Brigham Young University
BYU ScholarsArchive

Theses and Dissertations

2005-07-15

Biofilm Removal Using Bubbles and Sound

Michael R. Parini
Brigham Young University - Provo

Follow this and additional works at: https://scholarsarchive.byu.edu/etd

 Part of the Chemical Engineering Commons

BYU ScholarsArchive Citation

Parini, Michael R., "Biofilm Removal Using Bubbles and Sound" (2005). *Theses and Dissertations*. 619.
https://scholarsarchive.byu.edu/etd/619

This Thesis is brought to you for free and open access by BYU ScholarsArchive. It has been accepted for inclusion in Theses and Dissertations by an authorized administrator of BYU ScholarsArchive. For more information, please contact scholarsarchive@byu.edu, ellen_amatangelo@byu.edu.

www.manaraa.com

BIOFILM REMOVAL USING BUBBLES AND SOUND

by

Michael Robert Parini

A thesis submitted to the faculty of

Brigham Young University

in partial fulfillment of the requirements for the degree of

Master of Science

Department of Chemical Engineering

Brigham Young University

August 2005

www.manaraa.com

BRIGHAM YOUNG UNIVERSITY

GRADUATE COMMITTEE APPROVAL

of a thesis submitted by

Michael Robert Parini

This thesis has been read by each member of the following graduate committee and by majority vote has been found to be satisfactory.

_____	_____
Date	William G. Pitt, Chair
_____	_____
Date	Kenneth A. Solen
_____	_____
Date	William C. Hecker

www.manaraa.com

BRIGHAM YOUNG UNIVERSITY

As chair of the candidate's graduate committee, I have read the thesis of Michael Robert Parini in its final form and have found that (1) its format, citations, and bibliographical style are consistent and acceptable and fulfill university and department style requirements; (2) its illustrative materials including figures, tables, and charts are in place; (3) the final manuscript is satisfactory to the graduate committee and is ready for submission to the university library.

_____
Date

_____
William G. Pitt
Chair, Graduate Committee

Accepted for the Department

_____
W. Vincent Wilding
Department Chair

Accepted for the College

_____
Alan R. Parkinson
Dean, Ira A. Fulton College of Engineering and Technology

www.manaraa.com

المنارة للاستشارات
www.manaraa.com

ABSTRACT

BIOFILM REMOVAL USING BUBBLES AND SOUND

Michael Robert Parini

Department of Chemical Engineering

Master of Science

Bacteria in biofilms adhere well to surfaces and are quite difficult to remove. Oral plaque is one example of a biofilm. Many researchers have studied ways to remove plaque and bacteria from surfaces. It has been found that the passage of a bubble across a surface to which bacteria has adhered can remove the bacteria from the surface.

Biofilms of *Streptococcus mutans* were grown on glass coverslips as a simple model for oral plaque. The coverslips were mounted in a Plexiglas chamber filled with artificial saliva. A bubble stream was directed at the mounted biofilm. The velocity, gas fraction, median bubble diameter, and impingement angle were all varied to determine the effect of each parameter on removal and which parameter was the most significant.

To investigate the influence of sound on removal, a Ling oscillator was attached to the chamber, and was used simultaneously with and without a bubble stream. The acoustic intensity and the frequency were varied to determine if there was any effect on biofilm removal. Biofilm removal was also video taped.

www.manaraa.com

The results of these experiments confirmed that biofilms are removed by a stream of bubbles. Removal of biofilm is a function of stream velocity, gas fraction, and median bubble diameter, but not of impingement angle. The results of the acoustic experiments show that sound does not affect the removal of biofilm under the conditions used in these experiments.

Mathematical models relating the removal of biofilm as a function of time were also developed from the data obtained from the video recording of the experiments.

Additional tests using acoustic waves to remove biofilm should be performed to determine if more intense sound can remove biofilm. The intensity of the sound used in these experiments was low and the time of exposure was only 5 sec. Additional tests that more closely simulate the conditions of the mouth during brushing, like adding a surfactant, would also provide more insight as to whether bubbles in a clinical setting would remove biofilm.

www.manaraa.com

ACKNOWLEDGMENTS

I would like to thank Dr. William Pitt for all of his encouragement, guidance, and patience during these past few years. He has been invaluable in providing me direction, advice, challenges, and experiences to provide me with the best education possible. By being able to work in his lab, I have been blessed with the opportunity of working on many projects in addition to this present work, such as drug delivery in rats and rabbits, that might not have been available to me otherwise. He has provided me with opportunities to expand my knowledge and helped me to improve my ability to solve problems. I would also like to thank Dr. Kenneth Solen for his enthusiasm and instruction as I began my education in chemical engineering and his continuing encouragement. I also would like to thank Dr. William Hecker for his efforts to help me learn the principles of heat and mass transfer and for the opportunity of working with him as a TA.

I appreciate all of the efforts of my professors at Brigham Young University who have worked to provide me with an excellent education. I am especially grateful to the professors of the Chemical Engineering Department. They have been willing to drop what they are doing to help me, or any of my fellow students, with a problem. The department secretaries and staff have also been exceptional and I thank them for all the help they have given me.

www.manaraa.com

I would also like to thank the Chemical Engineering Department for the financial support it has provided. I extend a special thank you to Philips Oral Healthcare, who funded the majority of this project. This research would have been impossible if it was not for their support. I am also grateful to the NIH for the additional funding they provided.

I would also like to thank my friends and coworkers who have helped me to complete this research and to expand my knowledge. I am grateful to Jason Jones and the Precision Machining Lab at Brigham Young University for aiding in the design and for constructing many of the apparatuses used in this research. I also appreciate the help of Eric Richardson in assisting me with the more difficult experiments performed for this study. I also thank Mario Diaz for his insights and assistance in understanding many of the difficult concepts involved with chemical engineering.

None of this work would have been possible if it would not have been for my parents, Robert and Kathy Parini. They have always encouraged me and supported me throughout my life. I am extremely grateful for their love and for the many sacrifices they have made for me. I am also grateful to my mom for the dental advice she has provided me as a practicing dental hygienist.

Most importantly, I am eternally grateful to my Heavenly Father for his love, this life, and the gift of his son, Jesus Christ. He has provided us with this marvelous world and with the intelligence to learn more about this beautiful universe through study, experiment, and prayer. I am thankful for the atoning sacrifice of our Savior, Jesus Christ, which makes possible all of our life's experiences and the opportunity to return to the presence of our Heavenly Father.

www.manaraa.com

TABLE OF CONTENTS

www.manaraa.com

www.manaraa.com

www.manaraa.com

www.manaraa.com

LIST OF TABLES

www.manaraa.com

www.manaraa.com

LIST OF FIGURES

www.manaraa.com

www.manaraa.com

CHAPTER 1

INTRODUCTION

In traditional microbiology, bacteria are often studied as individual organisms in planktonic form. Many applications have shown that bacteria grow in communities, known as biofilms, and work symbiotically to enhance their ability to survive and obtain nutrients. (1-4) Biofilms adhere very well to surfaces and can be extremely difficult to remove.

One example of a biofilm that is dealt with on a daily basis is oral plaque. Oral plaque attaches strongly to teeth and cannot be removed by the natural flow of saliva in the mouth. While in the mouth, bacteria in the plaque digest the sugars present and produce acid as a byproduct. This acid dissolves the enamel of the teeth and irritates the gums. If this situation is not remedied quickly, the inside of the tooth will be destroyed and serious periodontal disease will result. In addition to producing acid, the bacteria also produce lipopolysaccharides, a toxin which elicits an immune response. If left untreated, the immune system will begin to damage the soft tissues of the mouth and could lead to systemic infection and disease. (5)

Previous studies have shown that the passage of an air bubble across a surface can effectively remove the particles and bacteria which had adhered to the surface. (6-10) However, many of these studies were limited to the passage of a single bubble across the surface. The use of a continuous stream of bubbles introduces other effects that may

www.manaraa.com

assist in the removal of biofilm; for example, shear forces and multiple collisions may enhance removal. The mixture of gas and liquid in the stream will change the viscosity of the solution impinging against the biofilm and will thus change the shear forces experienced by the biofilm.

Adams *et al.* conducted a study using a stream of bubbles, generated by the motion of a sonic toothbrush partially submersed in water, to remove biofilm. (11) This study showed that the bubbles from the toothbrush would remove biofilm from the walls of a narrow channel simulating the interproximal space between teeth. The bubbles used in this study were all generated from a sonic toothbrush that operates at a single speed. Factors such as velocity, fraction of gas in the fluid, size of the bubbles, and angle of impingement and their relationship to biofilm removal were not explored. In addition to these parameters, any effect of sonic waves in the fluid was not included in the study by Adams *et al*. Pitt has shown that the presence of sonic waves does remove biofilm. (12) It is possible that the sonic waves generated by the sonic toothbrush could have significantly influenced the amount of biofilm that was removed by the bubbles.

The goal of this research was to remove oral biofilm by collisions with bubbles in the presence of sonic waves and determine the effects of velocity, gas fraction, bubble size, angle of impingement, and the presence of sonic waves. In order to accomplish this goal, a continuous stream of bubbles of known velocity, gas fraction and size was passed across a biofilm of *Streptococcus mutans*, a common oral bacterium, at a specified angle. The *S. mutans* were grown on glass coverslips and mounted in a solution of artificial saliva. As the bubbles passed over the biofilm in the saliva, sound waves of fixed

www.manaraa.com

amplitude and wavelength were introduced into the solution by means of an oscillating piston suspended in the solution.

The impact angle of the bubbles onto the biofilm, the wavelength and amplitude of the acoustic wave, and the size and flow rate of the bubbles were the variables examined in this experiment. The amount of biofilm removed was measured as a function of these parameters.

www.manaraa.com

www.manaraa.com

CHAPTER 2

LITERATURE REVIEW

Chemical Removal of Biofilms

Many studies have been performed regarding the removal of biofilms, including oral biofilms within the mouth. (11, 13-16) Different interactions involved in the removal of biofilm have been studied, ranging from strictly chemical interactions, chemical with limited physical interactions, to solely physical methods of biofilm removal. An example of chemical removal was described in a study by Marais and Brozel who used electro-chemically activated water (ECAW) to remove biofilm from the inside of dental water lines. (17) At the commencement of the experiment the water lines in this facility contained 3×10^4 to 2×10^5 colony forming units per milliliter (CFU/mL). After one week the water lines with the ECAW had a bacterial concentration <1 CFU/mL while the control lines maintained the original bacterial concentration. At the end of the test, the biofilm was visually undetectable with SEM at 5000X magnification. (17) The use of ECAW is not limited to removing biofilm from tubing; Marais and Brozel believe that use of ECAW to keep teeth cool while being drilled would disinfect the cavities being treated. (17)

Bubbles

The use of bubbles as a means of removing particles from a surface has been explored in recent studies. (6, 7) Suarez *et al*. explored the removal of polystyrene

www.manaraa.com

lattices from quartz surfaces as a function of interfacial tension, velocity, and the number of air bubbles passing over the particles. The quartz was placed in a flow cell under a microscope in order to observe the interaction of the air-liquid-polystyrene interface. The polystyrene lattices were added to a potassium nitrate solution which was introduced into the flow cell to allow the lattices to adhere to the surface of the quartz. Flow of potassium nitrate was then introduced into the flow cell to remove any non-adhering lattices. (7)

Bubbles were passed over the surface to remove the particles. In order to manipulate the surface tension of the bubble/liquid interface, various amounts of 1-propanol were added to a potassium nitrate solution. The results of this study showed that the percentage of particles removed was proportional to the interfacial tension and number of bubbles involved in collisions, and inversely proportional to the velocity of the moving 3-phase interface. (7)

In addition to removing particles, bubbles have also been used as a means of removing adherent bacteria from a surface. Pitt *et al*. pumped bacteria through a flow cell containing a glass slide or a polymer substrate. After 1 hour of exposure to the bacterial suspension, the flow cell was rinsed with saline, then with ethanol, and finally with air. During the rinsing process, none of the bacteria adhering to the surface were displaced. This process was repeated using methanol in place of the ethanol, and again none of the bacteria moved. (10) The process was again repeated, but this time the alcohol rinse step was omitted. During the passage of the air-water interface through the flow cell, all of the bacteria were displaced. In another experiment a static air bubble, surrounded by water, formed on the surface of the flow cell. As the bubble expanded

www.manaraa.com

laterally, all of the bacteria in its path were displaced. Pitt *et al*. hypothesized that bacteria were displaced by the air-water interface as a result of the surface tension between air and water, but not by the lower surface tension of the air-alcohol interface. (10)

Use of Bubbles to Remove Biofilm

One common approach to removing biofilm is used by the general public on a daily basis. The use of mouth rinses or pre-brushing solutions are commonly employed in the attempt to remove biofilm, and Landa *et al*. have created an *in vitro* model to study the effectiveness of this approach. Biofilm was simulated by allowing *Streptococcus sobrinus* to adhere to a surface in a parallel plate flow chamber. After this preparation, a mouth rinse (Hibident®, or Scope®) or a pre-brushing solution (Plax®) was passed over the sample. Finally, air was introduced into the chamber so that bubbles would be present in the stream flowing over the sample. The interaction of the bubbles with the bacteria created a shear stress at the surface of the bacteria. (13)

The removal of bacteria in the presence of the mouth rinses was approximately 6% and 9% for Hibident® and Scope®, respectively, whereas Plax® removed 62% of the bacteria before the bubbles were introduced to the system. After the bubbles were introduced, the total percent of bacteria removed for the three rinses were 33%, 89%, and 81%, respectively. Control samples of the experiment, biofilms not exposed to a mouthrinse, were exposed to the bubble stream just as all of the other samples were; the amount of bacteria removed from the controls was approximately 26% of the total. (13) This control experiment shows that even though the chemical interactions are important

www.manaraa.com

in the removal of biofilm, the physical interactions of the bubbles also play an important role.

Companies like Braun, Oral-B, Interplak, and Philips have focused much of their attention on the development of toothbrushes that will provide the maximum amount of biofilm removal. There have been many studies performed on the different types of toothbrushes to determine which is best and why. (11, 15, 16, 18-22)

Yang *et al*. performed a study comparing three types of toothbrushes (manual, electric, and sonic) to determine which removes the greatest percentage of biofilm. Sonic and electric toothbrushes are both electrically powered, but the difference between a sonic toothbrush and an electric toothbrush is that the sonic toothbrush operates at speeds greater than 30,000 brushstrokes a minute whereas an electric toothbrush operates at only a few thousand brushstrokes a minute. From their experiment, two different sets of data were generated. The first set of data consisted of the number of bacteria per aggregate in the remaining biofilm, and the second set of data was the measurement of the percentage of biofilm removed. The distribution of the number of bacteria per aggregate was quite similar between the manual and electric toothbrush with values greater than five. On the other hand, over 80% of the remaining aggregates from the sonic toothbrush only contained one bacterium, and the largest aggregate contained two bacteria. (15)

With respect to biofilm removal, approximately 30% of the biofilm was removed by the manual brush, 60% of the biofilm by the electric, and the sonic toothbrush removed about 90%. (15) From this experiment it appears that the sonic toothbrush is superior to the other toothbrushes at removing biofilm. Other clinical studies also compared manual toothbrushes to sonic toothbrushes. The results of their studies also

www.manaraa.com

indicate that sonic toothbrushes are superior to manual toothbrushes at removing supragingival plaque. (20-22) The results from Tritten *et al.* showed that the sonic toothbrush was especially effective at removing plaque in the "hard to reach" places and in the surfaces lining the interproximal spaces. (21) It is important to note that in a clinical study comparing the removal of subgingival plaque by a mechanical toothbrush to the removal by a sonic toothbrush by Williams *et al.*, that there was no significant difference between the toothbrushes. In fact, there was no difference between the samples treated with the toothbrushes and the untreated control in the 1-to-3 mm region of the pocket (sulcus) below the gum line. (19)

Carter *et al*. also performed experiments to compare the difference in toothbrushes. Instead of focusing on whether the toothbrush was a manual, electric or sonic toothbrush, they tested 7 powered toothbrushes (6 electric and 1 sonic) from 6 different manufacturers for the best removal. Each toothbrush was placed over a 2-species biofilm of *S. sanguis* and *S. mutans*, and a compressive force was applied from the bristles to the film. Their results showed that the sonic toothbrush removed about the same total amount of biofilm as the other electric brushes with the exception of the Interplak by Bausch & Lomb, which removed significantly more biofilm than any of the other brushes tested. (16)

A third approach to studying the difference between sonic and electric toothbrushes focused on the ability of the brushes to remove biofilm in a model developed to replicate the interproximal spacing between human teeth, where the bristles cannot reach. In this experiment a slide covered in a biofilm of *S. mutans* was mounted behind two posts that represented two teeth. The toothbrush being tested was partially

www.manaraa.com

submerged in water and positioned to operate at the optimal performance angle. The sonic toothbrush removed more than twice the amount of biofilm than the electric toothbrush. An important observation from this study was that the sonic brush created more bubbles than the electric brush. (11)

The fluid dynamics of the sonic toothbrush were also of interest to Stanford *et al*. A study performed previous to their research by Wu-Yuan *et al.* reported that the fluid forces and cavitation generated by the sonic toothbrush were able to remove common oral bacteria (*S. mutans*, *Actinomyces viscosus*, and *Porphyromonas gingivalis*) from titanium and hydroxyapatite surfaces at distances of 4 mm. (23) Stanford *et al.* wanted to determine if the fluid forces would be able to remove oral plaque grown *in vivo* upon enamel. After the biofilm was grown, the enamel surface was placed either 2 or 3 mm from the tips of the bristles of the sonic toothbrush and were exposed for 5, 10 or 15 sec. After 5 sec of exposure at least 56 % of the bacteria were removed, and after 15 sec at least 65 % were removed. Thus the fluid forces generated by sonic toothbrushes are sufficient to remove oral plaque. (24)

Wu-Yuan *et al.* noted that both bubble cavitation and fluid forces were generated by the toothbrush during the experiments involving biofilm removal. (23) From Stanford *et al.* it is apparent that the fluid forces are sufficient to remove biofilm. (24) However, the impact of an air-liquid interface present when bubbles are in the solution and the effect of the acoustic waves generated by the toothbrush were not addressed. From the studies by Adams *et al*. and by Heersink *et al.*, it appears that the air-liquid interface of bubbles is also powerful enough to remove biofilm. (11, 25) What is not as clear is

www.manaraa.com

whether the acoustic vibrations created by sonic toothbrushes enhance the biofilm removal caused by bubbles.

Effect of Sound on Bacteria

McInnes *et al.* have studied the effect of sonic waves on planktonic *Actinomyces viscosus* and its adherence to hydroxyapatite discs. (26) The culture of *A. viscosus* was divided into three groups. The first group was exposed to sonic waves before being allowed to attach to the hydoxyapatite discs (pre-exposure group), the second group was first allowed to attach to the discs and was then sonicated (post-exposure group), and the third group was allowed to attach to the discs but was not sonicated (control group). Results from the pre-exposure group indicated that the bacteria had to be sonicated for at least 10 s before any significant reduction in the percentage of bacteria binding to the discs was observed. In this same group, an applied acoustic pressure of at least 20 kPa was required to reduce the percentage of binding for solutions of 10^7 bacteria/mL and a pressure of at least 35 kPa was required to reduce binding in solutions of 10^8 bacteria/mL.

Results from the study of the post-exposure group indicated that no significant removal occurred after 5 s of exposure to acoustic pressures of 50 kPa. After 15 s of exposure the difference in percent of bacteria bound to the discs between the post-exposure samples and the controls was statistically significant; however, the difference was only 10%. The study did show that the percentage of bacteria that remained bound to the discs decreased with time. After 480 s, the longest reported exposure, only 20% of the bacteria were still bound to the discs. As with the pre-exposure group, the post-exposure group was tested under various acoustic pressure conditions. It was shown that

www.manaraa.com

higher acoustic pressures resulted in greater removal. It was also noted that pressures lower than 30 kPa showed no significant removal of bacteria.

A later study by McInnes *et al.* was conducted to measure the effect of sonic waves on fimbriae. (27) It is believed that bacteria use fimbriae, pili, or polysaccharide layers to adhere to surfaces. In their work, both an acoustic generator and a Sonicare™ toothbrush were used to produce sonic waves. The acoustic generator was operated at 200 Hz and induced a peak pressure of about 50 kPa. The Sonicare™ was stated to have operated with similar parameters as the generator. The bacteria were exposed to sonic waves produced by either the generator for 15, 30, or 60 s, or to the Sonicare™ for 120 s. After exposure, the bacteria were suspended on a microscope grid and were then visualized by transmission electron microscopy. Micrographs taken by the transmission electron microscope showed that exposure for 30 s, 60 s, and 120 s caused significant damage to *A. viscosus* cells and their fimbriae. Exposure times of 15 s did not show any significant damage to either the cells or the fimbriae. Bacteria that were exposed to the Sonicare™ were severely damaged, with 10% of the cells being ruptured and extracellular particles covering the microscope grid.

The work performed by McInnes *et al.* suggests that the sound produced by sonic toothbrushes is effective at removing bacteria. Unfortunately, no information concerning the apparatus used for testing the toothbrush is described. However, a separate apparatus used in the same study to generate sound was described. This apparatus generates significant shear due to the small gap between the piston of the apparatus and the wall of the well containing the sample. In addition to the shear forces generated, there were bubbles present in the fluid.(27) It is doubtful that all the bacteria were subjected to pure

www.manaraa.com

sound (no shear and no bubbles). Further experiments must be performed to determine if sound alone will remove biofilm and whether it will enhance biofilm removal caused by a bubble stream.

Artificial Saliva

The ideal liquid solution for replicating the conditions of the mouth is obviously human saliva. Unfortunately obtaining large quantities of human saliva can be very expensive and impractical. Obviously, other solutions must be used. Many studies that require saliva use artificial saliva as a substitute. (28-32) Studies on different saliva substitutes have been performed to determine their physical properties. (33, 34) The viscosity of human saliva, as reported by Christersson *et al.*, is 1.9 centipoise. (34)

Ver der reijden *et al.* studied the rheological properties of different polysaccharide solutions to determine if any of the solutions exhibited rheological properties similar to that of saliva. The materials tested in this study were xanthan gum, alginic acid, carboxymethylcellulose, hydroxyethylcellulose, schleroglucan, guar gum, porcine gastric mucin, Saliva Orthana®, and whole human saliva. Each solid material was diluted in water and then each solution was analyzed using a rheometer. The results of this study showed that a 0.1 % (w/v) solution of schleroglucan had a viscosity and elasticity comparable to that of human saliva. (33) Schleroglucan is a branched homopolysaccharide which is composed of b-d-glucopyranosyl units linked together by a 1 to 3 linkage. An additional b-d-glucopyranosyl unit is linked on the sixth carbon of every third b-d-glucopyranosyl. This polysaccharide is commonly used in secondary oil recovery, paints, and in foods. It also has potential for use in drug delivery. (35)

www.manaraa.com

www.manaraa.com

CHAPTER 3

OBJECTIVES AND SIGNIFICANCE

Objectives

The objectives of this research were (1) to determine the effectiveness of gas bubbles in removing biofilm from surfaces within an acoustic field, (2) to determine which parameters have the greatest influence on the effectiveness of biofilm removal (the parameters of interest are volumetric fluid flow rate, gas volume fraction, bubble size, and angle of incidence of the bubbles on the biofilm), and (3) to determine the effect of different acoustic frequencies and amplitudes with respect to biofilm removal by the gas bubbles. In order to accomplish these objectives this project was divided into the following parts.

1. An apparatus was designed to create a constant stream of gas bubbles of uniform size which allowed the operator to determine the size and flow rate of the bubbles.
2. A chamber was designed and built that contained the biofilm in an artificial saliva solution that allowed for the introduction of the bubbles, manipulation of incidence angle, supported the generation and introduction of acoustic waves, and allowed for pressure measurements in situ.
3. The effects of volumetric flow rate, volume fraction, size, and incidence angle of the bubbles on the removal of biofilm were studied.
4. The effects of acoustic frequency and amplitude, in the presence of gas bubbles, on biofilm removal were studied.

www.manaraa.com

5. The viability of the biofilm after impingement by bubbles was studied to determine whether or not the bubbles would kill the bacteria.
6. Biofilm removal by bubble removal was described by a simple mathematical model.

Significance

The use of bubbles and acoustic waves in oral applications could lead to an increase of biofilm removal especially in the interproximal spacings of the teeth. By removing the biofilm the chances of developing gingivitis are greatly reduced; this will reduce the number of cases of more severe periodontal disease. This technology could easily be employed in a professional dental office, but even more advantageous would be the use of this technology on a daily basis with an instrument that could be used in the home of the consumer.

www.manaraa.com

CHAPTER 4

METHODS AND MATERIALS

Preparation of Artificial Saliva

To simulate a solution that would create bubbles with the same physical characteristics as those found in the mouth, an artificial saliva solution was developed. The complex biochemical reactions that occur in saliva were not of importance in this work, and so the enzymes typically found in saliva were not used. However, a solution with the same viscosity as human saliva was desired so that the Reynolds number in the experiments would be similar to that in the fluid found in the mouth.

Previous work performed by Philips Oral Healthcare had used a polysaccharide called schleroglucan (Clearogel CS 11D, MMP, Inc., So. Plainfield, NJ) as an additive to water to simulate the viscosity of human saliva. Douglas Dudgeon of Philips Oral Healthcare suggested that this polysaccharide be used in the artificial saliva solution. Many different concentrations of schleroglucan were tested as well as different techniques of preparation. The method that yielded a solution closest to the viscosity of human saliva was prepared in the following manner.

A flask containing 500 mL of deionized water was heated and continuously stirred on a heat/stir plate. Before coming to a boil, 2.0 gm of scleroglucan was added to the water. Scleroglucan is not completely soluble at this concentration, so it was added slowly to avoid creating clumps. After the solution came to a boil, it was vacuum filtered

www.manaraa.com

through a Whatman® 4 qualitative filter to remove any clumps from the solution. An additional 825 mL of deionized water was added to the solution.

The viscosity of the solution was measured using a capillary viscometer (Schott Gerate, capillary Typ 52503/0c, App Nr. 25030, K = 0.002539). To do so, it is assumed that the liquid is a Newtonian fluid with constant density. Newton's law of viscosity and Poiseuille flow can be applied under these assumptions. Measuring the viscosity of the schleroglucan solution with this method was performed by measuring the time it took a given volume of the solution to pass through a capillary tube and comparing that time to the time it took the same volume of distilled water to pass through that same capillary. This ratio is the relative viscosity. (36) To determine the absolute viscosity of the schleroglucan solution, the absolute viscosity of the water must be known. Since the absolute viscosity of water is a function of temperature, the temperature was measured with a digital thermometer. The absolute viscosity of the schleroglucan solution was then calculated from a tabulated value of viscosity for water at that temperature.

This solution had a viscosity of 1.4 centipoise. To determine if this value for saliva was adequate, a viscosity test of fresh human saliva from a BYU student was performed and yielded a value of 1.5 centipoise. Christersson *et al*. have also measured the viscosity of saliva and have reported that human saliva has a viscosity of approximately 1.9 centipoise. (34)

Preparation of Biofilm

Media

The *Streptococcus mutans* were grown in a solution of brain heart infusion supplemented with 2 wt % sucrose (BHI-S). This solution was prepared by adding 37

www.manaraa.com

grams of powdered brain heart infusion powder (BHI) into 1 L of distilled water. The mixture was placed onto a hot plate with magnetic stirring. This mixture was continuously stirred and heated until all of powder dissolved into solution. During this process 20 grams of sucrose were added. This solution was then covered and sterilized at 250ºF by autoclave for 20 minutes. The media was removed from the autoclave and left to cool to room temperature overnight.

Storage of Bacteria

To avoid mutation of the bacteria *Streptococcus mutans* (strain UA159), the bacteria was stored in a freezedown solution at a temperature near -80ºC (193 K). The freeze down solution was 50 % glycerol and 50 % BHI-S. Also, to facilitate inoculation of cultures, the suspension was aliquoted into separate 2 mL vials for storage.

Biofilm

The biofilm of *S. mutans* was grown on glass coverslips in the following manner. A 1 inch x 3 inch glass slide was placed into each of four chambers of a drip flow reactor (DFR). Three 1-inch squared coverslips were placed on top of the glass slide to form a single layer covering the slide. To secure the coverslips in place, 3 small drops (one for each coverslip) of sucrose syrup were placed onto the slide before adding the glass coverslips. The syrup was made by adding equal masses of sucrose crystals and water to a flask and then heating and stirring the flask until all of the sucrose had dissolved into the water. A Plexiglas cover, with a rubber septum at one end and an Acrodisc filter with 0.2 μm pores at the other, was then secured over each chamber with a set of screws. This "drip flow reactor" was then wrapped in aluminum foil and sterilized in an autoclave for 15 min at 250ºF and 29.82 psia. (37) It was then dried for 5 min in the autoclave. The

www.manaraa.com

reactor was then removed from the autoclave and allowed to cool to room temperature. (See Figure 1.) Using sterile technique, the reactor was removed from the foil and placed upon an aluminum leveling box inside a 37ºC incubator. A bulls-eye level was used to maintain a level platform for the reactor.

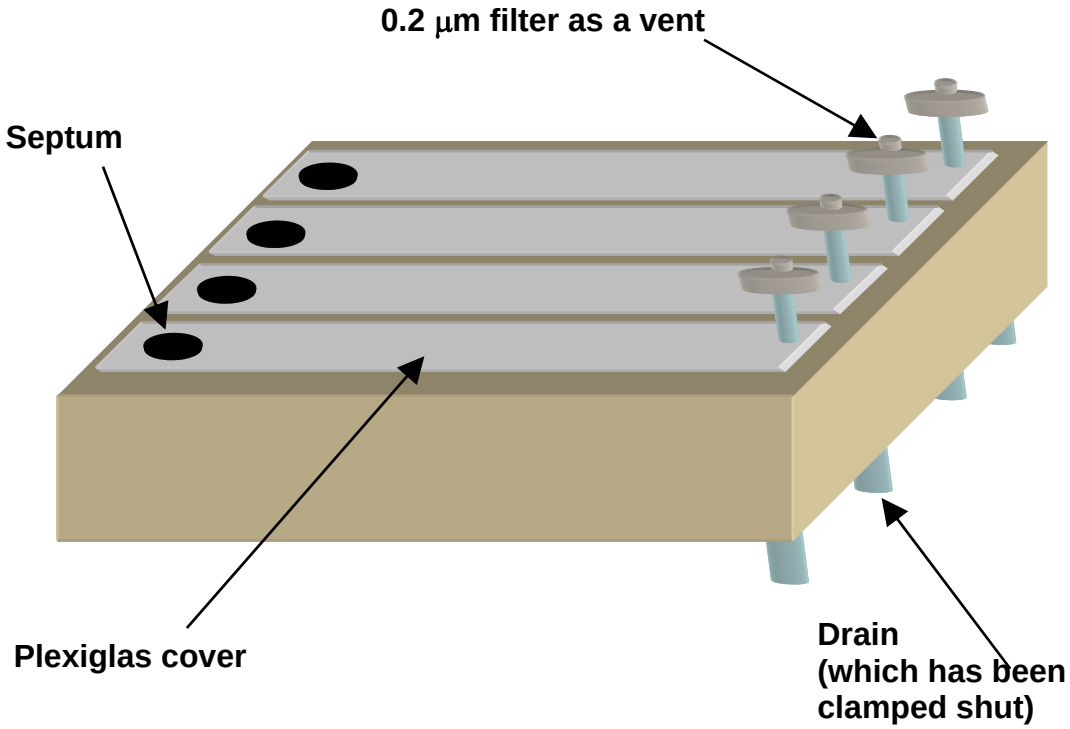

Figure 1. Drawing of the drip flow reactor.

Another important part of the biofilm formation was preparation of the bacterial culture. One vial of *S. mutans* was removed from the -80ºC freezer and was allowed to thaw just long enough to pipette out 10 μL of suspension and add it to 100 mL of sterile BHI-S in an Erlenmeyer flask. The vial was immediately placed into a -20ºC freezer where it was used to inoculate more cultures during a one week time period. After one week the vial and its contents were disposed of as biological hazard waste. The fresh

www.manaraa.com

culture in BHI-S was placed into a 1-gallon paint can, which has been thoroughly washed, and two CO_2 producing cartridges (Becton-Dickinson, Sparks, MD) were activated and added to the can. The can was sealed and placed into a 37ºC incubator for 14 to 24 hours. After this incubation period, the solution was removed from the incubator and the can. Of this solution, 6 mL were pipetted into 54 mL of sterile BHI-S. The rest of the overnight culture was later autoclaved and disposed of as waste. The new 60 mL solution was lightly swirled to create a homogeneous solution. Using sterile technique, 15 mL of the solution was pipetted into each of the four chambers of the drip flow reactor. (See Figure 2.)

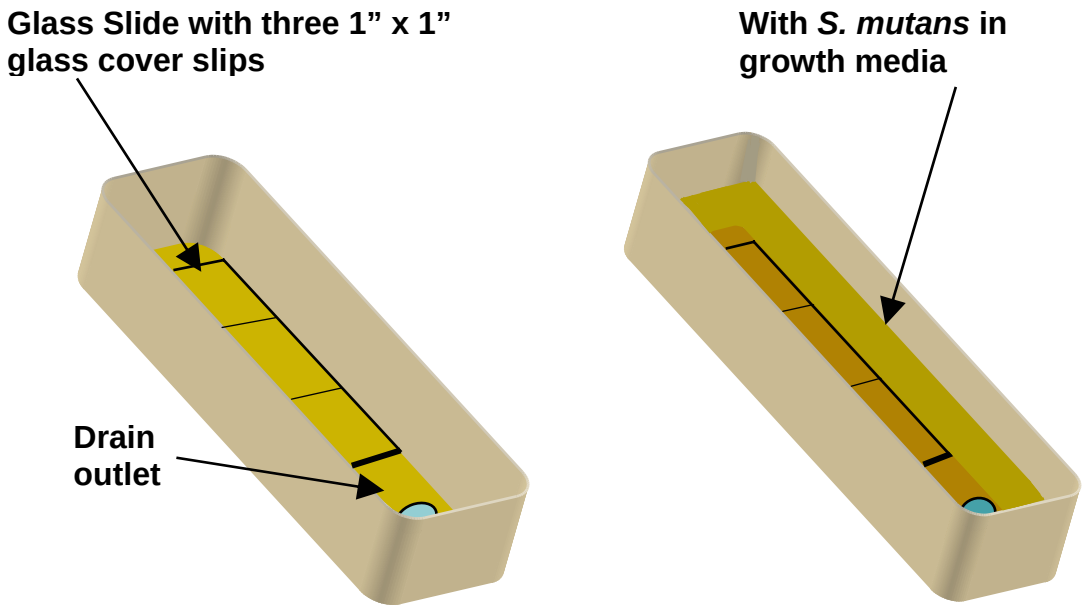

Figure 2. Drawing of chambers in drip flow reactor with a 1" x 3" glass slide and three 1" x 1" coverslips . The chamber on the left is sterile and has now growth media, while the chamber on the right has been inoculated with *S. mutans* in 15 mL of BHI-S.

To provide CO_2 to the *S. mutans*, 8 mL/min of CO_2 flowed through silicone rubber tubing from a compressed gas tank to an Acrodisc gas filter with 0.2 μm pores (Gelman, Pall

www.manaraa.com

Corporation, East Hills, NY). The small pores filtered the gas so that it was sterile. All of the tubing downstream of this filter was autoclaved before each use. The tubing branched into 4 streams, and at the end of each stream was a sterile 25 gauge needle (PrecisionGlide, Becton-Dickinson & Co., Franklin Lakes, NJ). The rubber septum in the Plexiglas cover of each chamber was then sprayed with a solution of 70% ethanol in water and the needle was inserted so as not to be orthogonal to the glass coverslips. By inserting the needle at an angle, the solution in the chamber was not displaced by the flow of gas since there is a sterile gas vent in each chamber. If the flow of gas were to cause significant shearing resulting in the displacement of the fluid surface, the layer of biofilm would not be of a uniform thickness across all of the coverslips. (See Figure 3.) The reactor was left in the incubator overnight for about 16 hours at a temperature of 37ºC.

Experimental Chamber

The experiments in which biofilms were exposed to gas bubbles and sound were performed in a rectangular box made of Plexiglas. Drawings of the box are found in the appendix. In the base of the box a small hole was drilled and a Pasteur pipette bulb was inserted to act as a septum. To insert the blunt needle used for the experiments, a larger, 20-gauge needle was inserted through the top of the septum. This needle acted as a sheath for the 25-gauge needle that was introduced up through the bottom of the septum. The use of the preliminary 20-gauge needle was necessitated as the bevel on the 25-gauge needle had been removed because the bevel imparted a spin to the column of bubbles. The bevel was removed using electrical discharge machining (EDM).

www.manaraa.com

Bubble Generation

To generate bubbles on the order of 10 – 100 microns, pressurized streams of gas and liquid were mixed together in the hub of the blunt 25-gauge needle and propelled through the needle into the experimental chamber. To create these gas and liquid streams, a cylinder of compressed air was connected to a tee joint of 0.5 inch schedule-80

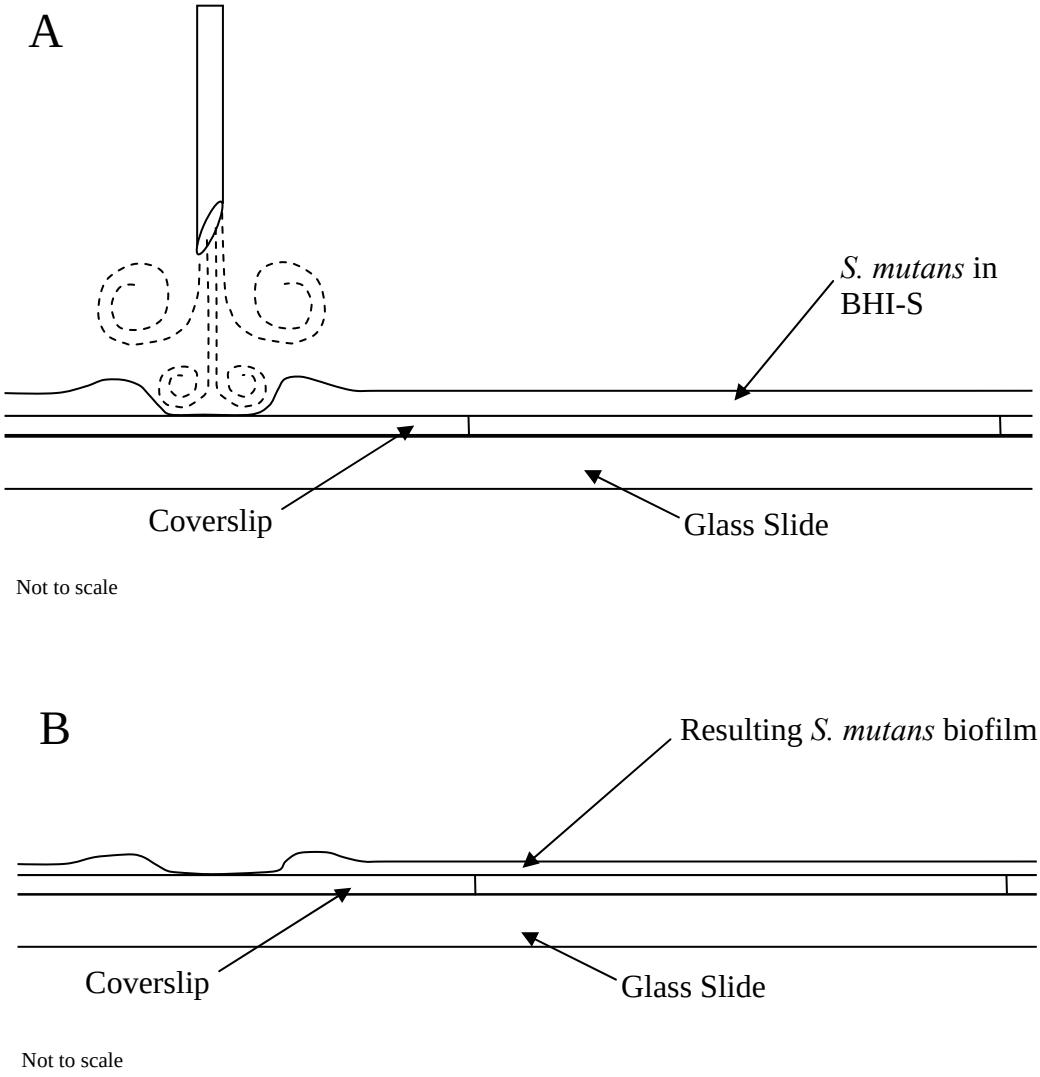

Figure 3. Drawings of biofilm growing on glass coverslips. A) Needle delivering CO_2 to growing bacteria which has been positioned orthogonally to the coverslips. B) Resultant biofilm formation. This was the situation that was avoided by inserting the needle at an angle.

www.manaraa.com

PVC pipe to which a 1.25 inch inner diameter pipe filled with artificial saliva solution was also attached. Through barbed fittings at the top and bottom of this tube, a pressurized air stream exited through the top and a pressurized artificial saliva stream exited out of the bottom. (See Figure 4.) Both of these streams were connected to ball valves which served as on and off switches. Needle valves were used to control the flow. These two streams were then directed through an aluminum block to which a blunt luer-lok needle could be affixed. In the hub of this needle is where the two streams mixed and created bubbles. This needle, which was previously inserted into the experimental chamber, then guided the bubble stream in the direction of the biofilm.

On the gas line, just before the ball valve, a pressure tap was inserted and connected to a pressure transducer. After the ball valve, the gas stream was tapped on both sides of the needle value, and a differential pressure transducer was connected to measure the pressure difference across this valve. The electrical signals from both transducers were sent to a National Instruments Data Acquisition card (NI-DAQ) which was connected to a PC. The analog voltage signals from the pressure transducers were converted into pressures by the computer program LabView (National Instruments).

Measuring Flow Rates

Calibrating Pressure Transducers

Each pressure transducer was calibrated independently. The electrical leads on the pressure transducer were connected to a Hewlett-Packard 3490A voltmeter which was accurate to 3 decimal places. The transducer was then connected to an Omega pressure calibrator PCL-200 which had been previously calibrated on May 27, 1999 and was accurate to within 0.10%. Voltage readings were taken for at least 12 pressures along

www.manaraa.com

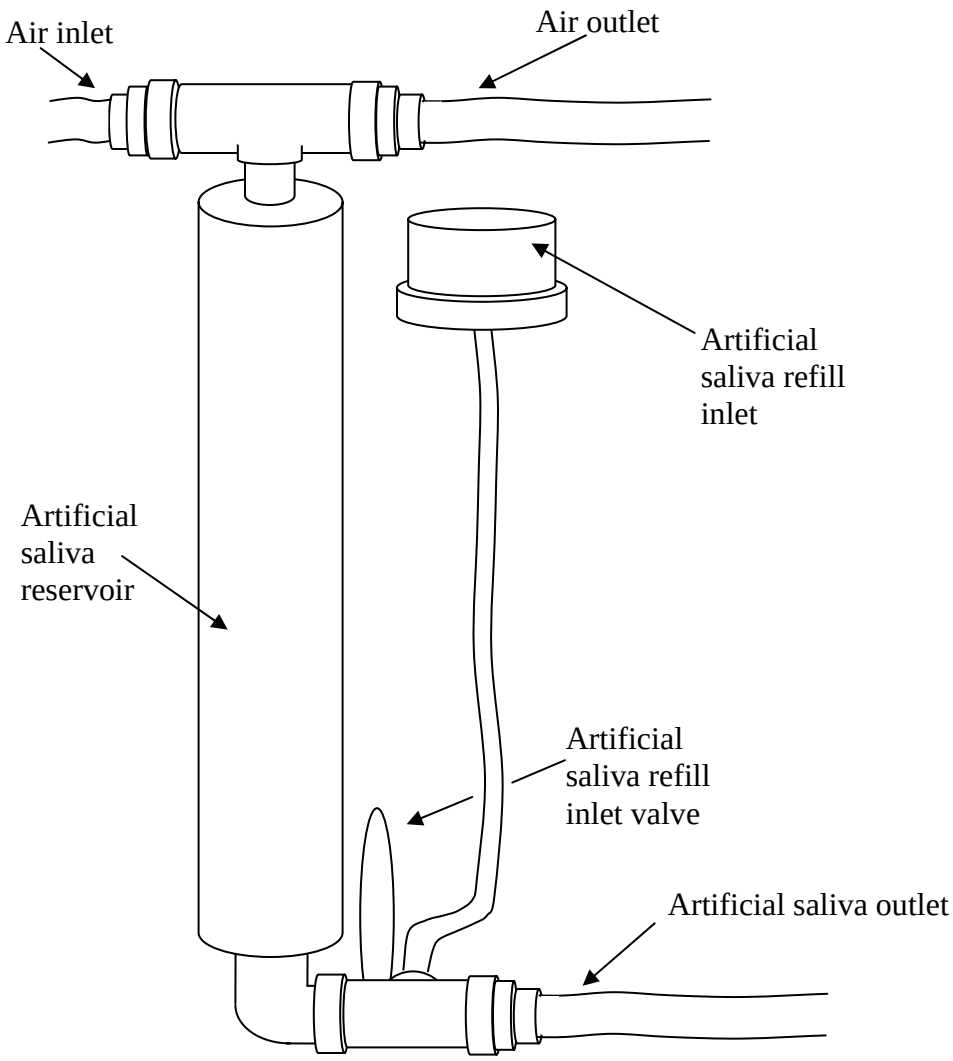

Figure 4. Drawing of the artificial saliva reservoir and pressurizing system.

the range of the transducer. Pressure-voltage plots were generated in MS Excel, which resulted in a linear relationship; the equations from these plots were then used in LabView so that the computer would display pressures. (See Figure 5.)

www.manaraa.com

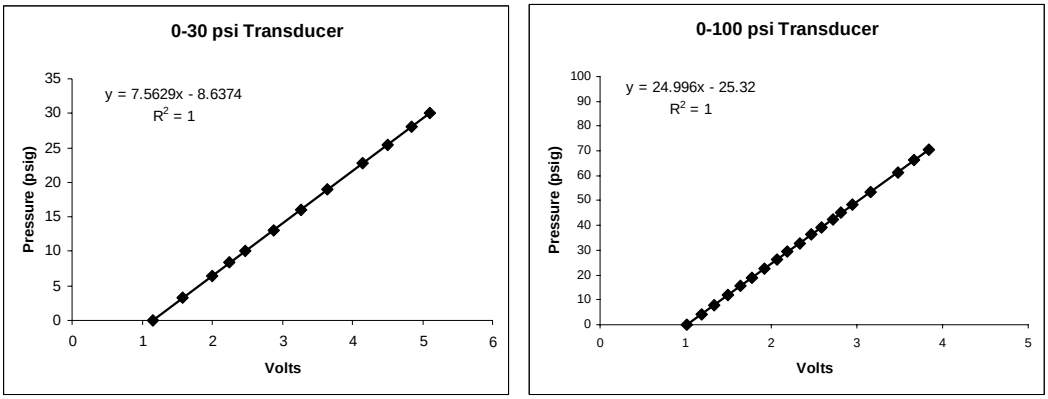

Figure 5. Calibration plots generated from experimental data used to create pressure scales in LabView.

Determination of Operating Pressures

The bubble generation system was operated at different pressures to determine the range of pressures that should be used in the experiments. In this experimentation it was noted that if both the liquid and air valves were completely open that the liquid would prevent the air from passing through the needle and then began to flow up the air lines. To prevent this, the needle valve on the liquid side was closed just enough so that air could pass through under all of the proposed experimental conditions.

Measuring Stream Velocity and Gas Fraction

The velocities of both gas and liquid streams were measured simultaneously by volumetric displacement as follows. Two 50 mL-burettes were connected in series by attaching latex tubing to the top of the first burette, connecting the other end of the latex tubing to a piece of copper tubing, and inserting the copper tubing into the bottom of the second burette. The first portion of latex tubing was wrapped with steel wire to prevent the tubing from pinching shut and then was allowed to hang freely. The latex tubing was then cut and a three-way valve was inserted into the tubing to act as a relief valve. All of

www.manaraa.com

the joints were checked for leaks using Snoop. (See Figure 6.) The first burette in the series only contained air and had a rubber septum through which the blunt needle passed. The second burette was filled with water and placed upside-down into a water bath. The bubble generator was turned on, and, after the pressure in the system had stabilized, the volumetric flow rates in the burettes were measured by recording the change in volume and the time elapsed. For the measurement of the liquid velocity at the needle exit, the volumetric flow rate was divided by the internal cross sectional area of the needle exit. The velocity of the air was determined in a similar matter. The volume of air in the first burette displaced by liquid was subtracted and the volumetric expansion of the air in the burette was also accounted for in the calculation. The gas fraction was calculated by dividing the volumetric gas flow rate by the total flow rate.

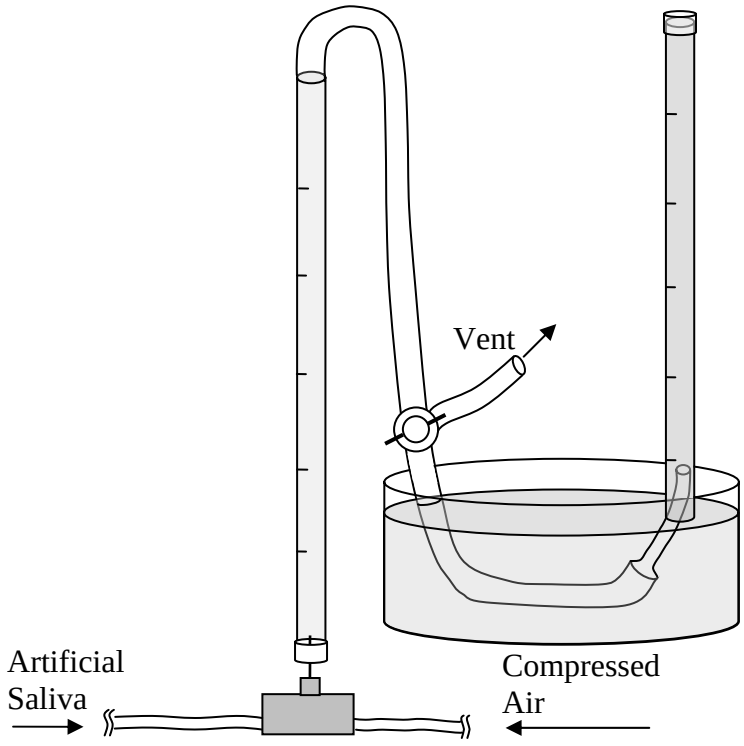

Figure 6. Apparatus used to determine fluid stream flow rates and gas fraction.

www.manaraa.com

Bubble Disruption of the Biofilm

Mounting the Coverslip

After the biofilm had grown on the coverslips in the drip flow reactor (DFR) overnight, one chamber of the DFR was opened and the slide with biofilm covered coverslips was removed with a pair of flat tweezers and placed in a Petri dish so that the edge of slide rested on the lip of the dish. This facilitated the removal of the coverslips from the slide and provided space in the Petri dish so that all of the coverslips could lay flat in the Petri dish. Distilled water was then pipetted into the dish to rinse the biofilms and keep them moist. Care was taken to ensure that the water was never applied directly over the biofilm so that shear forces would not remove additional biofilm.

After the rinse was performed one coverslip was removed from the Petri dish using the same flat tweezers and a dental curette. The tweezers were clamped onto the edge of coverslip so that the portion of biofilm disturbed by the tweezers would rest against a Plexiglas mount and out of the bubble stream. (See Figure 7.) This mount was designed so that the edge of the coverslip would come into contact on 3 sides with the Plexiglas. To secure the coverslip, optical microscope slide clamps were connected to the Plexiglas mount and the springs of the clamps pressed against the back of the coverslip.

www.manaraa.com

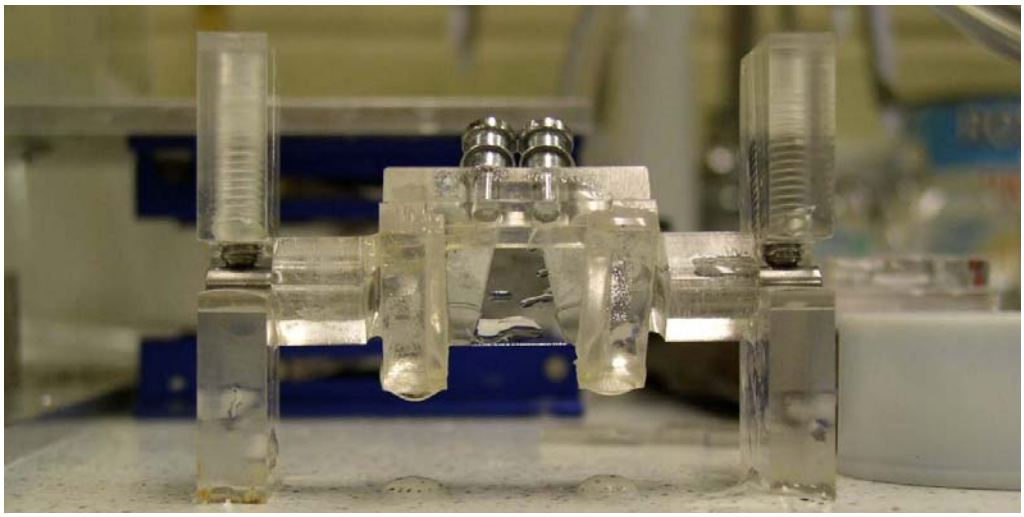

Figure 7. Picture of apparatus used to mount coverslips with biofilm.

A protractor with 5º graduations was fitted to the mount so that the angle of impingement with the bubble stream could be set. The mount was designed so that a glass slide could be slid in between the biofilm and the bubble stream. This shield was very useful because the biofilm could be placed in the experimental chamber, and thus protect the biofilm from bubbles before the bubble stream had reached steady state. At the commencement of the experiment, the shield was removed.

Visual Recording

Measuring Bubble Size

In order to generate bubbles at a desired size, a correlation between the bubble size and the system pressures was needed. The size of bubbles at different pressure settings were measured just after leaving the tip of the needle using a Sony CCD-IRIS/RGB video camera (DXC-151A, Park Ridge, New Jersey, USA) connected to a 10 inch laboratory telescope. The camera images were stored to a computer using image capturing software (Image-Pro® Plus, Media Cybernetics®, Silver Spring, Maryland, USA). The horizontal

www.manaraa.com

and vertical diameters of at least 30 bubbles were recorded for nine different pressure combinations of the two streams. To ensure that the images were not significantly distorted by the camera lens, a few of the conditions were repeated with the camera rotated at a 90º angle to its previous orientation, and these images were compared with those taken when the camera was at its original orientation.

Measuring Biofilm Removal – Radius

Many of the experiments performed were measured after exposure to the bubble stream. However, to achieve a greater understanding of how bubbles affected the removal of biofilm, real time measurements of the biofilm removal were recorded by positioning the experimental apparatus and bubble generator so that the center of the biofilm covered coverslip was in the focal plane of the aforementioned video camera and telescope. The output signal from the video camera was connected to a Sony VCR (SVO-1420) with a VHS tape set to record on short play (SP) setting. To ensure that the image was in focus, the signal was simultaneously transferred to a TV so that adjustments to the focus could be observed. Biofilm samples were then mounted into the experimental chamber and a glass slide, used as a protective shield, was placed in front of the biofilm. Then the bubble stream was introduced into the chamber. After the stream had come to equilibrium the biofilm shield was removed. The VCR continued to record until biofilm removal could no longer be visually detected. After all of the runs were recorded to tape, the video on the tape was then converted into a digital format that could be processed by a personal computer (PC).

One limitation to the setup was that the magnification of the telescope was such that not all of the biofilm removal pattern could be seen at once. Using Scion imaging

www.manaraa.com

software, the circle tool was used to find the center of the circular removal pattern by lining up the edge of the circle with the edge of the biofilm removed of the last frame of the run. The pixel at the middle of the circle was then used as the center point for the radial measurements corresponding to that experimental run.

Generation of Acoustic Field

A Ling oscillator (V203, Ling Dynamic Systems, Royston, Herts, United Kingdom) was mounted into a Plexiglas stand that was clamped on top of the Plexiglas chamber. Drawings of the mount and oscillator are located in the appendix. The oscillator was powered by a 25 W integrated stereo amplifier which received a signal from a waveform generator (Hewlett-Packard 31120A, Omaha, NE). In these experiments it was desired to reproduce the acoustic energy that would be received by a biofilm 1 mm from the tip of the bristles of a standard sonic toothbrush, the Sonicare *Elite* toothbrush (Philips Oral Healthcare, Snoqualmie, WA). To do so, the tip of a hydrophone (8130, Bruel & Kjaer) was placed in the Plexiglas chamber where the biofilm would be mounted during experiments.

A fully charged Sonicare *Elite* toothbrush was positioned 1 mm from the tip of the hydrophone. (See Figure 8.) The acoustic intensity of the toothbrush as measured by the oscilloscope was equal to 0.00154 mW/cm^2 and the frequency was 260 Hz. The toothbrush was removed from the tank, the Ling oscillator was attached to the tank, and the input voltage was adjusted until the acoustic signal received by the hydrophone from the oscillator was the same as the signal from the toothbrush. This value of acoustic intensity was defined as 1 toothbrush equivalent (TBE).

www.manaraa.com

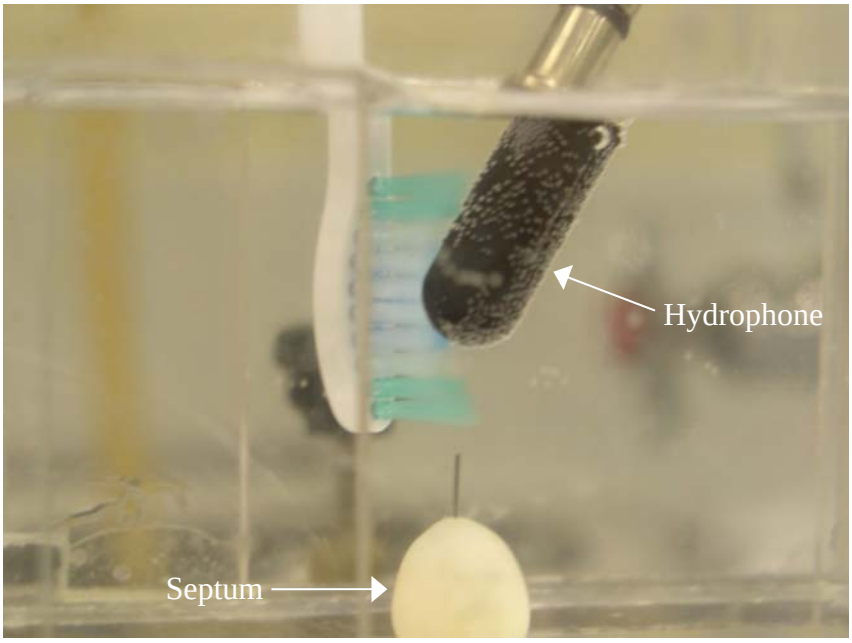

Figure 8. Picture of the Sonicare *Elite* toothbrush placed in the experiment chamber placed 1 mm from a hydrophone positioned where the biofilm would normally be.

Establishing Steady-state Conditions

The characteristics of the bubble stream (velocity, gas fraction, and median bubble diameter) were dependent upon the pressure of the system and also the difference in pressure between the air and the liquid sides of the bubble generator. By opening the valves to permit the air and liquid to flow through the needle, immediate changes in pressures were created. Adjustments were made to the pressure regulator and air side needle valve until the overall pressure and pressure drop across the air side needle valve appeared constant.

One complication to this processes involved the quality of the needle valves. It was noted that the flow of liquid through the needle valve was not always constant even though the valve was not adjusted. Because of this inconsistency the flow through the needle valves had to be recalibrated several times during a day.

www.manaraa.com

Phase 1: Influence of Stream Velocity, Gas Fraction, and Bubble Size on Biofilm Removal

The first objective of the study was to determine which factors (gas fraction, stream velocity, or size of the bubbles), or combination of factors, had the greatest influence on biofilm removal. To determine this, a 3 parameter (stream velocity, gas fraction, and bubble size) 2 level full factorial design with 3 replicates performed in random order was proposed. However, physical limitations of some combinations of parameters prevented the full design to be executed. Table 1 contains a summary of the conditions tested.

Table 1. Table of experimental conditions used in phase 1.

Experiment	Velocity (m/s)	Gas Fraction	Bubble Diameter (μm)
1	High (6.8)	High (0.5)	Low (136)
2	Low (4.0)	High (0.4)	Low (144)
3	High (10.1)	High (0.5)	High (256)
4	Low (3.3)	Low (0.3)	High (232)
5	High (12.2)	Low (0.3)	High (262)

Phase 2: Variation of Dominant Parameters

Once the dominant parameters and parameter interactions in biofilm removal were identified, a detailed study of how variations of each of these parameters affected the rate and area of biofilm removal was conducted. This was accomplished by repeating the same type of experiments as those used in phase 1, but instead of varying all of the parameters between high and low values, some selected dominant parameters were studied over a range of values. This resulted in 10 different experimental conditions that were executed twice each and in completely random order.

www.manaraa.com

Phase 3: Effect of Angle

For the first two phases of the experiment, the angle of bubble stream impingement was fixed at 45º. Once the effect of velocity, gas fraction, and bubble size were understood, the next study was how the impingement angle of the bubbles against the biofilm affected the biofilm removal. To determine the effect of the angle of fluid impingement, biofilms were exposed to one of two bubble stream conditions at one of three angles. The conditions of one of the bubble streams were a velocity of 1.5 m/s, a gas fraction of 0.04, and a median bubble diameter of 205 μm. The other stream consisted of bubbles of the same size as the previous stream but with a velocity of 4.3 m/s and a gas fraction of 0.41. The impingement angles used in this study were 5, 30, and 45 degrees. All combinations of bubble streams and angles were replicated four times.

Phase 4: Effect of Sound

Previous studies have shown that sonic toothbrushes remove more biofilm than manual and electric toothbrushes (11, 15); however, no study has validated the role of sound generated by the toothbrush as the cause for the enhanced removal. To determine whether or not sound plays a role in the biofilm removal, a pair of biofilms were exposed to bubble streams with the same velocity, gas fraction, and bubble size, but one biofilm was exposed simultaneously to an acoustic field, while the other biofilm was not exposed to such a field. In order to maximize the consistency of the bubble streams during the experiments, the bubble stream was started before the biofilm and the protective shield were inserted into the Plexiglas chamber. Once the stream had reached steady state at the desired parameters, the shield was opened for 5 seconds to expose the biofilm. After 5 seconds, the biofilm was removed from the path of the bubble stream and then removed

www.manaraa.com

from the chamber while the stream continued to flow; then the acoustic oscillator was activated. A second biofilm and shield were then placed into the chamber and exposed to the bubble stream and sound for 5 seconds and subsequently removed. Thus the paired experiments were done under identical bubble conditions, with only the acoustic field being different.

The frequencies used in this experiment were based around the frequency emitted by a common sonic toothbrush: the fundamental frequency, 260 Hz, twice that frequency, 520 Hz, and half that frequency, 130 Hz. At each frequency various intensities were employed to determine whether the frequency or the intensity of the sound was more dominant in removing biofilm. The acoustic intensities used with each of these frequencies were 0.2, 1, and 2 TBE; however, due to the mechanical limitations of the Ling oscillator, the maximum acoustic intensity achievable at 520 Hz was only 0.2 TBE.

Two different bubble streams were also used in these experiments. The parameters of one stream were a velocity of 10.8 m/s, a gas fraction of 0.27, and a median bubble diameter of 205 μm. The parameters of the other stream were 12 m/s, 0.65 gas fraction, and 300 μm diameter. The angle of impingement was set to 45º for all acoustic experiments. Experiments without bubble flow were also performed to measure the amount of removal caused by sound alone.

Phase 5: Video Photography of Biofilm Removal

The previous phases of the experiments have only provided a before and after image of the effects of bubbles on biofilm removal. Observation of real time experiments would allow for a more profound understanding as to the physical effect of bubbles when they come into contact with biofilm. To view the biofilm removal in real time, the

www.manaraa.com

bubble generator and biofilm experimental chamber were positioned in front of the Sony video camera attached to a 10” laboratory telescope. Bubble stream flow conditions used in the first 3 phases of the experiment were also used in this phase, and were observed to gain a qualitative understanding as to the interactions of the bubble stream with the biofilm.

Biofilm Image Capture

After a biofilm had been exposed to the bubble jet, it was removed from the experimental chamber and the mounting apparatus and placed, biofilm-side down, slowly onto a drop of deionized water in a clean Petri dish. A Petri dish lid, which had been lined with black paper, was then placed on top of the dish to provide a contrasting background to the white biofilm. The Petri dish was then placed on a flatbed scanner (C7710A, Hewlett-Packard, Omaha, NE) and scanned at 300 dots per inch (dpi).

The scanned image was then loaded as a grayscale image into an imaging software program (Scion Image). The first analysis dealt with determining the amount of biofilm that had been removed. This was done by assessing the grayscale of the regions where removal had taken place. Four sections where biofilm was completely absent, one near each corner of the image, were analyzed and returned a value close to 255 (black). The average of these values was used as the background value. Four additional sections, this time in sections where biofilm was believed to be undisturbed, were also analyzed and their average value was assigned the value of 100% biofilm present. The biofilm was sufficiently thin that the black background rendered the biofilm shades of gray (not white) even at thick undisturbed areas. The numerical grayscale values of regions impacted by bubble activity were used to calculate the amount of biofilm remaining

www.manaraa.com

based upon linear interpolation between the values of the black background and the unperturbed biofilm. Thus we assumed that the amount of light detected by the scanner was proportional to the thickness of bacteria in the biofilm.

Two measurements were made using Scion Image. First, a software tool was used to define the boundaries of the area perturbed by a numerical value for that area. Then the average grayscale value was calculated for the biofilm within the enclosed area. Using the linear interpolation discussed above, the average amount of biofilm removed was calculated in terms of a percent of thickness removed. This measure is called "deep removal". The product of the fraction of the coverslip area affected by the bubbles and of the average removal within that area produced a parameter called "total removal".

Measuring the Viability of the Biofilm

Viability Before Exposure to the Bubble Stream

Drop Plate Method

A fresh biofilm was removed from the DFR and rinsed with deionized water. The coverslip was then placed in a sterile 50 mL beaker containing 20 mL of sterile physiologic saline solution (PSS). A sterile rubber policeman, attached to the end of a glass hockey stick, was used to remove the biofilm from the coverslip into the solution and the coverslip was removed from the beaker. (See Figure 9.) The beaker was then placed under a tissue homogenizer (Ultra-Turrax, T25 basic, IKA-Werke) and the contents ground for at least 30 seconds at 17500 rpm.

www.manaraa.com

Figure 9. Picture of a rubber policeman attached to a glass hockey stick.

After the solution had been homogenized, 1 mL of this solution was added to a sterile test tube filled with 9 mL of PSS. This tube was capped and vortexed until the vortex spanned the entire test tube. 1 mL of this first dilution, labeled 10^1, was then added to the next test tube of 9 mL of PSS and the process (known as serial dilution) continued until the solution was diluted on the order of 10^6.

The drop plate method was used to quantify the serial dilutions as follows (38): The bottom of a Petri dish, containing sterile BHI-S agar media, was divided into four quadrants using a ruler and a red felt-tip pen. The quadrants were labeled 10^3,10^4, 10^5, 10^6, respectively. In each of the four quadrants 5 ten-μL drops of the serially diluted solution were deposited so that none of the drops were in contact with each other. After the plate was covered and the drops had absorbed into the agar, the Petri dish was placed upside down in an airtight container along with two activated CO_2 cartridges and then placed in a 37ºC incubator for 24 hours. After 24 hours had passed, two additional CO_2 cartridges were added to the container and incubation continued for another 24 hours.

www.manaraa.com

After the bacteria were incubated for 48 hours, the quadrant of the plate containing between 150-500 colony forming units, CFU, per quadrant was selected and the total number of colonies in that quadrant were counted. The total was then multiplied by the dilution and then converted to CFU/in^2 to determine the number of biofilm bacteria CFU there were per original coverslip.

Staining with Live/Dead Stain

A Live/Dead stain was prepared by adding 300 μL of sterile PSS to a small centrifuge tube. Next, 3 μL of SYTO 9 Nucleic Acid stain (Live/Dead BacLight Bacterial Viability Kit, L-7012, Molecular Probes, Eugene, OR) were added and then 3 μL of propidium iodide solution. This solution was gently swirled until it was evenly mixed. These are both fluorescent stains that can be observed by epifluorescence microscopy or by scanning laser confocal microscopy.

All cells that appear green have not had their membranes ruptured and are considered "alive". Cells with ruptured membranes appear red and are considered "dead". The green color comes from the STYO 9 nucleic acid stain. This stain labels all of the cells regardless whether the cell membrane is intact or not. Propidium iodide (PI) is what gives the cells their red color and overwhelms the green color. However, PI cannot pass through an intact cell membrane, and will only bind to the DNA if membrane is ruptured.

A biofilm sample was placed on a 3 inch glass slide and set in a Petri dish lined with a wet paper towel. Fifty microliters of the stain solution was then applied evenly to the biofilm sample. The Petri dish was then covered and placed in the refrigerator for a

www.manaraa.com

few hours. After a couple of hours the sample was removed from the refrigerator and was gently rinsed with PSS to remove excess stain.

Confocal Microscopy

The confocal microscope revealed the stains that were taken up by the cells. Since the intact biofilm only allows a view of the top layer and the dye can penetrate through the biofilm, after inspecting the top layer of the biofilm, a set of forceps was used to scratch off a line of biofilm down to the glass, so that the lower layers of the biofilm could be inspected.

Another reason for removing a thin strip of biofilm to the glass was to provide a baseline for measuring the thickness of the biofilm. When measuring thicknesses it is easy to find a valley in the biofilm and mistake it for the bottom of the sample. By scratching a line down to the glass a more precise measurement can be made. Measurements of biofilm height were taken at 5 locations along scratches made in the biofilm. Additional biofilms were grown for different durations of time (4 hr, 8 hr, 12 hr) to see how time of growth influenced the thickness of the biofilm. An ANOVA with a Posthoc was performed to determine statistical difference between the thicknesses of the samples.

Viability After Bubble Stream Exposure

Recovery

To determine whether the impact of the bubble jet against the bacteria was substantial enough to rupture the cell membranes, a sample of the bacteria that had been removed from the biofilm after exposure to the bubble jet was collected, stained, and

www.manaraa.com

analyzed by confocal microscopy. Preliminary experiments have shown that a solution with a bacterial count of approximately 8 x 10^6 CFU filtered through a sterile 47 mm polycarbonate black filter (Isopore Membrane Filters, Millipore, Billerica, MA) with 0.2 μm pores will provide enough bacteria to get a countable image. To recover this quantity of bacteria, the concentration of bacteria in the artificial saliva after the biofilm exposure to the bubble jet was determined. The experimental chamber was filled with 700 mL of artificial saliva solution. A biofilm covered coverslip was prepared and mounted into the experimental chamber as previously explained. The biofilm was then exposed to a bubble jet with a velocity of 15 m/s, gas fraction of 0.52, and a median bubble diameter of 291 μm at 45º for 5 seconds. To calculate the quantity of *S. mutans* removed from the coverslip, the calculated total CFU per coverslip was divided by the area of perturbed biofilm on the coverslip. The calculated average concentration of *S. mutans* in the chamber suggested that 14 mL of the liquid in the chamber would provide enough bacteria for a countable image. After gentle stirring of the solution in the chamber, this volume was pipetted from the chamber and into a beaker.

Staining and Microscopy

Then, 42 μL of SYTO 9 and 42 μL of propidium iodide solution were added, and the solution was gently swirled and then covered with aluminum foil and placed in the refrigerator for a few hours. The solution was then vacuum-filtrated through a polycarbonate black filter, following which the filter was placed onto a glass slide and visually analyzed through an epifluorescence microscope.

www.manaraa.com

www.manaraa.com

CHAPTER 5

RESULTS

Biofilm Viability

The viability of the biofilm was tested to determine if collisions with bubbles would kill the bacteria. From the drop plate method the average number of colony forming units (CFU) per coverslip before exposure to a fluid stream was 4.37×10^8 CFU/cm^2. The distribution of viability was assessed by staining with fluorescent Live/Dead stain. The fluorescence of the biofilm under the confocal microscope showed that more than 99% of the bacteria were viable at the surface. A set of tweezers was then used to scrape the biofilm down to the glass surface. Upon inspection of the underlying layers of biofilm, the biofilm was also observed to be more than 99% viable. The confocal microscope was also used to measure the thickness of the biofilm along a line scratched into the biofilm. The thickness was measured at 5 locations on 2 different coverslips with an average thickness of 40 μm and a standard deviation of 9 μm. Figure 10 shows an image taken of a vertical plane of the sample.

A biofilm that was exposed to a bubble stream was also stained and examined to determine the viability of the bacteria at the edge where the biofilm was removed. Again more than 99% were viable. The solution containing the biofilm removed by the bubble jet was sampled, stained, vacuum filtered, and examined under the microscope. More of the biofilm in this sample was dead than the biofilm observed in the previous samples, but more than 90% were still alive. It is believed that the biofilm is not killed during the

www.manaraa.com

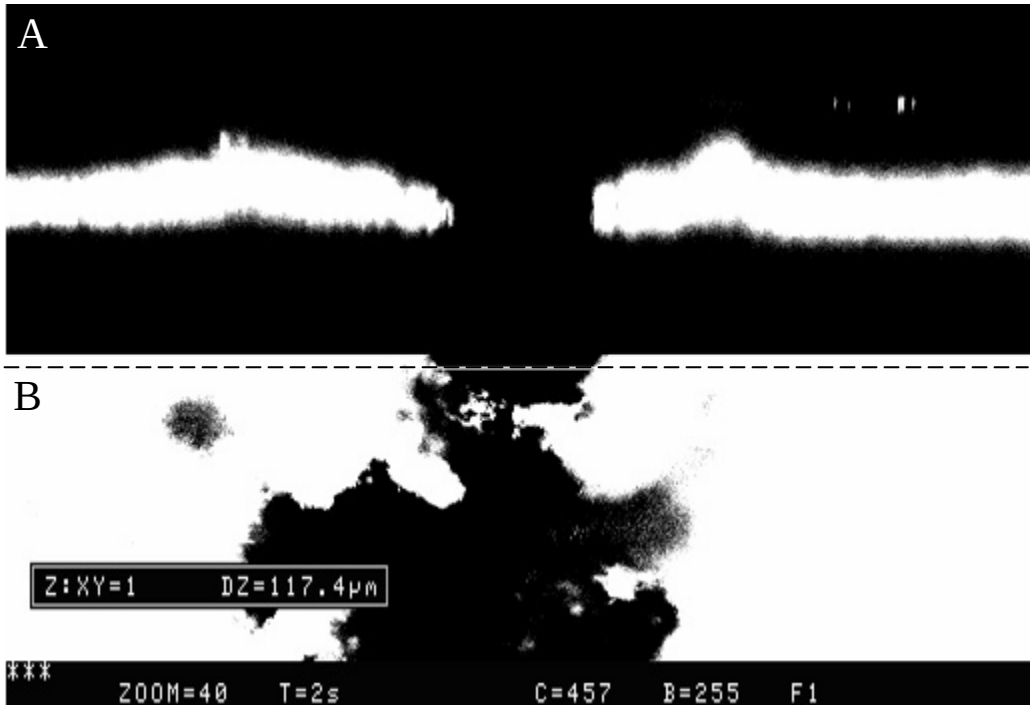

Figure 10. A) An image of a vertical plane in the biofilm taken with a confocal microscope. The biofilm is white. The black space in the middle of the image is where the biofilm was removed by scratching with tweezers. B) An image of a horizontal plane through the biofilm in the region where the biofilm has been removed from the middle of the sample, shown in black. The dashed line (– – –) indicates the position of the image of the vertical plane shown in part A.

removal process. Confocal microscopy showed no sign of damaged cells on the coverslip along the edge where the biofilm was removed. The cells along this edge would have also been killed if the bacteria removed were being killed. The small decrease in viability of the bacteria removed and then filtered could be attributed to the stresses caused by the homogenization process or the vacuum filtration.

Correlations for Stream Velocity, Gas Fraction, and Bubble Size as Functions of System Pressure and Pressure Difference

The data gathered for the stream velocity, gas fraction, and bubble sizes taken at different total system pressures and pressure differences (from the gas side to the total process) were analyzed with the aid of Dr. Dennis Eggett (Department of Statistics,

www.manaraa.com

Brigham Young University) and a statistical analysis software package called SAS (SAS Institute, Cary, North Carolina). The linear model for velocity as a function of the two different pressures is

$$Vel = A \cdot Line + B \cdot Diff + C \cdot Line \cdot Diff$$

where Vel = total stream velocity

$Line$ = total system pressure

$Diff$ = pressure difference between the total pressure and the gas pressure

and A, B, and C are constant. A regression of the data gave the best values for A, B, and C:

A = 1.343 m/(s x psi)

B = -2.498 m/(s x psi)

C = -0.037 m/(s x psi^2)

The regression coefficient R^2-value for this model is 0.584. The total system pressure and the pressure difference were very significant in this model ($p < 0.01$); however, the interaction between these two parameters was not very strong ($p < 0.15$).

A simple linear model for predicting the gas fraction of the stream is

$$Gas = D \cdot Line + E \cdot Diff + F \cdot Line \cdot Diff$$

where Gas = gas fraction in the stream, and the best fit parameters are:

D = 0.064/psig

E = -0.038/psid

and F = -0.005/(psig x psid)

www.manaraa.com

The regression coefficient R^2-value for the gas fraction model is 0.382 and the p-values for this model are found in Table 2. The p-value is the probability that the observation of the effect of a given parameter in the model occurs randomly.

Table 2. P-values of parameters for gas fraction model.

Parameter	p-value
Line	<0.0001
Diff	0.4313
Line x *Diff*	0.0002

These p-values indicate that total line pressure is the most significant factor in determining the gas fraction, and that the combination of total line pressure and pressure drop across the air side needle valve are likely to be significant as well. However, the differential pressure drop by itself has little if any significance on the gas fraction.

The linear model for the gas fraction in the fluid stream and the median bubble diameter are very similar to the velocity and gas fraction models, with the exceptions being that the coefficients are different and that the value for the bubble diameter is actually a rank which is checked against a chart to determine the diameter.

$$Size = G \cdot Line + H \cdot Diff + J \cdot Line \cdot Diff$$

where *Size* = rank of horizontal bubble diameter

G = 18.519/psig

H = 32.283/psid

and *J* = -2.052/(psig x psid)

for the bubble diameter. The F-values and p-values for each parameter and the cross-interaction are shown in Table 3.

www.manaraa.com

Table 3. P-values for bubble diameter model.

Parameter	F-values	p-value
Line	1497.10	<0.0001
Diff	31.95	<0.0001
Line x *Diff*	145.08	<0.0001

In this case each parameter and the cross-interaction are significant in determining the median bubble diameter.

Phase 1: Influence of Stream Velocity, Gas Fraction, and Bubble Size on Biofilm Removal

Biofilm removal data for the different combinations of bubble stream velocity, gas fraction, and median bubble size were analyzed with the aid of Dr. Eggett and the SAS software package. The data show that there is not just one parameter that is the most influential in biofilm removal, but that all of the parameters are interrelated and affect the amount of removal.

Table 4. P-Values of parameters for biofilm removal.

Parameter	p-value
Velocity	0.0124
Gas Fraction	0.0210
Bubble Size	0.0108
Velocity x *Bubble Size*	0.0148
Gas Fraction x *Bubble Size*	0.0342

The optimized p-values in Table 4 show a greater likelihood that the removal of biofilm is related to the stream velocity, gas fraction, and median bubble diameter.

www.manaraa.com

However, there is not one parameter that is significantly dominant. Hence, the experiments for phase 2 had to be performed for all of the variables.

Phase 2: Variation of Dominant Parameters

Bubbles vs. Liquid Only

Before determining whether bubble velocity, size, or the fraction of gas in the stream was the most significant factor in removing biofilm, it was important to determine if the presence of bubbles in the liquid jet removed more biofilm than a stream without them. Figure 11 shows that the stream with bubbles (right) removed more biofilm than the stream without bubbles (left). (39)

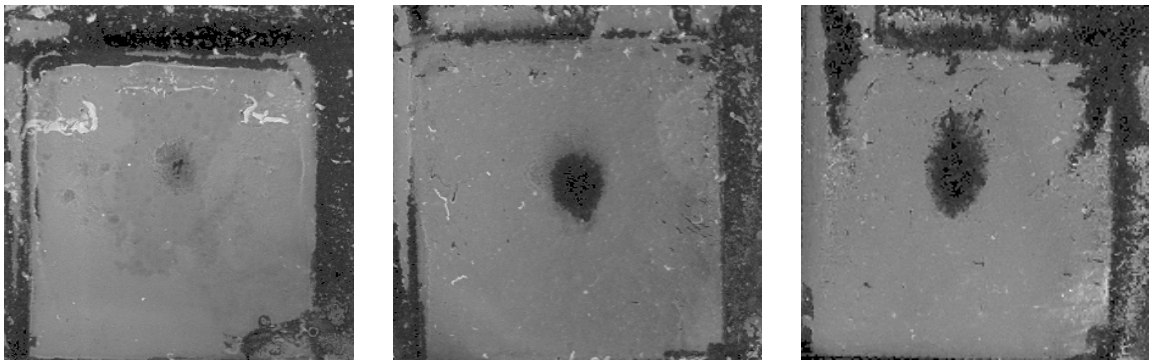

Figure 11. Biofilm of *S. mutans* after exposed to liquid jet stream. (Left) Biofilm exposed to a 3.3 m/s stream without bubbles. (Center) Biofilm exposed to a stream of bubbles. The velocity of the stream was 3.3 m/s, the gas fraction was 0.29, and the average bubble diameter was 231 μm. (Right) The velocity of the bubble stream was 7.3 m/s, gas fraction was 0.30, and the average bubble diameter was 246 μm.

At a low velocity of only 3.3 m/s, the addition of bubbles to the liquid stream removed about twice the biofilm than without bubbles. For example, the liquid stream alone removed an average of 27 ± 9 % of the biofilm in the affected area, while the jet with bubbles removed about 56 ± 5 %. As the velocities of the flow in the streams

www.manaraa.com

increased, the amount removed, both with or without bubbles, increased. However, at higher velocities, the addition of bubbles did not increase removal. For example at 11 m/s, the average amount removed was 81 ± 8 % and 61 ± 5 %, without and with bubbles, respectively. However, velocities of this magnitude are over an order of magnitude greater than those produced by commercially available toothbrushes. (11) In the velocity range at which toothbrushes currently propel bubbles, bubbles assist in biofilm removal.

Biofilm Removal with Bubbles

The removal of biofilm is not a simple function with dependence upon one variable; rather it is dependent upon the stream velocity, the gas fraction, and the bubble size. The data of the percentage removed as a function of these three variables was analyzed statistically using SAS software and fit to a linear model with cross interactions terms. After removing all terms that had a $p > 0.03$, the remaining terms in the model were the stream velocity, the gas fraction, the bubble size, and the interactions between velocity and gas fraction and between velocity and bubble size. (The p-values for these parameters are found in Table 5.) The resulting mathematical model that best predicted the depth of removal was

$$R = A \cdot Vel + B \cdot Gas + C \cdot Size + D \cdot (Vel \cdot Gas) + E \cdot (Vel \cdot Size)$$

where R = average fraction of biofilm thickness removed within the region of bubble impact

Vel = velocity

Gas = gas fraction

$Size$ = bubble diameter size

and A, B, C, D, and E are constants with the following regression values:

www.manaraa.com

A = 8.064 s/m

B = -113.8

C = 0.3806 /μm

D = 12.85 /μm

E = -0.04836 s/m/μm.

This model has a regression coefficient R^2-value of 0.975 (see Appendix B). Figure 12 illustrates how the data compare with predicted values from the mathematical model.

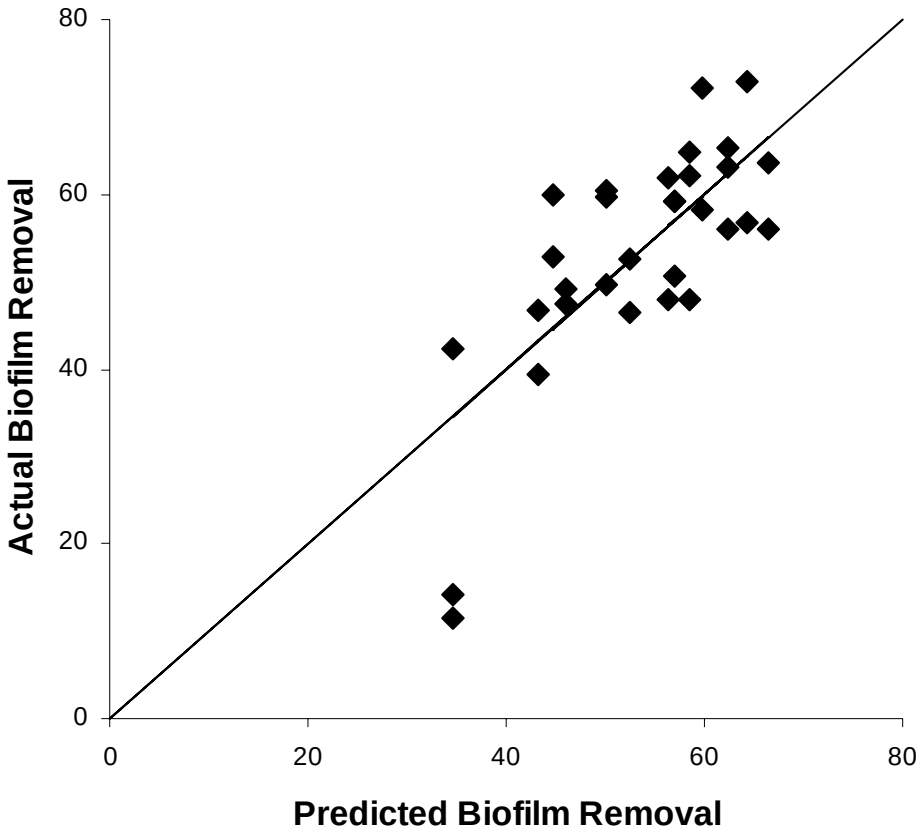

Figure 12. Plot comparing actual biofilm removal data (individual points) to the predicted biofilm removal values from the mathematical model. The solid line is a guide to the eyes showing a 45º line.

www.manaraa.com

Table 5. P-values of the parameters used in the statistical model

Parameter	p-value
Velocity	0.0002
Gas Fraction	0.0044
Bubble Size	<0.0001
Velocity x *Bubble Size*	0.0252
Gas Fraction x *Bubble Size*	0.0002

Biofilm Removal as a Function of Velocity

To show how the removal of biofilm is related to the velocity of the stream, the partial derivative of the fraction removed with respect to velocity can be calculated:

$$\frac{\partial R}{\partial Vel} = A + D \cdot Gas + E \cdot Size = 8.064 + 12.85 \cdot Gas - 0.04836 \cdot Size$$

This equation shows that velocity affects biofilm removal in a complex manner. For example, if the gas fraction is 0.30 and the bubble diameter is 246 μm or less, higher velocities will remove more biofilm ($\partial R / \partial Vel$ is positive). On the other hand, if the gas fraction is 0.30 but the bubble diameter is greater than 246 μm, the model predicts that removal decreases as velocity increases.

Figure 11 shows the images of two biofilms after being exposed to bubble streams of 3.3 and 7.3 m/s. The gas fraction for these two biofilms is approximately 0.30. Since the bubble diameter is not greater than 246 μm, the model predicts that the removal of biofilm should be greater at the higher velocity.

Figure 11 shows that, in fact, more biofilm is removed from the sample exposed to the higher velocity stream.

www.manaraa.com

Biofilm Removal as a Function of Gas Fraction

The effect of gas fraction on the amount of biofilm removed is difficult to determine due to the error in the coefficients associated with gas fraction. Though there is much scatter in the data, gas fraction is still a statistically significant parameter. The partial derivative of biofilm removal with respect to gas fraction is

$$\frac{\partial R}{\partial Gas} = B + C \cdot Vel = -113.8 + 0.3806 \cdot Vel$$

Within the range of velocities used in these experiments (2 to 12 m/s), this equation suggests that an increase in gas fraction will reduce the amount of biofilm removed for velocities less than 8.85 m/s.

Figure 13 shows the difference between two biofilms that have been exposed to bubble streams of differing gas fractions. The image on the left is of a biofilm that has been exposed to a large gas fraction of 0.48, whereas the biofilm shown on the right was exposed to a stream with a gas fraction of 0.05. Though the amount of removal is greater for the stream with the lower gas fraction, the difference in removal is small relative to the order of magnitude difference in gas fraction.

Biofilm Removal as a Function of Bubble Size

The partial derivative of the amount of biofilm removal with respect to average bubble diameter is

$$\frac{\partial R}{\partial Size} = C + E \cdot Vel = 0.3807 - 0.04836 \cdot Vel$$

This equation shows that if the velocity is greater than 7.87 m/s, the amount of removal increases as bubble size decreases.

www.manaraa.com

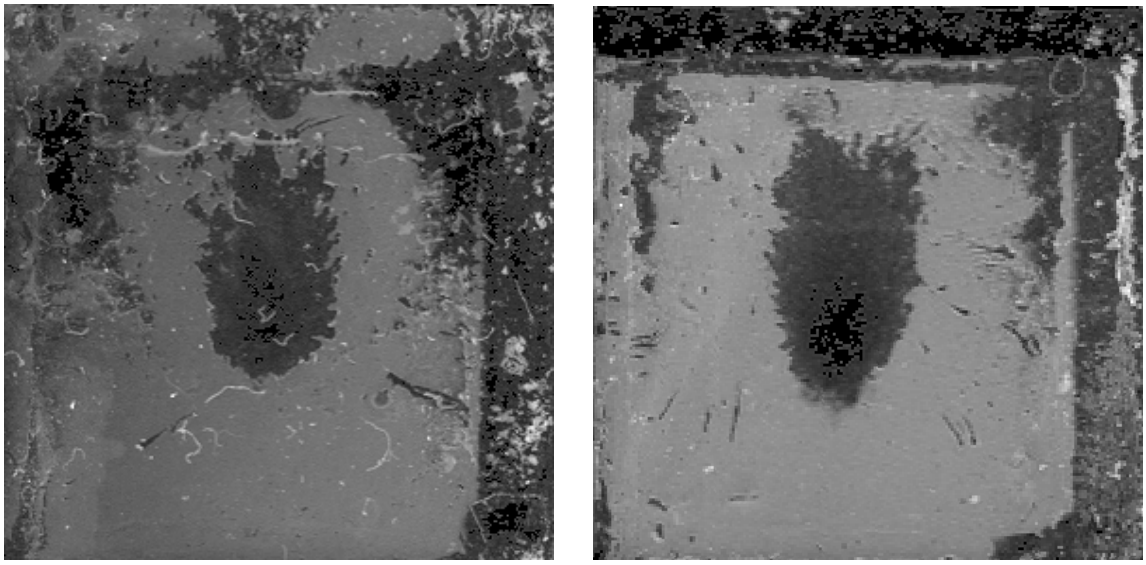

Figure 13. Biofilms after exposure to bubble streams of different gas fractions. Left, velocity of the stream was 6.7 m/s, gas fraction was 0.48, and the bubble diameter was 205 μm. Right, velocity of the stream was 6.5 m/s, gas fraction was 0.05, and the bubble diameter was 200 μm.

Figure 14 displays the images of two biofilms that have been exposed to bubble streams with similar gas fractions and velocities less than 7.87 m/s. As predicted, there is greater biofilm removal on the coverslip that was exposed to the larger bubbles (see Figure 14, left).

Phase 3: Effect of Angle

Figure 15 shows the thickness percentage of biofilm removed after 5 seconds of exposure to a bubble stream at 3 different angles. The data show that the angle at which the bubbles impinge upon the biofilm has no significant effect upon the amount removed. (40) Figure 16 shows the shape of the removal differs as the angles change, becoming more narrow and elongated at low angles and more rounded at high angles. However, the amount of total removal, deep removal, and area of removal are the same.

www.manaraa.com

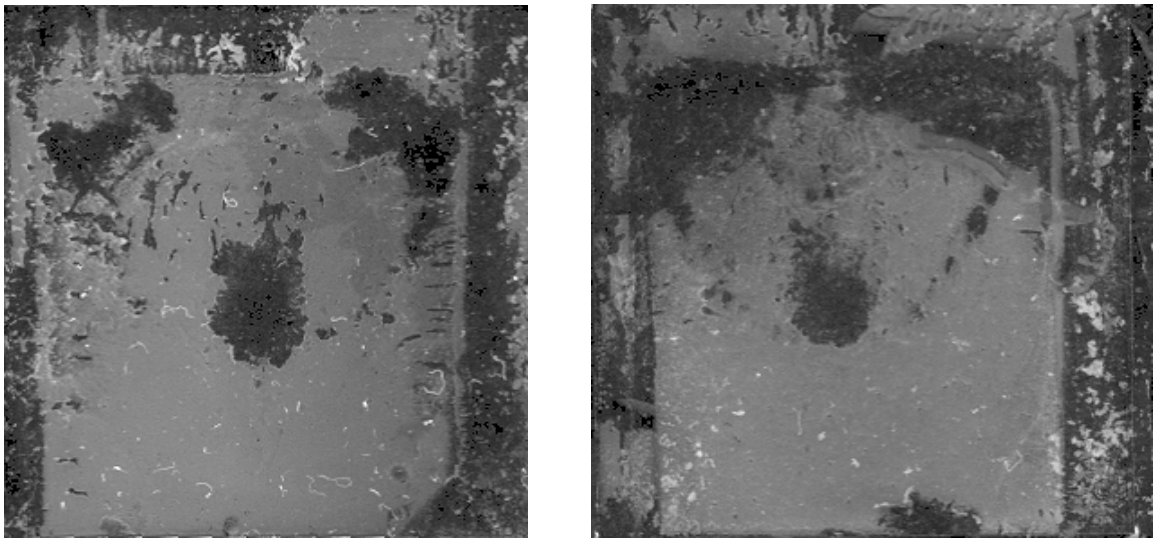

Figure 14. Biofilms after exposure to bubble streams of different bubble sizes. Left, velocity of the stream was 6.8 m/s, gas fraction was 0.42, and the bubble diameter was 246 μm. Right, velocity of the stream was 6.8 m/s, gas fraction was 0.45, and the bubble diameter was 135 μm. The black spots in the top corners are where biofilm had been removed by bubbles that had been trapped in the lip of the fixture clipping the coverslip in place.

It was originally hypothesized that bubbles that impinged against the biofilms at more direct angles (45º) would remove more biofilm than those that impinged at more glancing angles (5º). From 3-dimensional geometry it is apparent that the area of a surface exposed to a column of fluid is greater at glancing angles than at more direct angles. (See Figure 17) Yet, when the biofilms were exposed to the column of bubbles at different angles the amount of removal was the same. It is postulated that this is because the different samples were exposed to the same number of bubbles. Since the bubbles impinging at the more glancing angles were spread over a larger area, there was a lower bubble density. So less biofilm was removed per area. These experiments support the hypothesis that the angle at which the bubbles impinge against the biofilm does not affect the amount of biofilm removed, but it is actually the number of bubbles that collide with

www.manaraa.com

the biofilm that determine the amount of removal. Thus a bubble stream does not have to be perpendicular to the surface of the biofilm to effectively remove it.

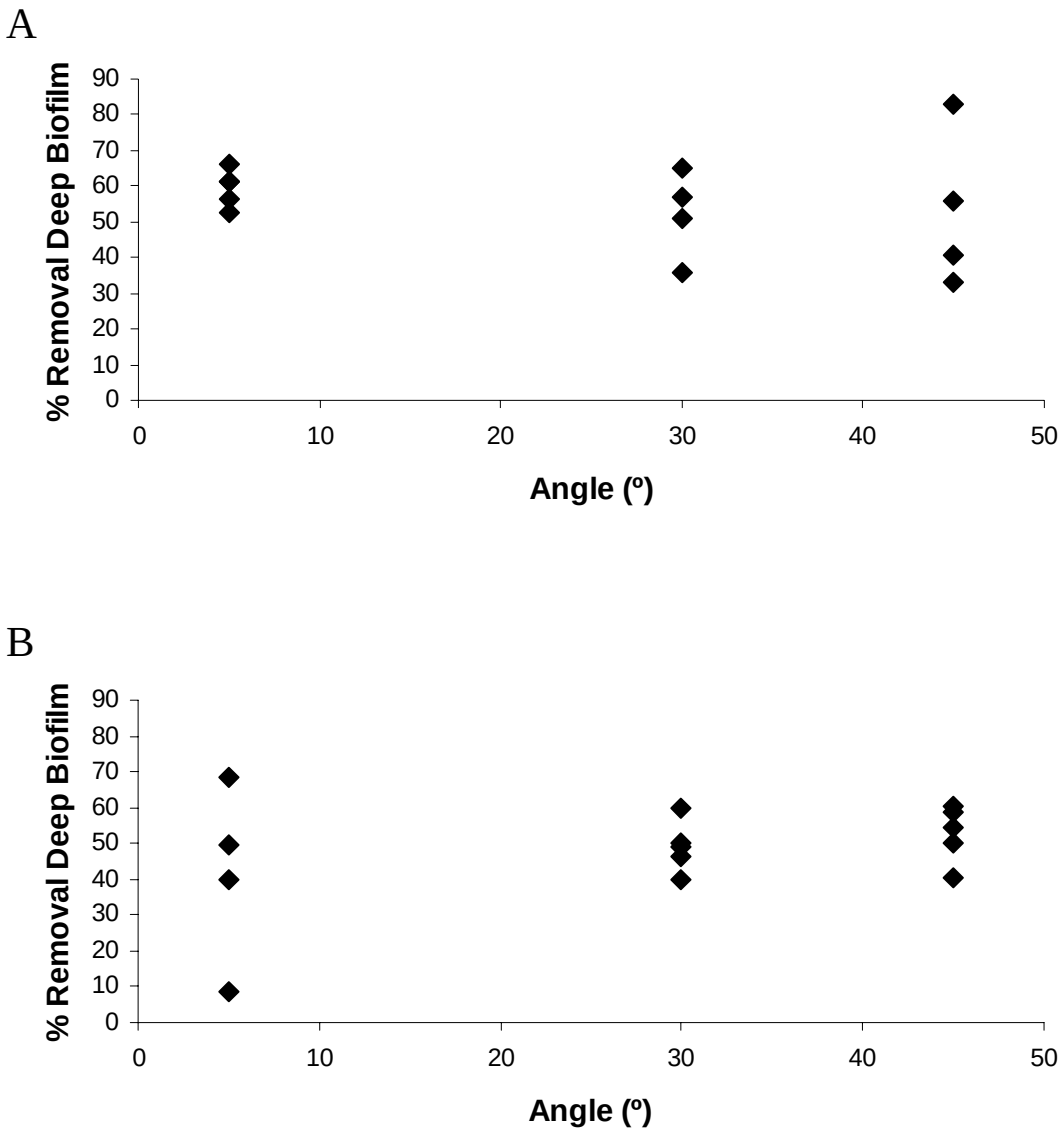

Figure 15. Amount of biofilm removed by bubbles at different contact angles. A) Bubble stream velocity is 1.5 m/s, fraction of gas in the stream is 0.04, and the median bubble diameter is 205 μm. B) Bubble stream velocity is 4.3 m/s, fraction of gas in the stream is 0.41, and the median bubble diameter is 205 μm.

www.manaraa.com

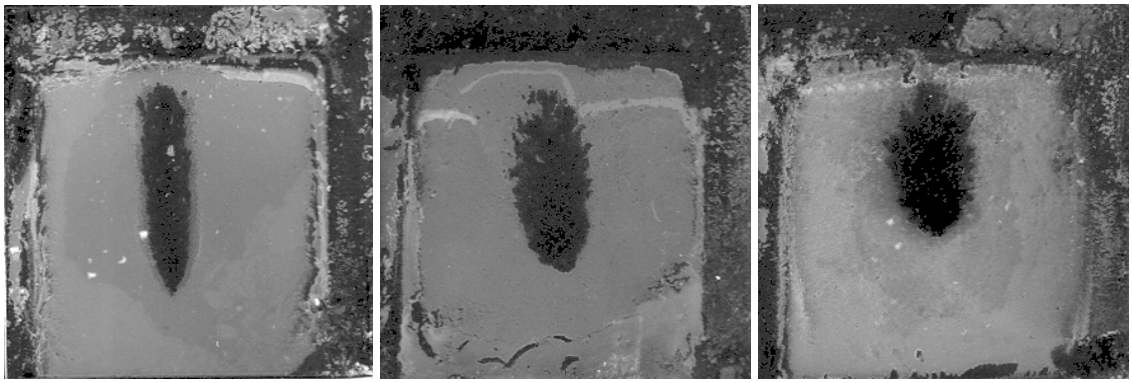

Figure 16. Removal of biofilm by bubbles at different angles of impact. All bubble streams had a velocity of 1.5 m/s, a gas fraction of 0.04, and a median bubble diameter of 205 μm. The angles of impact were (Left) 5º, (Center) 30º, and (Right) 45º.

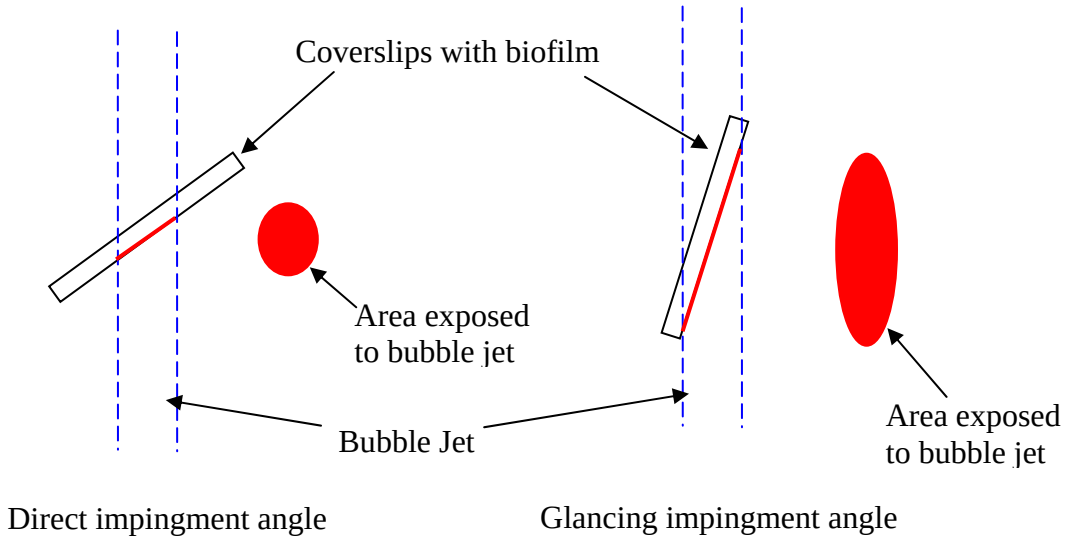

Figure 17. Comparison of surface areas in a column of fluid at different angles of exposure.

Phase 4: Effect of Sound

Figure 18 shows paired comparisons of *S. mutans* biofilm removal by bubble streams with and without the addition of 1 TBE of acoustic pressure. Figure 19 shows

www.manaraa.com

the same comparison but at a larger gas fraction and flow rate. As these figures indicate, and as all the numerical data (amounts of removal) indicate, there is no significant difference in either deep removal or total removal by a bubble stream caused by the absence or presence of sonic phenomena equivalent to that produced by the *Elite* toothbrush.

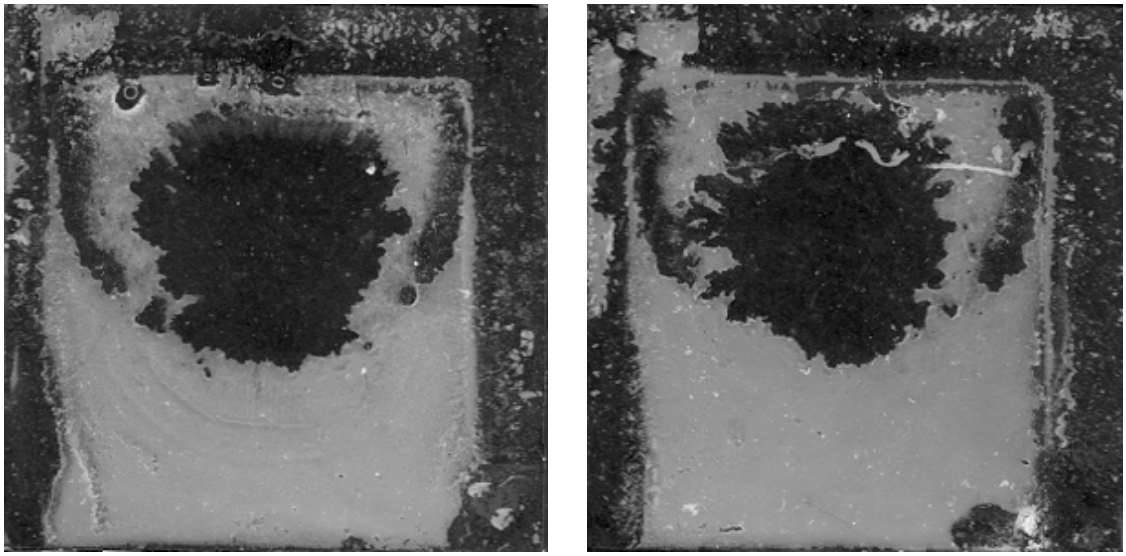

Figure 18. Biofilm after exposure to bubble stream. The border of disturbed biofilm that exists on the top and the sides is caused by the apparatus to which the slip is mounted. Both biofilms have been subjected to a bubble stream with the following properties: Velocity = 10.8 m/s, Gas fraction = 0.27, Bubble Diameter Size = 205 μm, Impact angle 45°. The image of the biofilm on the left has also been exposed to sound with the sound frequency = 260 Hz, and power = power output of Sonicare *Elite* Toothbrush on High. The biofilm on the right has not been treated with sound.

Figure 20 shows the removal, or lack thereof, caused by 1 TBE in the absence of any fluid flow or bubbles. This image is compared to the lack of removal of biofilm in a sham experiment in which the biofilm was placed in the holder in the chamber, and removed, but without any fluid flow or application of sound. The handling process itself removes some biofilm from the edges of the cover slip, but not any measurable amount

www.manaraa.com

from the center test area; neither does application of sound alone remove any measurable amount of biofilm from the test area.

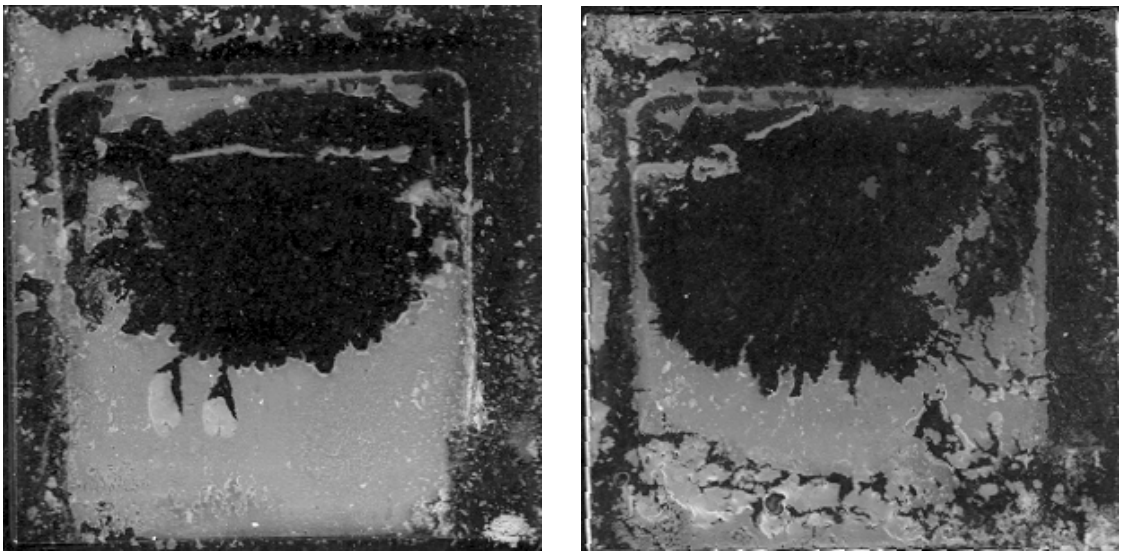

Figure 19. Biofilms of *S. mutans* after 5 sec. exposure to bubble stream at an impact angle of 45º, velocity is approx 12 m/s, gas fraction is approximately 0.65, bubble diameter is on the order of 300 μm. The one on the right has sound at the same frequency and intensity as that produced from the Sonicare *Elite*, while the one on the left has had no sound added.

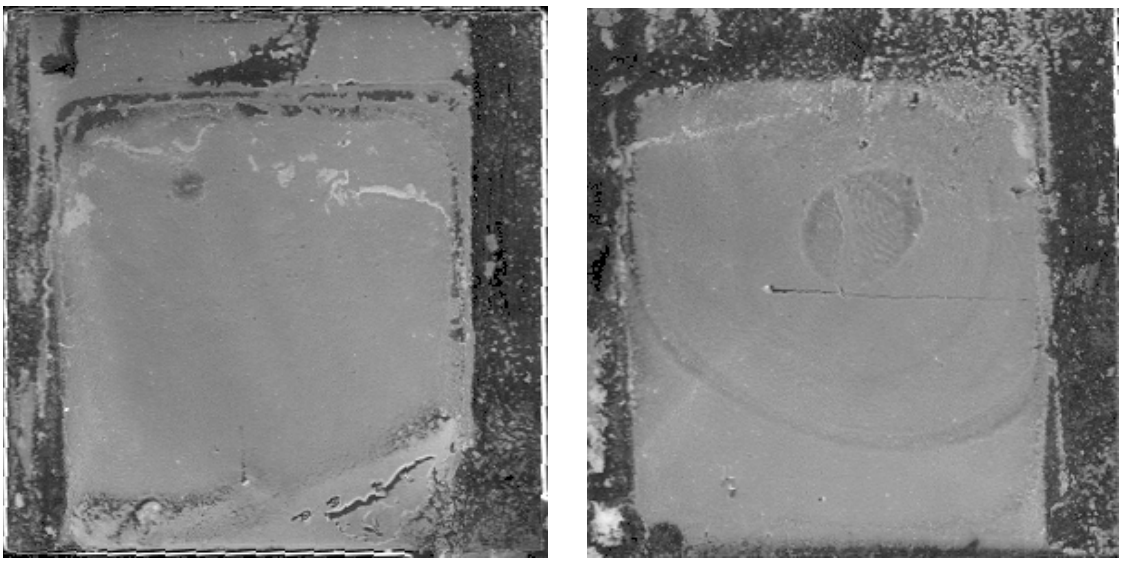

Figure 20. The image on the left was placed into the mounting apparatus and exposed to the sound of the same intensity and frequency emitted by the Sonicare *Elite* toothbrush. The image on the right was mounted into the apparatus, but no sound or bubbles were applied. (Note: The rings on the image were caused when the cover slip was mounted onto a Petri dish for imaging.)

www.manaraa.com

A few experiments were performed in which the acoustic intensity and frequency were increased to examine whether these more severe conditions would impact biofilm removal. In experiments at 260 Hz and 2 TBE there was no additional removal attributed to the addition of the sound. Likewise in experiments employing 520 Hz and 0.2 TBE there was no additional removal attributed to sonic exposure. Because of the lack of removal by sound at these extreme conditions, the full matrix of experiments at lesser frequencies and intensities was not completed.

McInnes claims that sound reduces adhesion of planktonic bacteria to surfaces and to cause damage to fimbria on exposed cells. (26, 27) However, the application of audible sound at the intensity of a toothbrush was not shown to remove biofilm, or to enhance the removal of biofilm in the presence of a bubble stream. Although it is possible for sonic pressure waves to remove bacteria, if this removal occurred in this research, it was so small that the removal contributed by sound was negligible compared to the removal caused by the action of bubbles striking the surface of the biofilm. Likewise, Stoodley *et al.* have shown that the removal caused by bubble and fluid action is less than the removal caused by direct contact with the bristles of the toothbrush. (11, 25)

There still exists the observation that intense sound can remove small amounts of biofilm. (12) However, the intensities used were much greater than those produced by any sonic toothbrushes currently available. There are also reports of intense ultrasound removing biofilm, most likely through cavitation phenomena. (41, 42)

www.manaraa.com

Phase 5: Video Photography of Biofilm Removal

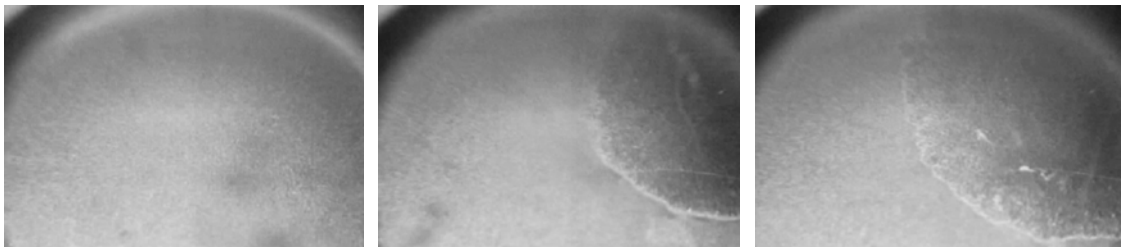

Figure 21. Video frames of *S. mutans* exposed to a bubble jet with a velocity of 12.1 m/s, gas fraction of 0.34 and median bubble diameters of 261 microns. The images are taken at different times of exposure to the jet. From left to right, t = 0 s, 0.1 s, and 1.0 s.

By videotaping experiments in real time, it was possible to observe the bubbles plucking the biofilm off of the glass surface. It was observed that as the jet first comes into contact with the biofilm a large quantity is rapidly removed near the center of the jet. Continued exposure to the jet removes more biofilm, increasing the radius of biofilm removed with time; however, the rate of removal decreases rapidly with time. (See Figure 21.)

www.manaraa.com

CHAPTER 6

MATHEMATICAL MODEL OF BIOFILM REMOVAL

Mathematical Model

To assist in the analysis of dynamic biofilm removal, a mathematical model was constructed. (43) In developing this model, the following assumptions were made.

1. All bubbles have the same footprint area.
2. Each bubble strike removes a constant fraction *f* of biofilm within the footprint.
3. At an initial time ($t = 0$), the thickness of the biofilm is uniform throughout the sample.
4. The sample substrate is sufficiently wide that there are no edge effects.
5. Bubbles hit the biofilm only once.

The amount of biofilm at radius *r* and time *t* is given by $A(r,t)$ and has dimensions of CFU per area. As the bubbles strike the biofilm-coated surface they remove a portion of the biofilm. Initially, it is assumed that the amount of biofilm removed at a given radius *r* is proportional to the remaining amount ($A(r,t)$), the footprint of the bubbles ($\mathcal{A}$), the removal fraction (f), and the local flux of bubbles that collide with the biofilm ($N''(r)$), which is a function of radial position (r) from the center of the jet. The change in the amount of biofilm with respect to time is given by

$$\frac{-dA(r,t)}{dt} = A(r,t)\mathcal{A}fN''(r) \qquad (1)$$

The derivative is negative because the remaining amount of biofilm decreases with time.

www.manaraa.com

To solve this equation we must first determine the local bubble flux $N''(r)$, which is related to the total number of bubbles leaving the needle per unit time ($\dot{N}_0$).

Since $N''(r)$ is a function of radial position from the center of the jet, the total number of bubbles leaving the jet is the integral of the local flux of bubbles:

$$\dot{N}_0 = \int_0^{2\pi} \int_0^{\infty} N''(r) r dr d\theta \qquad (2)$$

Unfortunately, the form of the bubble distribution ($N''(r)$) is not known *a priori.* Work by Iguchi *et al*. reports that the radial distribution of bubbles in a liquid-gas stream follows a Gaussian distribution, when the gas fraction is less than 50%. (44) We have applied this distribution, as well as a decaying exponential function, to the mathematical model to test which distribution fits the data best. The flux for a general distribution would be defined as follows

$$N''(r) = N' \cdot G(r) \qquad (3)$$

where $G(r)$ is the bubble distribution function (either Gaussian or decaying exponential in this example) and N' is a scaling factor to scale the distribution to the local flux. The local fluxes for a Gaussian distribution and a decaying exponential function are

$$N''(r) = N' \frac{e^{\frac{-1}{2}\frac{r^2}{\sigma^2}}}{\sigma\sqrt{2\pi}} \qquad \text{(Gaussian)} \qquad (4a)$$

$$N''(r) = N' \cdot e^{-kr} \qquad \text{(decaying exponential)} \qquad (4b)$$

where σ is one standard deviation of the Gaussian function, and k indicates the tightness of the bubble dispersion. For example, when k is large the bubbles are clustered tightly near the center of the jet. The value of $1/k$ is a characteristic length of the bubble distribution.

www.manaraa.com

When the distribution function for $N''(r)$ is substituted into Equation 2 and the distribution is integrated from 0 to ∞, the equation becomes

$$\dot{N}_0 = \int_0^{2\pi} \int_0^{\infty} N' \cdot G(r) r dr d\theta \tag{5}$$

$$\dot{N}_0 = 2\pi N' \int_0^{\infty} r G(r) dr \tag{6}$$

$\dot{N}_0$ is also equal to the total fluid flow rate (Q) multiplied by the volume fraction of gas in the stream (f_g) and divided by the average bubble volume ($\overline{V_b}$).

$$\dot{N}_0 = \frac{Q f_g}{\overline{V_b}} \tag{7}$$

$\dot{N}_0$ can easily be calculated, and then Equation 6 can be integrated and rearranged to solve for N'. For the Gaussian and the decaying exponential functions, the values of N' are respectively

$$N' = \frac{\dot{N}_0}{\sigma\sqrt{2\pi}} \tag{8a}$$

$$N' = \frac{\dot{N}_0 k^2}{2\pi} \tag{8b}$$

We can now combine Equations 1, 4, and 8 and then integrate to obtain

$$A(r,t) = \exp\left[-\not{A} f \dot{N}_0 \frac{e^{\frac{-1\, r^2}{2\, \sigma^2}}}{4\pi\sigma^2} t - C \right] \tag{9a}$$

$$A(r,t) = \exp\left[-\not{A} f \dot{N}_0 \frac{k^2 \cdot e^{-kr}}{2\pi} t - C \right] \tag{9b}$$

www.manaraa.com

where C is a constant of integration that can be obtained from the initial condition that when all of the biofilm is present, at $t = 0$. Because the biofilm is uniform at $t = 0$, the original amount of biofilm is A_0 for all values of r. Therefore

$$C = -\ln(A_0) \tag{10}$$

Now we can substitute C into our equations to yield

$$\frac{A(r,t)}{A_0} = \exp\left[-\mathscr{A}f\dot{N}_0 \frac{e^{\frac{-1}{2}\frac{r^2}{\sigma^2}}}{4\pi\sigma^2} t\right] \tag{11a}$$

$$\frac{A(r,t)}{A_0} = \exp\left[-\mathscr{A}f\dot{N}_0 \frac{k^2 \cdot e^{-kr}}{2\pi} t\right] \tag{11b}$$

It is difficult experimentally to measure the removal of the amount of biofilm at a radius r as a function of time from the video microscopy. However, from the video recordings, we could easily measure the radius at which the glass slide was cleaned of nearly all the biofilm. We can invert Equation 11 to obtain the radius at which 95% removal occurs, calling this R_{95}(t)

$$R_{95}(t) = \sqrt{-2\sigma^2 \ln\left[\frac{2\pi\sigma^2}{-\mathscr{A}f\dot{N}_0 t}\ln(0.95)\right]} \tag{12a}$$

$$R_{95}(t) = -\frac{1}{k}\ln\left[\frac{2\pi}{-\mathscr{A}f\dot{N}_0 k^2 t}\ln(0.95)\right] \tag{12b}$$

These two equations were fit to the biofilm removal data obtained from the video recording.

When the data are compared to the Gaussian distribution and the decaying exponential function, we see that both distributions fit the data quite well (see Figure 22).

www.manaraa.com

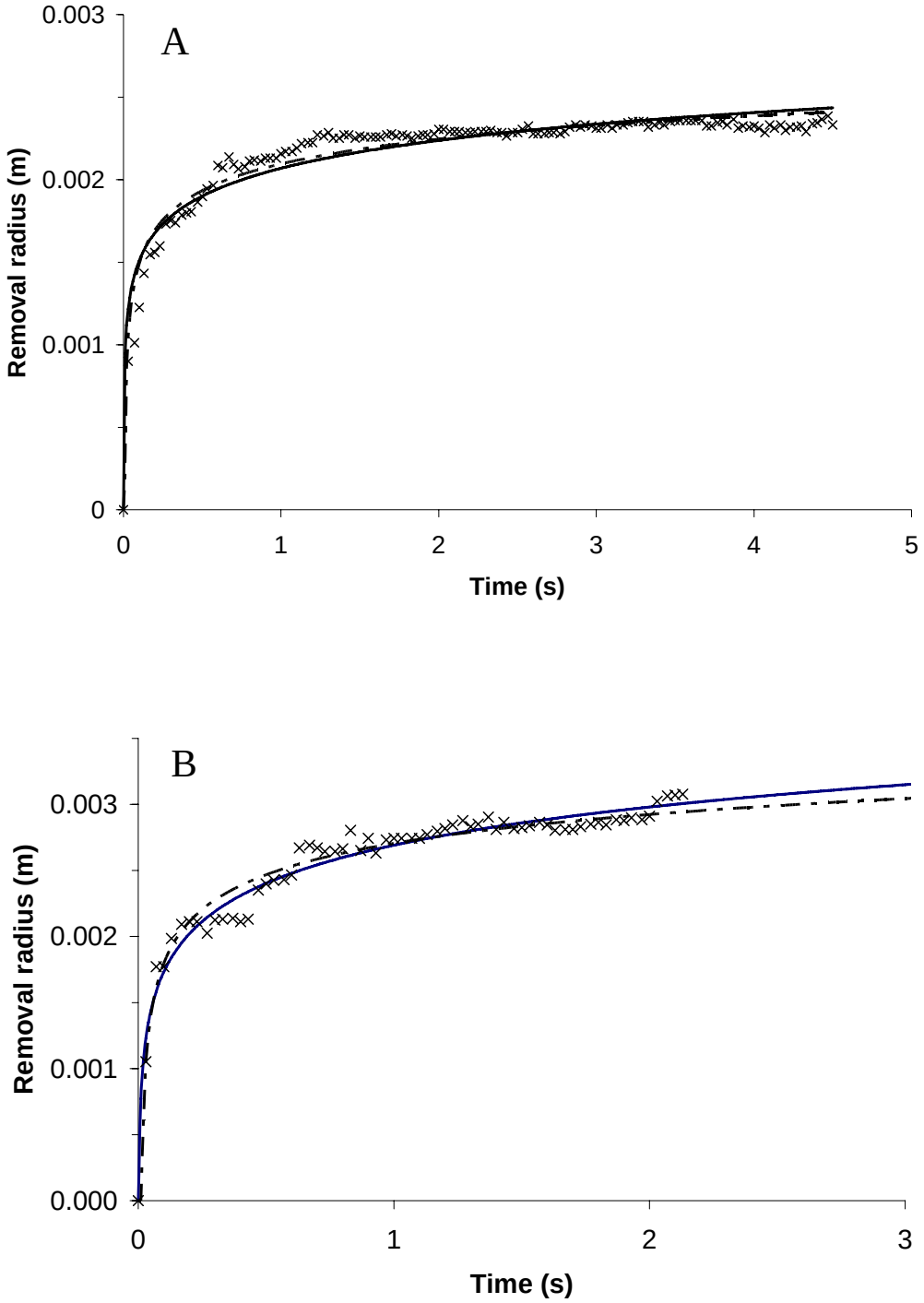

Figure 22. Plots of the size of the radius of the area of 95 % of the biofilm removed (x) versus the time of exposure to a bubble jet. The mathematical models are also plotted as removal radius versus time, where the Gaussian model and the decaying exponential model are represented as (— – —) and (———), respectively. The bubble jet properties were A) velocity = 12.0 m/s, gas fraction = 0.34, and median bubble diameter = 261 μm. B) velocity = 10.1 m/s, gas fraction = 0.55, and median bubble diameter = 257 μm.

www.manaraa.com

In regressing the coefficients to the data, the value f (the fraction removed within the footprint) for the Gaussian model is 0.40 and for the decaying exponential model ranges between 0.19 and 0.65. This seems reasonable that f is a number between 0 and 1. From the regressed value of f, it appears that the effectiveness of an individual collision is on the order of 40% removal. The value of f is based on the assumption that the bubble footprint $\mathscr{A}$ is equal to the cross sectional area of the spherical bubble. However, an alternative explanation is that the bubble removes all the biofilm within the contact area, but the contact area is less than the area with the diameter equal to the bubble diameter. In this scenario of 100% removal, the footprint diameter for a bubble with a diameter of 261 μm would be 162 μm and 211 μm for the Gaussian and exponential models respectively. In this same scenario, but with a bubble diameter of 257 μm, the footprint diameter would be 162 μm and 113 μm, respectively.

The values for σ and $1/k$ were optimized using a least-squares regression, and range from 1 to 2 mm and 0.2 to 0.4 mm, respectively. They were found to be dependant upon the conditions of the bubble jet. The values for σ appear reasonable because 99% of the bubbles should impinge upon the biofilm within a distance of 3σ from the center of the jet, and the cleaned area is usually 1 cm in diameter. It is postulated that these parameters are dependant upon the gas fraction (and thus the bubble density) of the bubble jet. More tests would be required to determine whether gas fraction has a statistically significant effect on the values of σ and $1/k$.

www.manaraa.com

Discussion of Model

This model was founded upon 5 key assumptions, whose validity should be considered. The first assumption, that all bubbles have an equal footprint, is not strictly valid because there is a distribution of bubble sizes in the actual stream. However, there is an average size, and thus an average area of removal per collision, assuming that f is constant for each collision. This latter assumption assumes that the relative deformation of the bubble during contact is independent of bubble size, a reasonable assumption because they are equally compressible and nearly equally deformable. The next assumption, that the thickness of the biofilm is uniform at $t = 0$, is not an accurate representation of biofilms. Measurements of biofilm thickness show that biofilms of *S. mutans* are not uniform in thickness. However, the standard deviation in the thickness of a biofilm is only 23%. The assumption that edge effects can be neglected due to the sufficiently wide substrate is well supported by observation. All of the biofilm removal measured occurred in the middle of the coverslip. The biofilm on the edges of the coverslip was not disturbed by the bubble stream. The fifth assumption, that the bubble only hits the biofilm once is not supported by observations made during this study. Though many of the bubbles only came into contact with the biofilm once, there were a few that collided with the biofilm more than once.

Both the Gaussian and decaying exponential models fit the biofilm removal data. The fact that the Gaussian model follows the data supports the statement of Iguchi *et al*. that bubble distribution is Gaussian. (44) As the bubbles leave the blunt needle they do not stay in a perfect cylinder along the axis of the needle, but the bubbles on the edge of the cylinder diffuse out radially. This creates a region that has a lower bubble density

www.manaraa.com

than at the center of the stream. Thus, when the stream comes into contact with the biofilm, a lot of bubbles collide with the middle of the sample and remove almost all of the biofilm from the middle of the sample instantly. However, farther from the center of the bubble stream there are fewer collisions, so it takes longer for enough collisions to occur to cause observable removal.

The main difference between the Gaussian distribution and the decaying exponential distribution is that the former is a function of e^{-r^2} and the latter is only a function of e^{-r} (see Equation 11). Thus the Gaussian has an initial change in slope that is quite sharp. Using the more general decaying exponential distribution in the model permits a more gradual change in slope. Though the results show that either model fits the data fairly well, the value for f for the two bubble sizes is consistent in the Gaussian model. However, for the decaying exponential model the values for f are less consistent (0.19 and 0.65). This provides additional support for the Gaussian model.

www.manaraa.com

CHAPTER 7

DISCUSSION

Biofilm Removal

Biofilm removal cannot be described by a simple relationship between velocity, gas fraction, and bubble size, but requires a more sophisticated mathematical model that includes the interactions between these three variables. This more complex model includes numerical coefficients that were determined by statistical regression of the data from these experiments. The statistical results of this research show bubble streams with velocities in the range of 2 m/s to 9 m/s remove more biofilm when the bubbles are larger and the gas fraction is smaller (in other words, bigger and fewer bubbles). However, for bubble streams traveling at higher velocities, smaller bubbles and higher gas fractions (more bubbles) are predicted to remove more biofilm. It is important to note that though the statistical model predicts that these conditions are the optimum for removing biofilm, the difference in the amount of removal is only a few percent. Thus, variation of these parameters creates a statistically significant difference in removal, but the differences are small. It is also important to note that given all the variations within the human population in oral biofilms and salivary chemistry, removal in the human mouth may be different from removal measured in this study. However, it is believed that trends in biofilm removal *in vivo* with respect to bubble parameters (velocity, size, etc.) would be similar to those observed in this *in vitro* study.

www.manaraa.com

During the experiments, the removal of biofilm by streams without bubbles was observed. It is believed that the removal of the biofilm by liquid is caused by shear forces when the liquid jet impinges on the biofilm. In the situation of a liquid jet impinging on a surface, the shear rate is highest near the point of impingement, and decreases as the fluid flows out radially along the flat surface. Thus the velocity gradient on the biofilm decreases radially from the impingement point. It is hypothesize that there is a critical velocity gradient on the surface, above which biofilm is removed because shear stresses are larger than biofilm adhesion strength. This point of critical velocity gradient will move outward radially at higher flows, and inward at slower flows, encompassing a region in which the biofilm is sheared off. This critical area of shear will increase with fluid velocity.

The data also show that a fluid stream with no bubbles at high velocity removes a larger area and amount of biofilm than does a stream containing bubbles at the same velocity. It appears that the removal forces caused by the liquid flow alone may be greater than forces caused by a mixture of liquid and bubbles at high velocities. Why might a liquid at high velocities produce more removal force than a gas-liquid mixture at the same velocity? It is postulated that the presence of the bubbles decreases the shear and momentum forces (at the same overall fluid velocity) which act on the biofilm. Shear forces are proportional to the viscosity of the fluid, and forces produced by a change in momentum are proportional to the density of the fluid. The apparent viscosity of two immiscible fluids is an intermediate value of the viscosities of the two pure fluids. (45) Thus, by introducing bubbles into the liquid stream, the apparent viscosity of the fluid decreases. Similarly, the density of the mixture is a volume average of the liquid

www.manaraa.com

and gas densities. Consequently at high velocities, when shear and momentum forces dominate, the removal forces are reduced in a gas-liquid mixture as compared to liquid alone.

However, at lower velocities, the addition of bubbles increases the biofilm removal compared to a stream without bubbles. Visual observation of the bubbles exiting the needle indicates that they do not exit in a perfect linear stream, but their flow is turbulent and chaotic. There is some spread in the position of the bubbles within the flow stream, thus creating a column of bubbles instead of a line of bubbles. It is postulated that at lower velocities the area of contact of the bubble column with the biofilm is larger than the critical area of shear created by the liquid flow alone, and thus (at lower velocities) the stream with bubbles removes more biofilm. In addition to shear forces, bubbles are capable of removing bacteria from a surface as the three-phase line (surface, liquid, gas) contacts the bacteria. (12) As a bubble collides with the surface, the three-phase boundary plucks off some biofilm. Thus with bubbles in the stream there are two forces that can remove the bacteria, the shear forces of the fluid and the surface tension of bubbles.

Previous work by Suarez has shown that a single bubble moving at slower velocities removes more bacteria or particles than a bubble moving at higher velocities. (7, 9) The overall efficiency of a bubble removing a bacterium was described as the product of three efficiencies: bubble-bacterium collision, bubble-bacterium attachment, and the stability of the bubble-bacterium aggregate. By decreasing the velocity of the bubble, the liquid film surrounding the bacterium becomes thinner and increases the probability that the air-liquid interface of the bubble will come into contact with the

www.manaraa.com

bacterium. In so doing, the efficiency of the bubble-bacterium collision is increased. Another advantage of a decreased velocity is that the bubble has more time to attach to the bacterium and form a stable aggregate, thus increasing the efficiencies of the bubble-bacterium attachment and the bubble-bacterium aggregate stability. This description supports the results obtained in this present study when there are few slow moving bubbles and the bubble size is large. The statistics show that when the number of bubbles is increased, under these conditions, the amount of removal is decreased. It is postulated that the introduction of additional bubbles lowers the efficiency of the bubbles-bacterium attachment as they crowd each other.

The major difference between the studies of Gomez-Suarez *et al.* and this present study is that they reported that bacterium removal always increased as flow velocity decreased, whereas it has been shown in this study that, when the size of the bubbles is small, biofilm removal increased as flow velocity increased. This divergence of observation is attributed to two factors. First, the fully developed biofilms used in this study are different than a distribution of adherent bacteria on a surface. Second, and perhaps more importantly, the experiments of Gomez-Suarez *et al.* were done with large bubbles (25 mm x 5 mm) at low velocities (0.001 m/s) compared to those in the experiments of this study (135 to 270 μm and 2 to 12 m/s). Both sets of data confirm the importance of both fluid dynamics and surface tension in removal of bacteria and biofilms from surfaces. Both proposed mechanisms of removal are probably valid in their respective flow regimes. It would be informative to determine if the Gomez-Suarez *et al.* model in slow flow and large bubbles applies to biofilms, and if the model from this study applies to a submonolayer of particles or bacteria with small bubbles in fast flow.

www.manaraa.com

The study of Gomez-Suarez *et al.* did not consider the angle of collision of the bubble with the surface. However, my study considered angle but found that the angle of impingement of the bulk fluid does not affect the amount of removal. The chaotic flow that has been observed in this study may also cause the bubbles to impinge upon the biofilm at different angles. It is hypothesized that the angle at which an individual bubble impinges does not affect the amount of biofilm that it removes. Thus the mathematical model derived earlier neglects any angle of attack as part of the derivation.

Though the sound used in these experiments did not appear to affect the amount of biofilm removal, the intensities used were quite low as compared to those of the ultrasound used in therapeutic medicine. Additional experiments using sound waves of greater intensities would provide some insight as to whether or not the sound would have the same synergistic effect with a bubble jet as it does with very few bubbles. However, high intensity sounds within the acoustic range might not lead to practical in-home products.

Dental Implications

To take advantage of the capacity of bubbles to remove biofilm when teeth are brushed, a toothbrush that propels bubbles at the surfaces of the teeth is desired. A powered toothbrush that is able to rapidly propel bubbles towards the teeth would be able to clean beyond the reach of the bristles; i.e., be able to clean the proximal surfaces and sulci of the teeth. Thus, the ability to propel many small bubbles at high velocity should be an important criterion for powered toothbrush design. In addition the angle at which the bubbles impinge against the biofilm does not affect the amount of biofilm removed; thus a bubble stream does not have to be perpendicular to the surface of the biofilm to

www.manaraa.com

effectively remove it. For example, if the buccal or lingual surfaces of the teeth are exposed to a stream of bubbles, the bubbles that pass through the interproximal spaces of the teeth will remove biofilm from the surfaces with which they come in contact.

One caution that should be considered in the design of these dental apparatus is that since the bubbles are powerful enough to shear biofilm off of the teeth, they have the potential to shear off layers of living cells of the host, i.e. gums, tongue, and cheek cells. Granted, the viability study on the biofilm suggests that the membranes of the bacterial cells are not lysed by the bubbles, so the bubbles may not destroy the human cells. However, the displacement of the human cells might still be painful.

Though the experiments performed were intended to have the same fluid characteristics as saliva in the mouth, toothpaste is often used during regular brushing. If toothpaste were added to the system, the surface tension of the bubbles would decrease significantly because many toothpastes contain sodium lauryl sulfate, a powerful surfactant. The decrease in surface tension modifies the biofilm removal in two different and compensating manners. First, the decrease in surface tension decreases the capacity of the bubble to pluck off bacterium. (7) On the other hand, the decrease in surface tension allows for smaller bubbles to form, and thus there will be many more bubbles (at the same gas fraction) that will collide with the surface. The net effect of adding a surfactant upon biofilm removal cannot be predicted from our data.

www.manaraa.com

CHAPTER 8

CONCLUSIONS AND RECOMMENDATIONS

Conclusions

The *S. mutans* biofilms covering the glass coverslips before exposure to the bubble stream contained 4.37 x 10^8 CFU/cm^2 and were 99% viable. The average thickness of the biofilms was approximately 40 μm. After exposure to the bubble stream the viability of the biofilm was 90%. This decrease in viability could be caused by the bubble stream, but the decrease is most likely attributed to the homogenation and filtration processes.

Though the bubble stream may not kill the biofilm, it is effective at removing biofilms from a surface. However, the removal of biofilm by a stream of bubbles is not dependent on one single factor, but is dependent upon the velocity of the bubble stream, gas fraction, and the size of the bubbles in the stream. A mathematical model relating these three parameters to the amount of removal was determined statistically. The model indicates that if the bubble stream is moving at a velocity of 9 m/s or greater, a large gas fraction and small bubble size is most effective in removing biofilm. If the stream is moving at a velocity between 2 m/s and 9 m/s, then a small gas fraction and large bubble size are more efficient. It is important to note that though these conditions are the most efficient statistically, the difference in removal is only a few percent.

For the range of velocities in which sonic toothbrushes propel bubbles, the presence of bubbles enhances the amount of biofilm removal. However, if the velocity is

www.manaraa.com

increased beyond a value on the order of 10 m/s, the bacteria removing efficiency of the stream decreases when bubbles are present. A stream of liquid will remove more biofilm than a stream that contains bubbles at the higher velocities.

Though it was originally believed that the angle at which the bubbles came into contact with the biofilm affected the amount of removal, this is not the case. A stream of bubbles that impinged upon the biofilm at a 5º angle removed the same amount of biofilm as the stream than impinged at a 45º angle. The change of angle only changes the shape of the removal. When the angle of impingement is small, the shape of the removal is elongated; whereas larger angles have a rounded shape. These results showed that it is not the angle, but rather the number of bubbles that came into contact with the biofilm that affect the amount of removal.

The addition of sound, equivalent to the sound generated by the Sonicare *Elite* toothbrush, did not affect the amount of biofilm removed during the 5 sec exposure to the bubble stream. Increasing the frequency or the intensity of the sound did not have any measurable affect on the amount of biofilm removed. No removal was detected for biofilms that were only exposed to acoustic waves. It is likely that no removal occurred due to the extremely short exposure time.

Two mathematical models were developed to describe the removal of biofilm with respect to time. Both models are based on functions that describe the radial distribution of bubbles in the bubble stream. The first model was based on the Gaussian distribution of bubbles in a column and the second model was based on a decaying exponential distribution. The results from both of these models are consistent with data for biofilm removal as a function of time.

www.manaraa.com

Recommendations

Additional research needs to be conducted with respect to acoustic waves removing biofilm. From the experiments performed in this study it appears that sound does not affect biofilm; however, the work by McInnes *et al.* (26, 27) implicates that acoustic waves generated at the levels used in this study should remove bacteria from the surface and damage the bacteria. The apparatus used for this study does not allow any air to be entrained into the solution and come into contact with the biofilm; this makes it a very practical device for studying the effects of acoustic waves on biofilms. McInnes *et al.* showed that exposures less than 15 sec did not have any apparent removal but there probably were air bubbles in his their experiment. Increasing the time of exposure of biofilm to acoustic waves would provide additional insight as to whether or not acoustic waves will remove biofilm. Increasing the intensity of the acoustic waves will also provide insight as to whether sounds of audible frequencies can remove biofilm, as there might be a threshold value that must be surpassed to cause any removal.

If any biofilm removal is observed to be caused by acoustic waves, a high speed video of the removal might be beneficial in understanding the physical mechanism causing the removal. The use of high speed video would also be helpful for observing biofilm removal by bubbles and also the bubble distribution as the stream exits the tip of the needle. The video used in this study provided insight as to how the bubbles removed biofilm, but there was too much time between frames to observe the mechanical interaction of the bubble against the biofilm. A high speed video of the bubbles would also allow for a more exact description of the radial distribution of bubbles as they leave the needle tip. A macroscopic view of the bubble stream provides an approximate shape

www.manaraa.com

as to the nature of the distribution, but the video obtained does not provide more definitive information. In addition to the distribution, a faster video capture would allow for more accurate size measurement of the bubbles leaving the needle tip and would clarify whether a bubble in the image was leaving the needle tip or being recirculated back into the image.

One of the difficulties involved in the performance of the experiments in this study was the necessity of recalibrating the needle valve of the liquid solution throughout the day. One of the reasons for this problem was the artificial saliva solution. The schleroglucan was not completely soluble in water. The small particles in the solution would then clog the needle valve and thus change the flow of the system. Another problem with schleroglucan was that it does not make a clear, transparent solution. In order to capture real-time video the schleroglucan would have to be exchanged for clean water. Finding another substitute for artificial saliva that was clear and that would not stick to any portion of the apparatus would be ideal.

Finally, future experiments could be improved by taking additional steps to mimic an environment similar to the mouth while the teeth are being brushed. Oral plaque does not consist of one single strain of bacteria. There are over twenty strains of bacteria in the mouth; *S. mutans* is one of the more prevalent. The addition of other species of bacteria, such as *Actinomyces viscosus* or *Porphyromonas gingivalis*, would provide a more realistic model of plaque. To improve upon the model of the biofilm further, it would also need to be attached to a surface more like that found in the mouth. Covering the teeth is a layer of proteins referred to as the salivary pellicle. Coating the glass

www.manaraa.com

coverslips with this pellicle would provide a more realistic surface to which the bacteria could adhere.

Another aspect to creating an environment similar to that of the mouth during brushing is the introduction of a surfactant containing dentifrice. The addition of a surfactant would change the viscosity of the solution and the surface tension of the bubbles within the solution. Additional studies would have to be performed to determine if the bubbles of this solution would be able to remove biofilm.

www.manaraa.com

www.manaraa.com

REFERENCES

1. Miller, M.B. and B.L. Bassler, *Quorum sensing in bacteria.* Annual Review of Microbiology, 2001. **55**: p. 165-199.
2. Donlan, R.M., *Biofilms: Microbial Life on Surfaces.* Emerging Infectious Diseases, 2002. **8**(9): p. 881-890.
3. Costerton, J.W., Z. Lewandowski, D.E. Caldwell, D.R. Korber, and H.M. Lappinscott, *Microbial Biofilms.* Annual Review of Microbiology, 1995. **49**: p. 711-745.
4. Costerton, W.J. and P.S. Stewart, *Battling Biofilms.* Scientific America, 2001. **285**(1): p. 74-81.
5. Scannapieco, F.A., *Inflammation: From Gingivitis to Systemic Disease.* Compendium of Continuing Education in Dentistry, 2004. **25**(7 (Supplement 1)): p. 16-24.
6. Suarez, C.G., J. Noordmans, H.C. Van der Mei, and H.J. Busscher, *Detachment of colloidal particles from collector surfaces with different electrostatic charge and hydrophobicity by attachment to air bubbles in a parallel plate flow chamber.* Physical Chemistry Chemical Physics, 1999. **1**(18): p. 4423-4427.
7. Suarez, C.G., J. Noordmans, H.C. Van der Mei, and H.J. Busscher, *Removal of colloidal particles from quartz collector surfaces as stimulated by the passage of liquid-air interfaces.* Langmuir, 1999. **15**(15): p. 5123-5127.

www.manaraa.com

8. Busscher, H.J., M. Rustema-Abbing, G.M. Bruinsma, M. de Jager, B. Gottenbos, and H.C. van der Mei, *Non-contact removal of coadhering and non-coadhering bacterial pairs from pellicle surfaces by sonic brushing and de novo adhesion.* European Journal of Oral Sciences, 2003. **111**(6): p. 459-464.

9. Gomez-Suarez, C., H.J. Busscher, and H.C. van der Mei, *Analysis of bacterial detachment from substratum surfaces by the passage of air-liquid interfaces.* Applied and Environmental Microbiology, 2001. **67**(6): p. 2531-2537.

10. Pitt, W.G., M.O. Mcbride, A.J. Barton, and R.D. Sagers, *Air-Water-Interface Displaces Adsorbed Bacteria.* Biomaterials, 1993. **14**(8): p. 605-608.

11. Adams, H., M.T. Winston, J. Heersink, K.A. Buckingham-Meyer, J.W. Costerton, and P. Stoodley, *Development of a laboratory model to assess the removal of biofilm from interproximal spaces by powered tooth brushing.* American Journal of Dentistry, 2002. **15 Spec No**: p. 12B-17b.

12. Pitt, W.G., *Removal of Oral Biofilm by Sonic Phenomena.* American Journal of Dentistry, 2005: p. (In Press).

13. Landa, A.S., H.C. van der Mei, and H.J. Busscher, *A comparison of the detachment of an adhering oral streptococcal strain stimulated by mouthrinses and a pre-brushing rinse.* Biofouling, 1996. **9**(4): p. 327-339.

14. Poortinga, A.T., J. Smit, H.C. van der Mei, and H.J. Busscher, *Electric field induced desorption of bacteria from a conditioning film covered substratum.* Biotechnology and Bioengineering, 2001. **76**(4): p. 395-399.

www.manaraa.com

15. Yang, J., R. Bos, G.F. Belder, and H.J. Busscher, *Co-adhesion and removal of adhering bacteria from salivary pellicles by three different modes of brushing.* European Journal of Oral Sciences, 2001. **109**(5): p. 325-329.

16. Carter, K., G. Landini, and A.D. Walmsley, *Plaque removal characteristics of electric toothbrushes using an in vitro plaque model.* Journal of Clinical Periodontology, 2001. **28**(11): p. 1045-1049.

17. Marais, J.T. and V.S. Brozel, *Electro-chemically activated water in dental unit water lines.* British Dental Journal, 1999. **187**(3): p. 156-158.

18. Emling, R.C. and S.L. Yankell, *The application of sonic technology to oral hygiene: The third generation of powered toothbrushes.* Journal of Clinical Dentistry, 1997. **8**(1): p. 1-3.

19. Williams, K.B., C.M. Cobb, H.J. Taylor, A.R. Brown, and K.K. Bray, *Effect of sonic and mechanical toothbrushes on subgingival microbial flora: A comparative in vivo scanning electron microscopy study of 8 subjects.* Quintessence International, 2001. **32**(2): p. 147-154.

20. Zimmer, S., M. Fosca, and J.F. Roulet, *Clinical study on the effectiveness of two sonic toothbrushes.* Journal of Dental Research, 1998. **77**: p. 716-716.

21. Tritten, C.B. and G.C. Armitage, *Comparison of a sonic and a manual toothbrush for efficacy in supragingival plaque removal and reduction of gingivitis.* Journal of Clinical Periodontology, 1996. **23**(7): p. 641-648.

22. OBeirne, G., R.H. Johnson, G.R. Persson, and M.D. Spektor, *Efficacy of a sonic toothbrush on inflammation and probing depth in adult periodontitis.* Journal of Periodontology, 1996. **67**(9): p. 900-908.

www.manaraa.com

23. Wu-Yuan, C.D., R.D. Anderson, and C. McInnes, *Ability of the Sonicare Electronic Toothbrush to Generate Dynamic Fluid Activity that Removes Bacteria.* Journal of Clinical Dentistry, 1994. **5**: p. 89-93.

24. Stanford, C.M., R. Srikantha, and C.D. Wu, *Efficacy of the Sonicare(R) toothbrush fluid dynamic action on removal of human supragingival plaque.* Journal of Clinical Dentistry, 1997. **8**(1): p. 10-14.

25. Heersink, J., W.J. Costerton, and P. Stoodley, *Influence of the Sonicare toothbrush on the structure and thickness of laboratory grown Streptococcus mutans biofilms.* American Journal of Dentistry, 2003. **16**(2): p. 79-83.

26. McInnes, C., D. Engel, B.J. Moncla, and R.W. Martin, *Reduction in Adherence of Actinomyces-Viscosus after Exposure to Low-Frequency Acoustic Energy.* Oral Microbiology and Immunology, 1992. **7**(3): p. 171-176.

27. McInnes, C., D. Engel, and R.W. Martin, *Fimbria Damage and Removal of Adherent Bacteria after Exposure to Acoustic Energy.* Oral Microbiology and Immunology, 1993. **8**(5): p. 277-282.

28. Wong, L. and C.H. Sissions, *A comparison of human dental plaque microcosm biofilms grown in an undefined medium and a chemically defined artificial saliva.* Archives of Oral Biology, 2001. **46**(6): p. 477-486.

29. Wataha, J.C., P.E. Lockwood, S. Bouillaguet, and M. Noda, *In vitro biological response to core and flowable dental restorative materials.* Dental Materials, 2003. **19**(1): p. 25-31.

www.manaraa.com

30. Pedrazzi, V., E.H.G. Lara, J.O.D. Ciampo, and H. Panzeri, *Tensile bond strength of a polymeric intra-buccal bioadhesive: the mucin role.* Bollettino Chimico Farmaceutica, 2001. **140**(6): p. 471-474.

31. Friel, E.N. and A.J. Taylor, *Effect of salivary components on volatile partitioning from solutions.* Journal of Agricultural and Food Chemistry, 2001. **49**(8): p. 3898-3905.

32. Matharu, S., D.A. Spratt, J. Pratten, Y.L. Ng, N. Mordan, M. Wilson, and K. Gulabivala, *A new in vitro model for the study of microbial microleakage around dental restorations: a preliminary qualitative evaluation.* International Endodontic Journal, 2001. **34**(7): p. 547-553.

33. Van der reijden, W.A., E.C.I. Veerman, and A.V.N. Amerongen, *Rheological Properties of Commercially Available Polysaccharides with Potential Use in Saliva Substitutes.* Biorheology, 1994. **31**(6): p. 631-642.

34. Christersson, C.E., L. Lindh, and T. Arnebrant, *Film-forming properties and viscosities of saliva substitutes and human whole saliva.* European Journal of Oral Sciences, 2000. **108**(5): p. 418-425.

35. Coviello, T., M. Grassi, R. Lapasin, A. Marino, and F. Alhaique, *Scleroglucan/borax: characterization of a novel hydrogel system suitable for drug delivery.* Biomaterials, 2003. **24**(16): p. 2789-2798.

36. Rodriguez, F., *Principles of Polymer Systems*. 4 ed. 1996, Washington D.C.: Taylor & Francis. 732.

37. Smith, J.M., H.C. Van Ness, and M.M. Abbott, *Introduction to Chemical Engineering Thermodynamics*. 6th ed. McGraw-Hill Chemical Engineering

www.manaraa.com

Series, ed. E.D. Glandt, M.T. Klein, and T.F. Edgar. 2001, New York: McGraw-Hill. 789.

38. Herigstad, B., M. Hamilton, and J. Heersink, *How to optimize the drop plate method for enumerating bacteria.* Journal of Microbiological Methods, 2001. **44**: p. 121-129.

39. Parini, M.R., D. Eggett, and W.G. Pitt, *Removal of Streptococcus mutans Biofilm by Bubbles.* Journal of Clinical Periodontology, 2005(In Press).

40. Parini, M.R. and W.G. Pitt, *Removal of Oral Biofilm by Bubbles: The Effect of Trajectory and Sonic Waves.* Journal of the American Dental Association, 2005(In Press).

41. Zips, A., G. Schaule, and H.C. Flemming, *Ultrasound as a Means of Detaching Biofilms.* Biofouling, 1990. **2**: p. 323-333.

42. Mott, I.E.C., D.J. Stickler, W.T. Coakley, and T.R. Bott, *The removal of bacterial biofilm from water-filled tubes using axially propagated ultrasound.* Journal of Applied Microbiology, 1998. **84**(4): p. 509-514.

43. Parini, M.R. and W.G. Pitt, *Model of Biofilm Removal by a Bubble Jet.* Colloids and Surfaces B: Biointerfaces, 2005(submitted).

44. Iguchi, M., A. Kawajiri, H. Tomida, and Z. Morita, *Effects of the Viscosity of Liquid on the Characteristics of Vertical Bubbling Jet in a Cylindrical Vessel.* Isij International, 1993. **33**(3): p. 361-368.

45. Perry, R.H., *Chemical Engineers' Handbook*. Seventh ed, ed. R.H. Perry, D.W. Green, and J.O. Maloney. 1997, New York: McGraw-Hill.

www.manaraa.com

APPENDICES

www.manaraa.com

www.manaraa.com

APPENDIX A

Biofilm Removal Data

www.manaraa.com

www.manaraa.com

المنارة للاستشارات

Biofilm Removal at a 45º Angle of Impingement

Velocity (m/s)	Gas Fraction	Bubble Size (μm)	Run	% Deep Removal	Deep Area (in^2)	Total Deep Removal	% Removal in Region
1.9	0.34	206	1	52.83%	0.05	2.64%	7.06%
1.9	0.34	206	2	59.91%	0.04	2.40%	19.51%
2.8	0.10	211	1	56.01%	0.07	3.92%	12.53%
2.8	0.10	211	2	63.55%	0.04	2.54%	4.18%
3.3	0.29	231	1	59.19%	0.02	1.18%	3.71%
3.3	0.29	231	3	59.10%	0.04	2.36%	10.41%
3.3	0.29	231	2	50.65%	0.01	0.51%	3.10%
4.0	0.39	143	1	14.21%	0.01	0.14%	1.56%
4.0	0.39	143	2	11.51%	0.01	0.12%	0.54%
4.0	0.39	143	3	42.27%	0.01	0.42%	1.18%
4.3	0.41	205	1	47.34%	0.12	5.68%	24.98%
4.3	0.41	205	2	49.07%	0.03	1.47%	11.76%
5.7	0.43	139	1	39.31%	0.03	1.18%	9.88%
5.7	0.43	139	2	46.68%	0.13	6.07%	24.00%
6.5	0.05	200	1	72.86%	0.07	5.10%	14.93%
6.5	0.05	200	2	56.83%	0.10	5.68%	15.15%
6.7	0.48	205	1	46.56%	0.07	3.26%	11.93%
6.7	0.48	205	2	52.62%	0.04	2.10%	11.50%
6.8	0.42	246	1	48.04%	0.03	1.44%	6.35%
6.8	0.42	246	2	61.79%	0.09	5.56%	13.27%
6.8	0.45	135	1	60.51%	0.02	1.21%	9.61%
6.8	0.45	135	2	49.71%	0.04	1.99%	13.82%
6.8	0.45	135	3	59.71%	0.27	16.12%	37.74%
7.3	0.30	246	1	58.17%	0.02	1.16%	4.96%
7.3	0.30	246	2	72.07%	0.02	1.44%	9.46%
10.1	0.55	257	1	55.91%	0.02	1.12%	8.71%
10.1	0.55	257	2	65.30%	0.02	1.31%	8.51%
10.1	0.55	257	3	63.10%	0.10	6.31%	34.29%
12.2	0.34	261	1	62.15%	0.08	4.97%	20.68%
12.2	0.34	261	2	47.98%	0.02	0.96%	3.96%
12.2	0.34	261	3	64.73%	0.16	10.36%	31.50%

www.manaraa.com

المنارة للاستشارات

Biofilm Removal by Bubbles at Impingement Angles of 5, 30,and 45 Degrees

Velocity (m/s)	Gas Fraction	Bubble Size (μm)	Angle	Run	% Deep Removal	Deep Area (in^2)	Total Deep Removal	% Removal in Region
1.5	0.05	205	5	1	52.59%	0.03	1.58%	4.00%
1.5	0.05	205	5	2	61.48%	0.05	3.07%	13.73%
1.5	0.05	205	5	3	66.09%	0.10	6.61%	17.55%
1.5	0.05	205	5	4	56.56%	0.11	6.22%	23.30%
4.3	0.41	205	5	1	39.73%	0.01	0.40%	4.21%
4.3	0.41	205	5	2	49.82%	0.01	0.50%	7.29%
4.3	0.41	205	5	3	68.21%	0.05	3.41%	9.87%
4.3	0.41	205	5	4	8.64%	0.01	0.09%	0.13%
1.5	0.05	205	30	1	56.93%	0.07	3.99%	11.42%
1.5	0.05	205	30	2	51.17%	0.04	2.05%	7.08%
1.5	0.05	205	30	3	64.87%	0.07	4.54%	11.47%
1.5	0.05	205	30	4	35.85%	0.02	0.72%	7.59%
4.3	0.41	205	30	1	46.43%	0.01	0.46%	2.25%
4.3	0.41	205	30	2	39.83%	0.02	0.80%	6.54%
4.3	0.41	205	30	3	59.77%	0.02	1.20%	4.65%
4.3	0.41	205	30	4	50.08%	0.06	3.00%	11.93%
1.5	0.05	205	45	1	82.80%	0.06	4.97%	17.22%
1.5	0.05	205	45	3	40.60%	0.12	4.87%	13.92%
1.5	0.05	205	45	4	55.78%	0.22	12.27%	35.37%
1.5	0.05	205	45	5	32.89%	0.01	0.33%	0.56%
4.3	0.41	205	45	1	60.10%	0.09	5.41%	19.23%
4.3	0.41	205	45	2	49.91%	0.04	2.00%	11.41%
4.3	0.41	205	45	1**	47.34%	0.12	5.68%	24.98%
4.3	0.41	205	45	2**	49.07%	0.03	1.47%	11.76%

** Data taken from the first two phases of the experiment.

www.manaraa.com

المنارة للاستشارات

Biofilm Removal by Sound at an Impingement Angel of 45 Degrees

Frequency (Hz)	Intensity (TBE)	% Deep Removal	Deep Area (in^2)	% Removal in Region
0	0	20.19%	0.03	0.00%
0	0	0.00%	0	6.47%
0	0	0.00%	0	0.00%
260	0.174	0.00%	0	3.64%
260	1	0.00%	0	0.00%
260	2	0.00%	0	0.00%
260	2	0.00%	0	2.00%
260	2	0.00%	0	3.18%
520	0.174	24.02%	0.02	4.51%
520	0.174	20.86%	0.03	3.36%
520	0.174	0.00%	0	2.21%

www.manaraa.com

المنارة للاستشارات

Biofilm Removal by Bubbles and Sound at an Impingement Angel of 45 Degrees

Frequency (Hz)	Intensity (TBE)	% Deep Removal	Deep Area (in^2)	% Removal in Region	Velocity (m/s)	Gas Fraction	Bubble Size (μm)
0	0	70.67%	0.06	19.41%	10.4	0.25	205
0	0	85.37%	0.19	39.52%	10.8	0.27	205
0	0	79.75%	0.3	56.85%	10.8	0.27	205
0	0	56.58%	0.11	17.36%	10.8	0.27	205
0	0	89.04%	0.17	47.58%	10.8	0.27	205
0	0	79.84%	0.04	18.12%	10.8	0.27	205
0	0	74.58%	0.06	15.28%	10.8	0.27	205
0	0	81.19%	0.13	35.29%	10.8	0.27	205
0	0	91.89%	0.24	65.41%	10.8	0.27	205
0	0	93.22%	0.16	48.45%	10.8	0.27	205
150	2	73.60%	0.06	13.86%	10.8	0.27	205
150	2	80.51%	0.05	20.63%	10.8	0.27	205
150	2	81.15%	0.15	34.03%	10.8	0.27	205
260	0.174	73.48%	0.02	19.30%	10.4	0.25	205
260	0.174	83.64%	0.17	35.42%	10.8	0.27	205
260	0.174	88.66%	0.15	33.62%	10.8	0.27	205
260	1	76.50%	0.05	17.07%	10.8	0.27	205
260	1	86.77%	0.25	54.84%	10.8	0.27	205
260	1	79.06%	0.13	26.59%	10.8	0.27	205
260	2	65.84%	0.16	26.83%	10.8	0.27	205
260	2	87.14%	0.33	68.22%	10.8	0.27	205
260	2	83.86%	0.14	31.12%	10.8	0.27	205
260	2	83.03%	0.17	42.12%	10.8	0.27	205
520	0.174	91.28%	0.15	39.07%	10.8	0.27	205
520	0.174	85.63%	0.17	40.03%	10.8	0.27	205

www.manaraa.com

APPENDIX B

Statistical Analysis Software (SAS) Reports

www.manaraa.com

www.manaraa.com

The SAS System
13:13 Wednesday, June 15, 2005

The GLM Procedure

Dependent Variable: % Deep Removal

Source	DF	Sum of Squares	Mean Square	F Value	Pr > F
Model	5	90874.98156	18174.99631	201.92	<.0001
Error	26	2340.23068	90.00887		
Uncorrected Total	31	93215.21224			

R-Square	Coeff Var	Root MSE	% Deep Removal Mean
0.974894	17.82820	9.487301	53.21513

NOTE: No intercept term is used: R-square is not corrected for the mean.

Source	DF	Type I SS	Mean Square	F Value	Pr > F
Velocity	1	76914.15768	76914.15768	854.52	<.0001
Gas_Fraction	1	2673.16640	2673.16640	29.70	<.0001
Bubble_Size	1	9217.05569	9217.05569	102.40	<.0001
Velocity*Gas_Fractio	1	339.23512	339.23512	3.77	0.0631
Velocity*Bubble_Size	1	1731.36668	1731.36668	19.24	0.0002

Source	DF	Type III SS	Mean Square	F Value	Pr > F
Velocity	1	1711.702136	1711.702136	19.02	0.0002
Gas_Fraction	1	875.298746	875.298746	9.72	0.0044
Bubble_Size	1	4737.100418	4737.100418	52.63	<.0001
Velocity*Gas_Fractio	1	507.611982	507.611982	5.64	0.0252
Velocity*Bubble_Size	1	1731.366682	1731.366682	19.24	0.0002

Parameter	Estimate	Standard Error	Value	Pr > |t|
Velocity	8.0635095	1.84906707	4.36	0.0002
Gas_Fraction	-113.8012009	36.49314999	-3.12	0.0044
Bubble_Size	0.3806869	0.05247523	7.25	<.0001
Velocity*Gas_Fractio	12.8536202	5.41255337	2.37	0.0252
Velocity*Bubble_Size	-0.0483648	0.01102751	-4.39	0.0002

www.manaraa.com

The SAS System
13:13 Wednesday, June 15, 2005

The GLM Procedure

Dependent Variable: % Removal in Region

Source	DF	Sum of Squares	Mean Square	F Value	Pr > F
Model	2	5319.174768	2659.587384	32.38	<.0001
Error	29	2381.857938	82.133032		
Uncorrected Total	31	7701.032706			

R-Square	Coeff Var	Root MSE	% Removal in Region Mean
0.690709	71.89643	9.062728	12.60525

NOTE: No intercept term is used: R-square is not corrected for the mean.

Source	DF	Type I SS	Mean Square	F Value	Pr > F
Velocity	1	5073.535410	5073.535410	61.77	<.0001
Velocity*Bubble_Size	1	245.639358	245.639358	2.99	0.0944

Source	DF	Type III SS	Mean Square	F Value	Pr > F
Velocity	1	859.2378047	859.2378047	10.46	0.0030
Velocity*Bubble_Size	1	245.6393584	245.6393584	2.99	0.0944

Parameter	Estimate	Standard Error	t Value	Pr > |t|
Velocity	3.907454979	1.20808147	3.23	0.0030
Velocity*Bubble_Size	-0.009021334	0.00521652	-1.73	0.0944

www.manaraa.com

The SAS System
13:13 Wednesday, June 15, 2005

The GLM Procedure

Dependent Variable: Deep Area

Source	DF	Sum of Squares	Mean Square	F Value	Pr > F
Model	2	0.11355773	0.05677887	20.12	<.0001
Error	29	0.08184227	0.00282215		
Uncorrected Total	31	0.19540000			

R-Square	Coeff Var	Root MSE	Deep Area Mean
0.581155	92.51912	0.053124	0.057419

NOTE: No intercept term is used: R-square is not corrected for the mean.

Source	DF	Type I SS	Mean Square	F Value	Pr > F
Velocity	1	0.10088095	0.10088095	35.75	<.0001
Velocity*Bubble_Size	1	0.01267679	0.01267679	4.49	0.0427

Source	DF	Type III SS	Mean Square	F Value	Pr > F
Velocity	1	0.02978624	0.02978624	10.55	0.0029
Velocity*Bubble_Size	1	0.01267679	0.01267679	4.49	0.0427

Parameter	Estimate	Standard Error	t Value	Pr > |t|
Velocity	0.0230062146	0.00708153	3.25	0.0029
Velocity*Bubble_Siz	-.0000648077	0.00003058	-2.12	0.0427

www.manaraa.com

The SAS System
13:13 Wednesday, June 15, 2005

The GLM Procedure

Dependent Variable: Total Deep Removal

Source	DF	Sum of Squares	Mean Square	F Value	Pr > F
Model	2	368.5746769	184.2873385	18.00	<.0001
Error	29	296.9465199	10.2395352		
Uncorrected Total	31	665.5211968			

R-Square	Coeff Var	Root MSE	Total Deep Removal Mean
0.553814	98.47435	3.199927	3.249504

NOTE: No intercept term is used: R-square is not corrected for the mean.

Source	DF	Type I SS	Mean Square	F Value	Pr > F
Velocity	1	340.4373297	340.4373297	33.25	<.0001
Velocity*Bubble_Size	1	28.1373473	28.1373473	2.75	0.1082

Source	DF	Type III SS	Mean Square	F Value	Pr > F
Velocity	1	77.68007063	77.68007063	7.59	0.0100
Velocity*Bubble_Size	1	28.13734726	28.13734726	2.75	0.1082

Parameter	Estimate	Standard Error	t Value	Pr > |t|
Velocity	1.174876184	0.42655734	2.75	0.0100
Velocity*Bubble_Siz	-0.003053257	0.00184188	-1.66	0.1082

www.manaraa.com

APPENDIX C

Mechanical Drawings

www.manaraa.com

www.manaraa.com

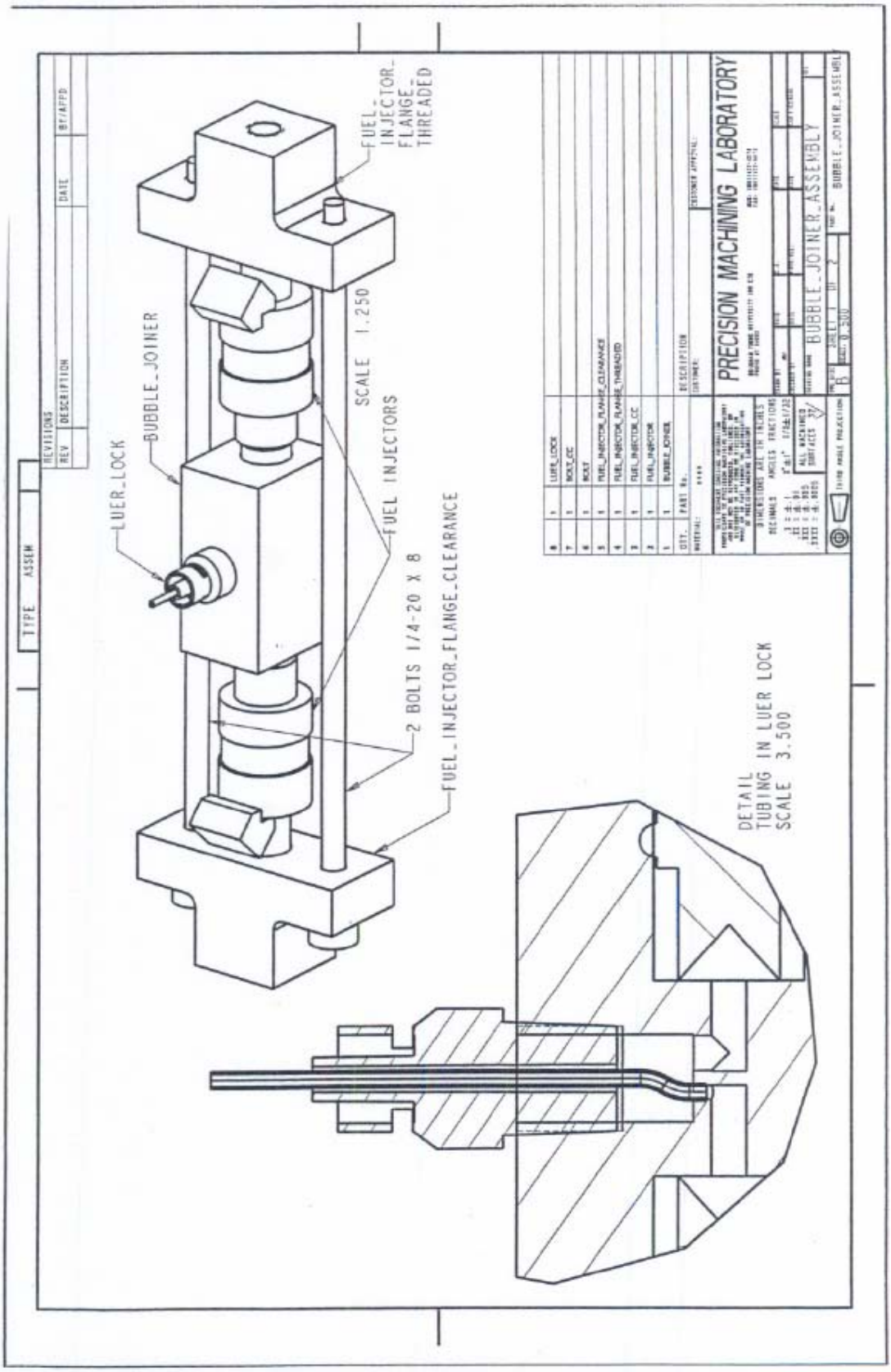

www.manaraa.com

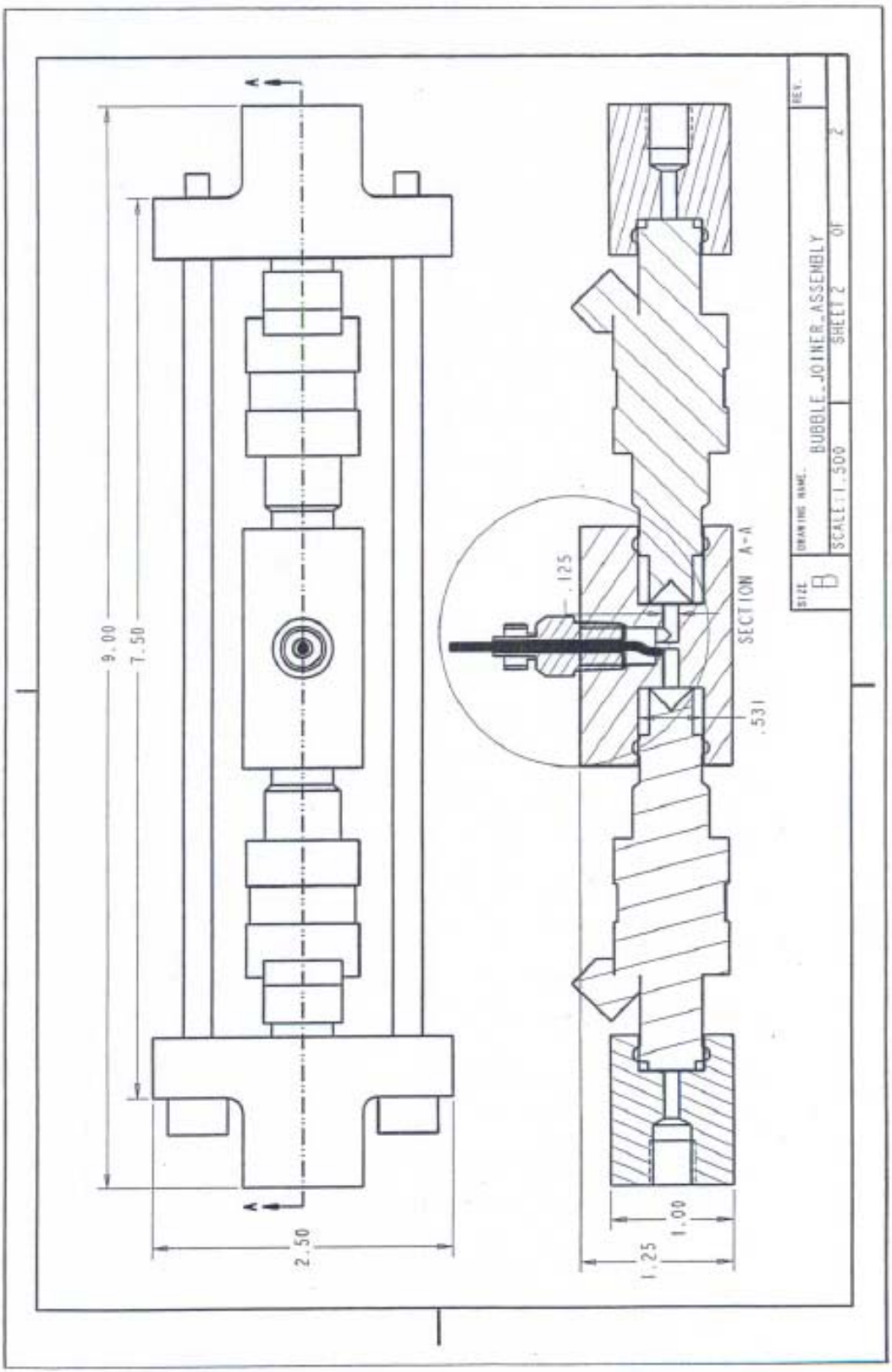

www.manaraa.com

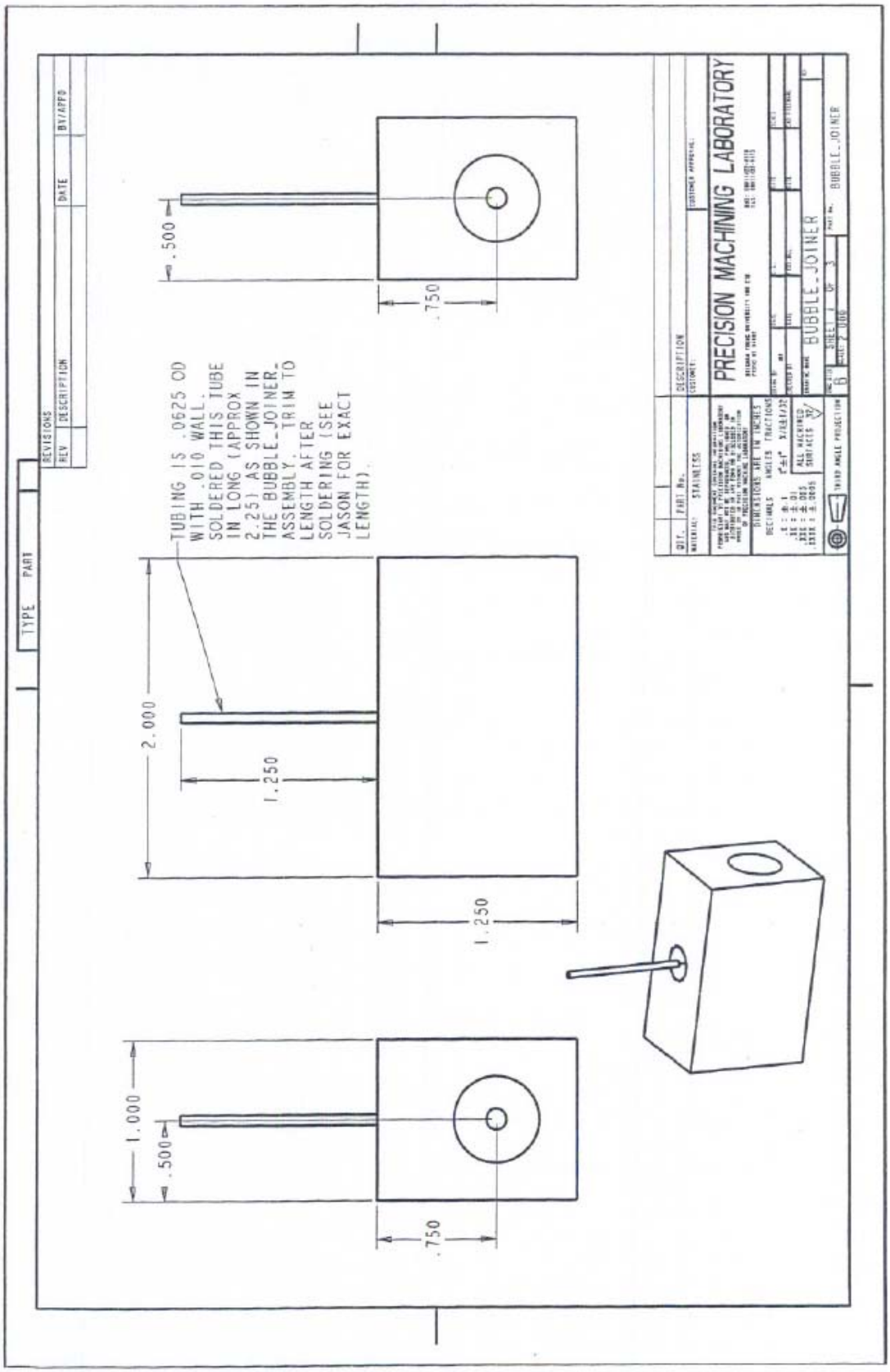

www.manaraa.com

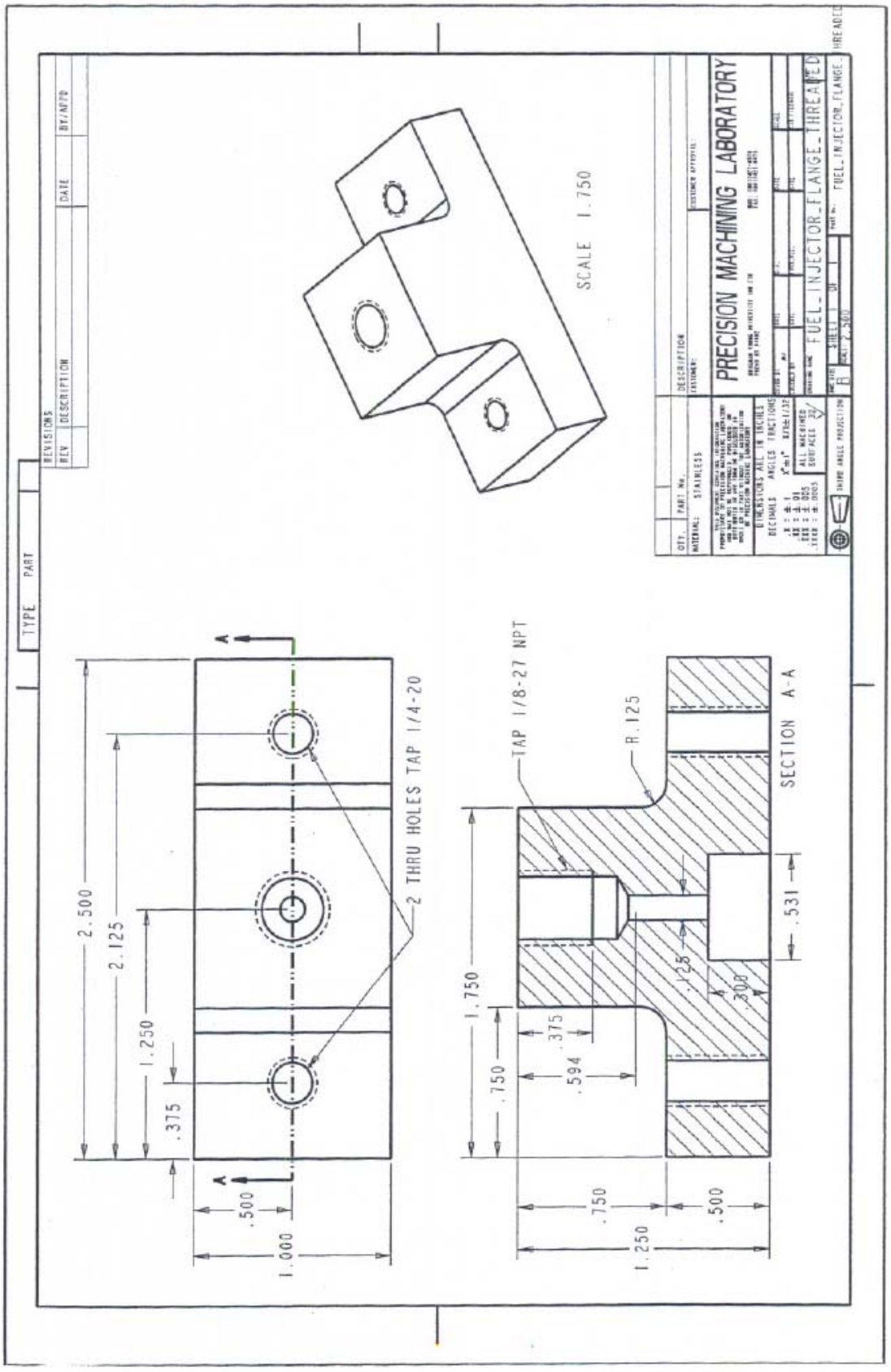

www.manaraa.com

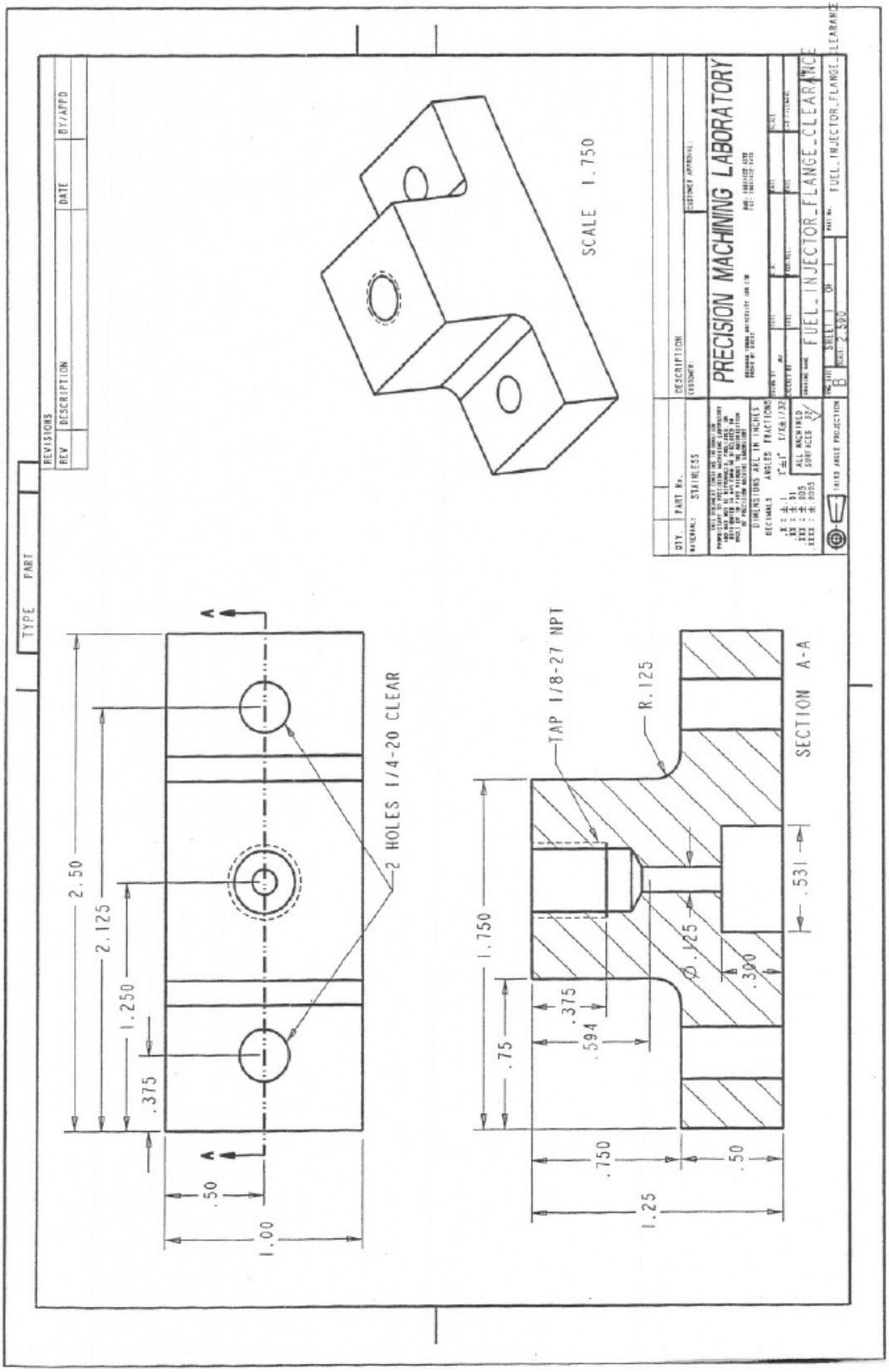

www.manaraa.com

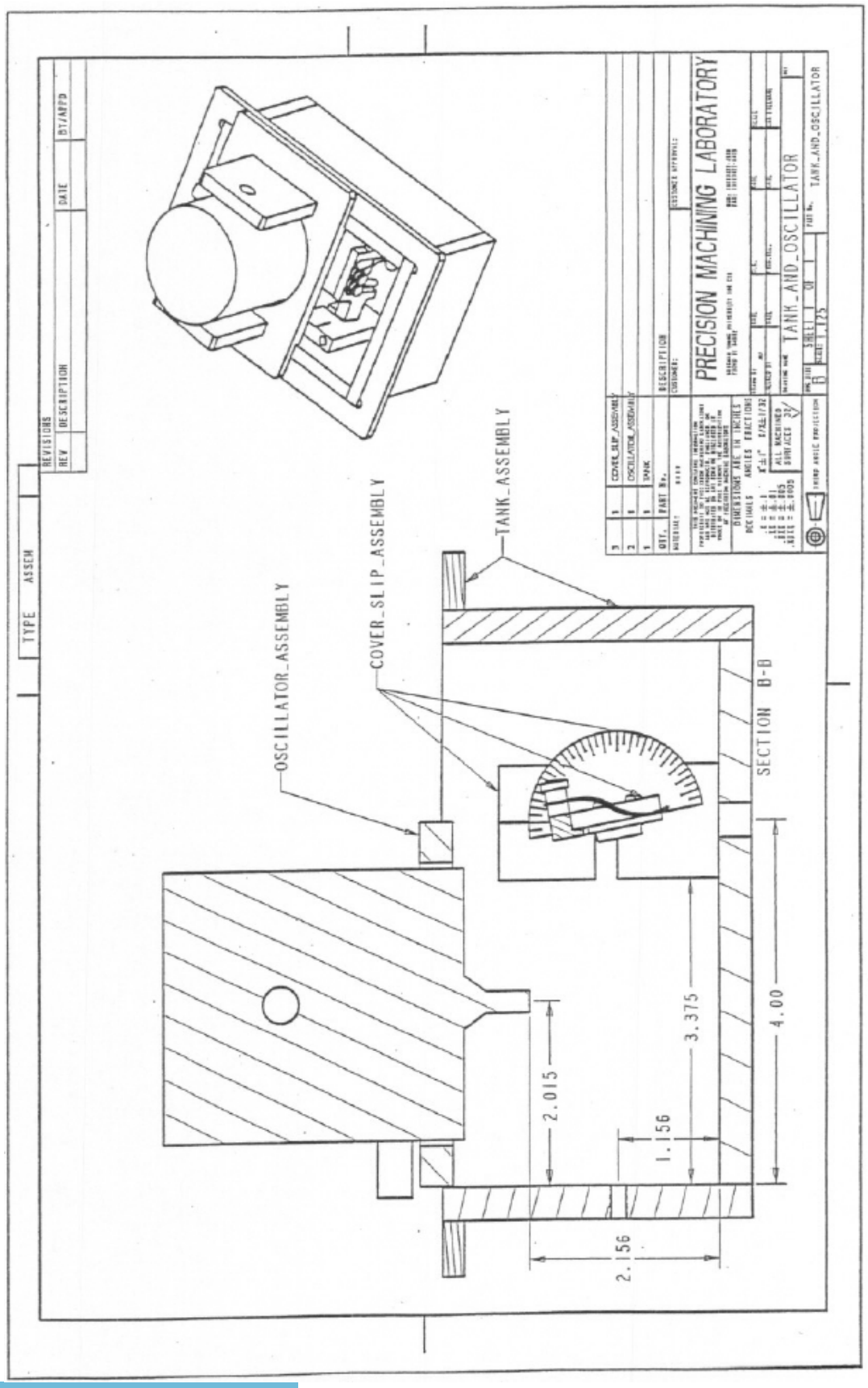

www.manaraa.com

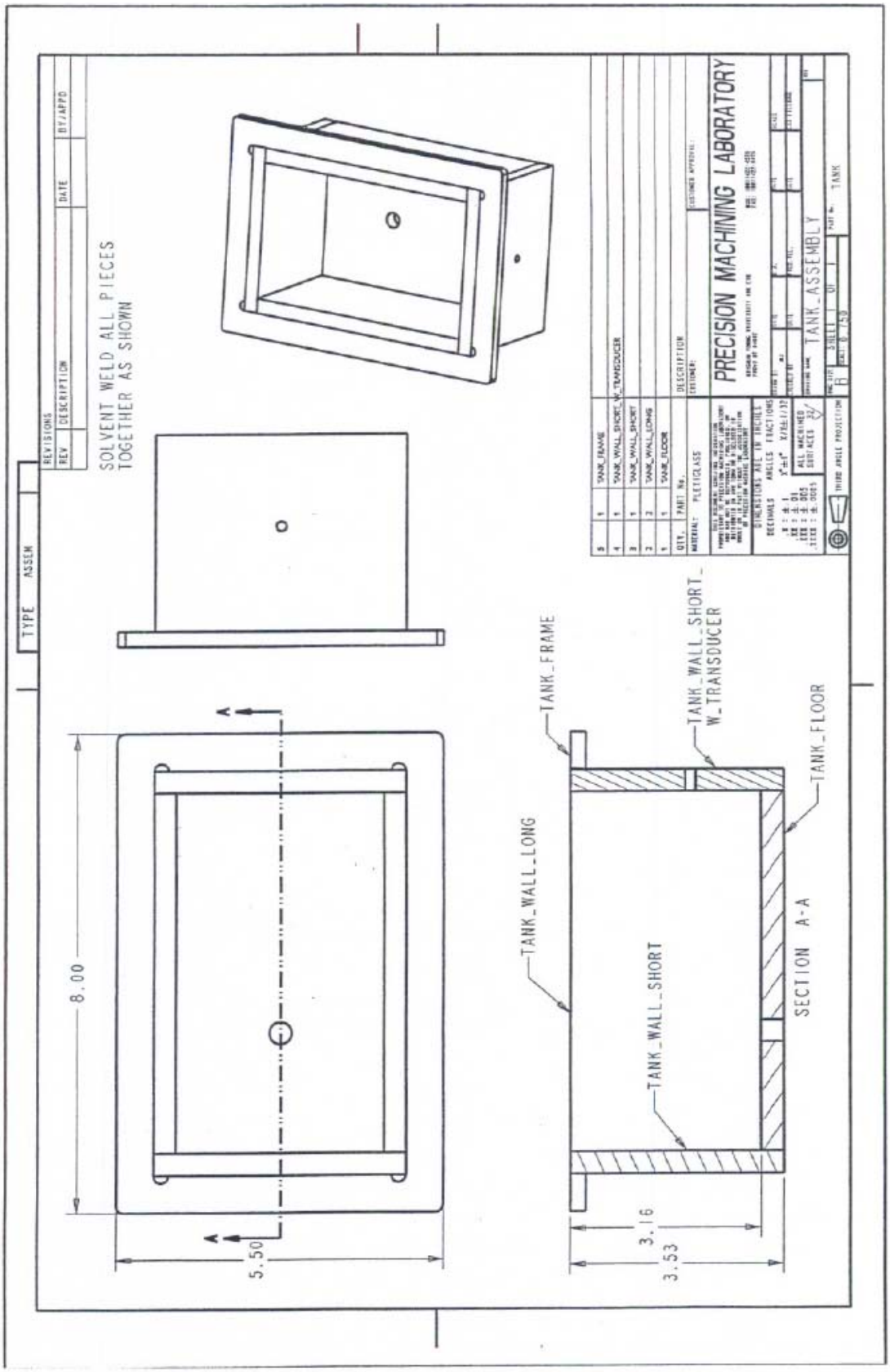

www.manaraa.com

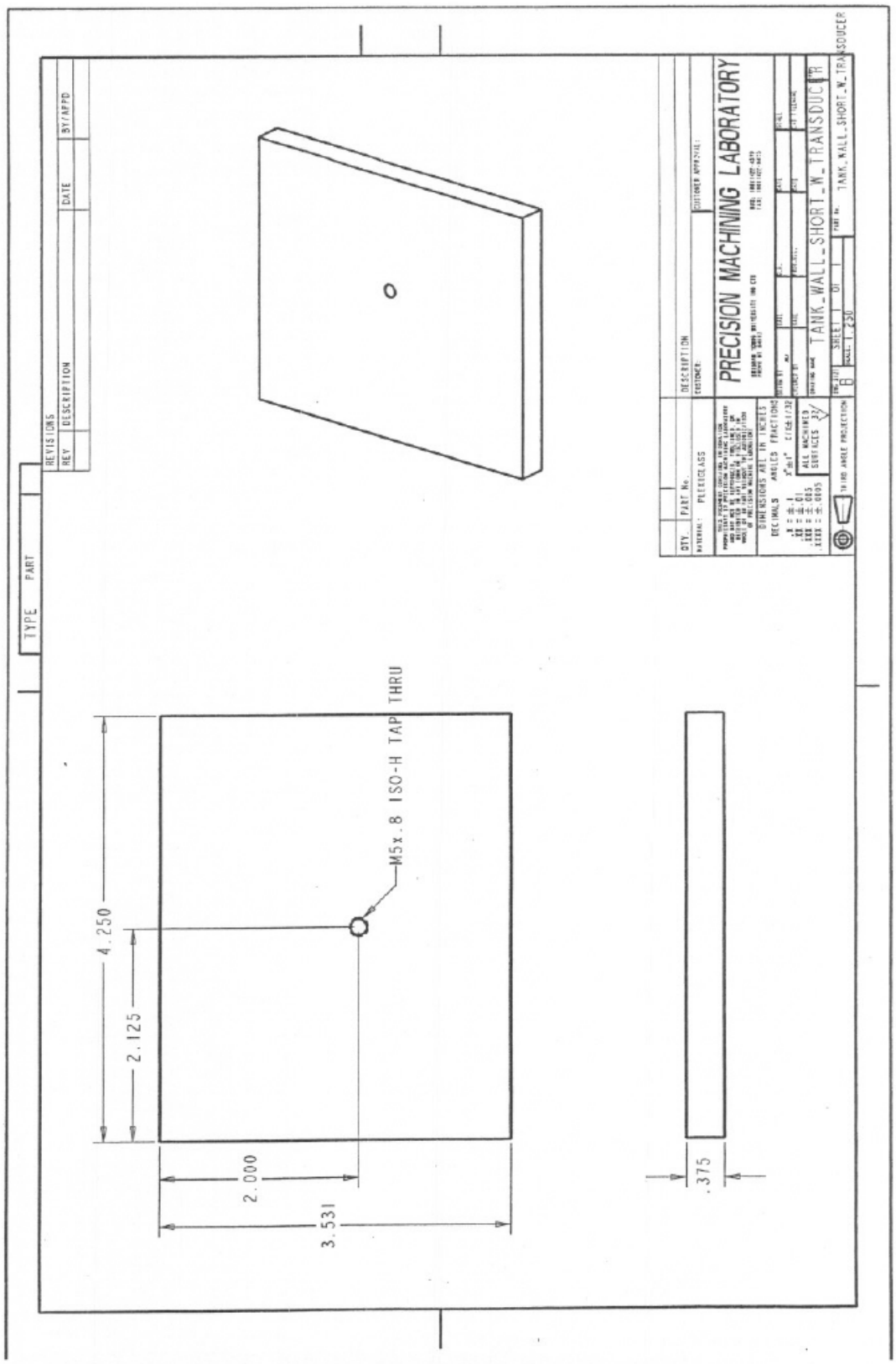

www.manaraa.com

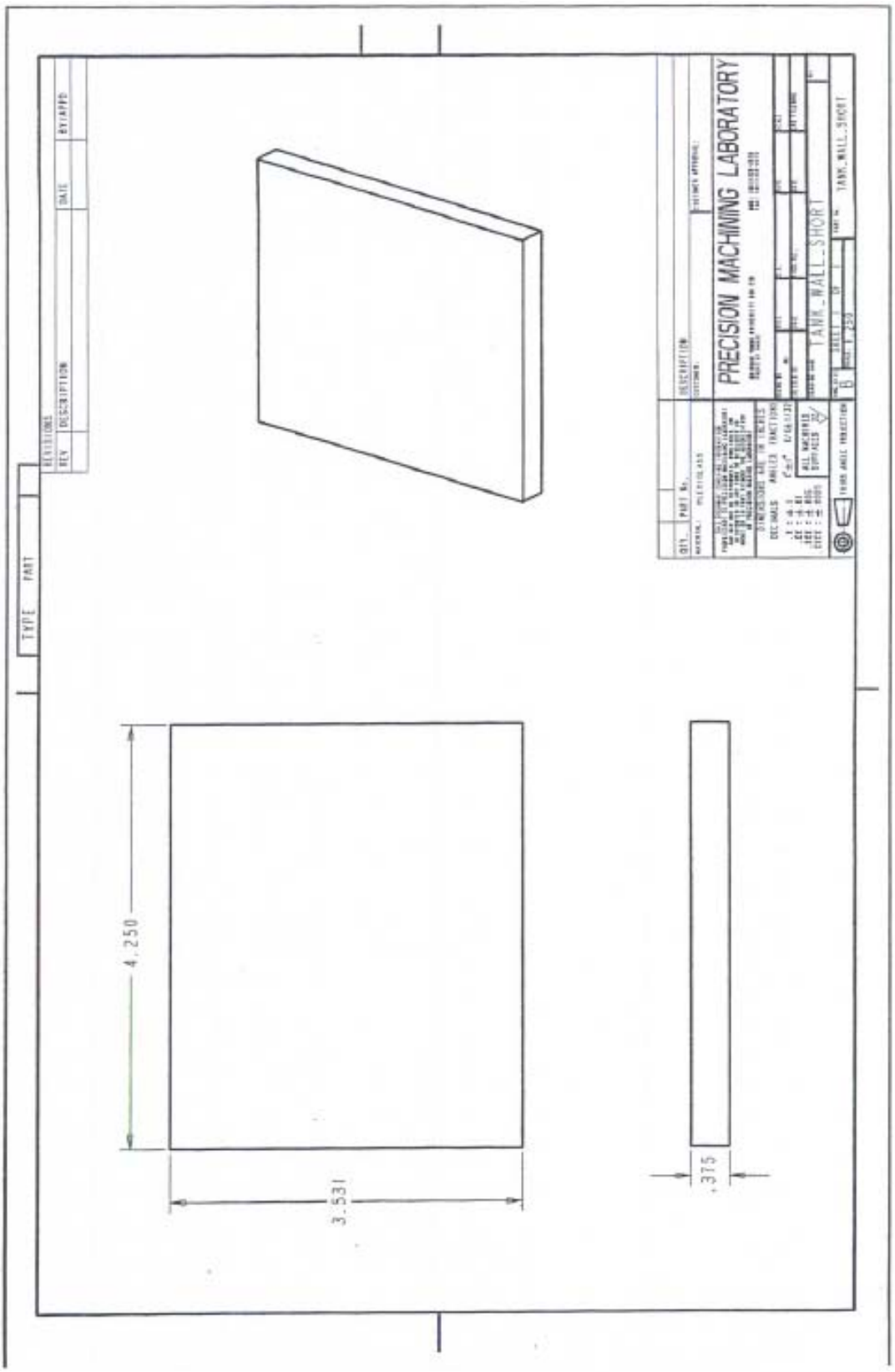

www.manaraa.com

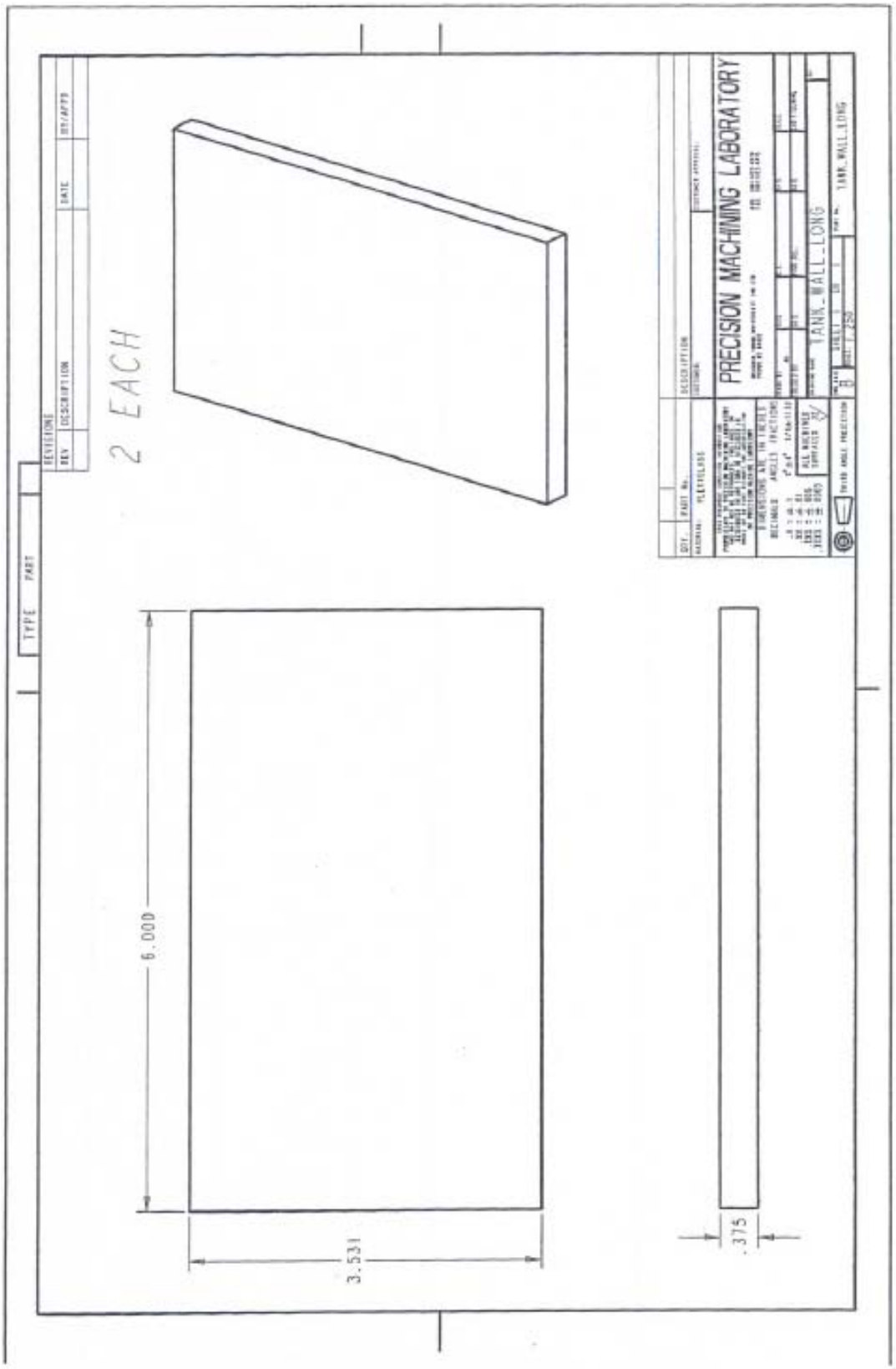

www.manaraa.com

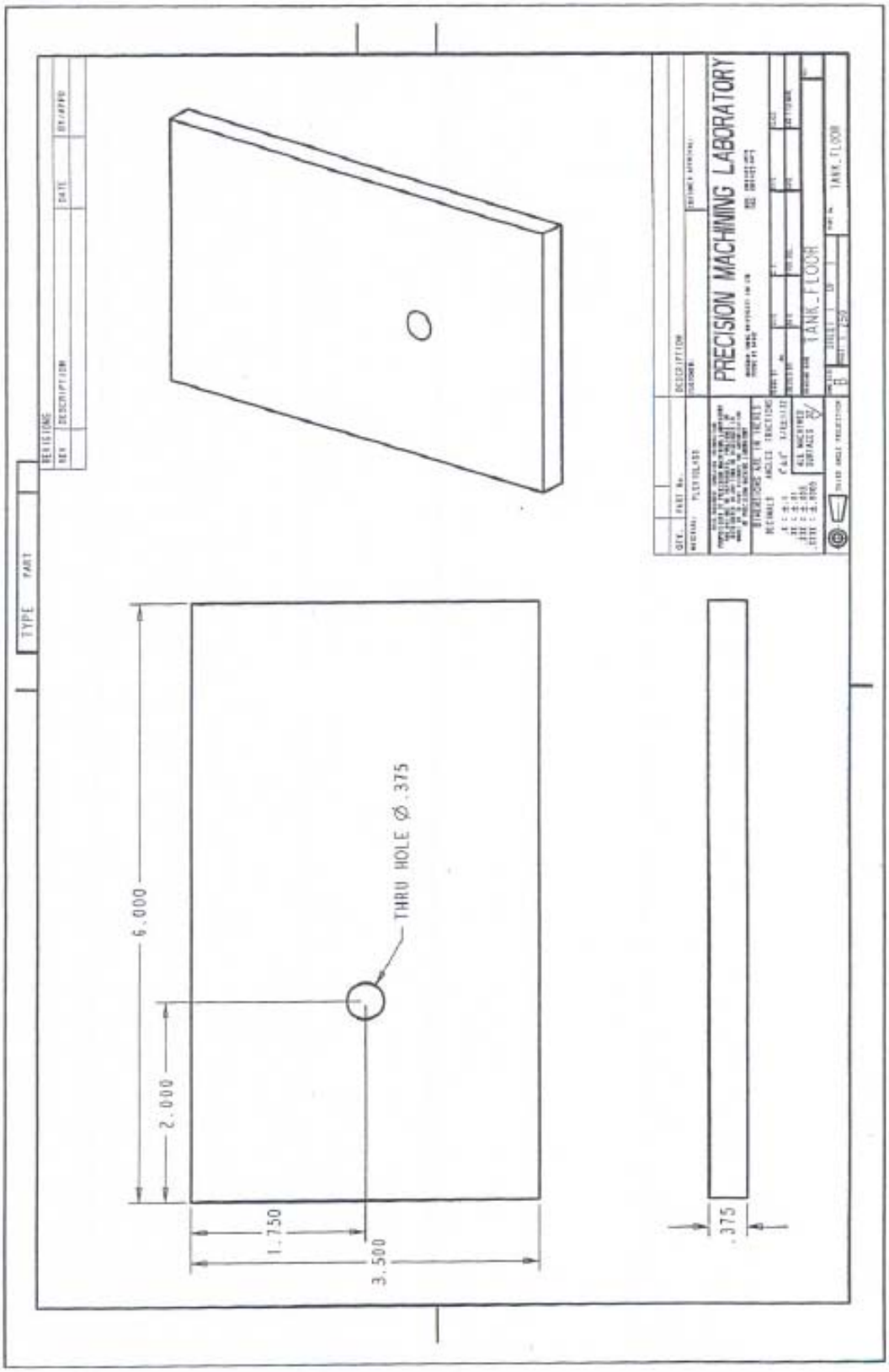

www.manaraa.com

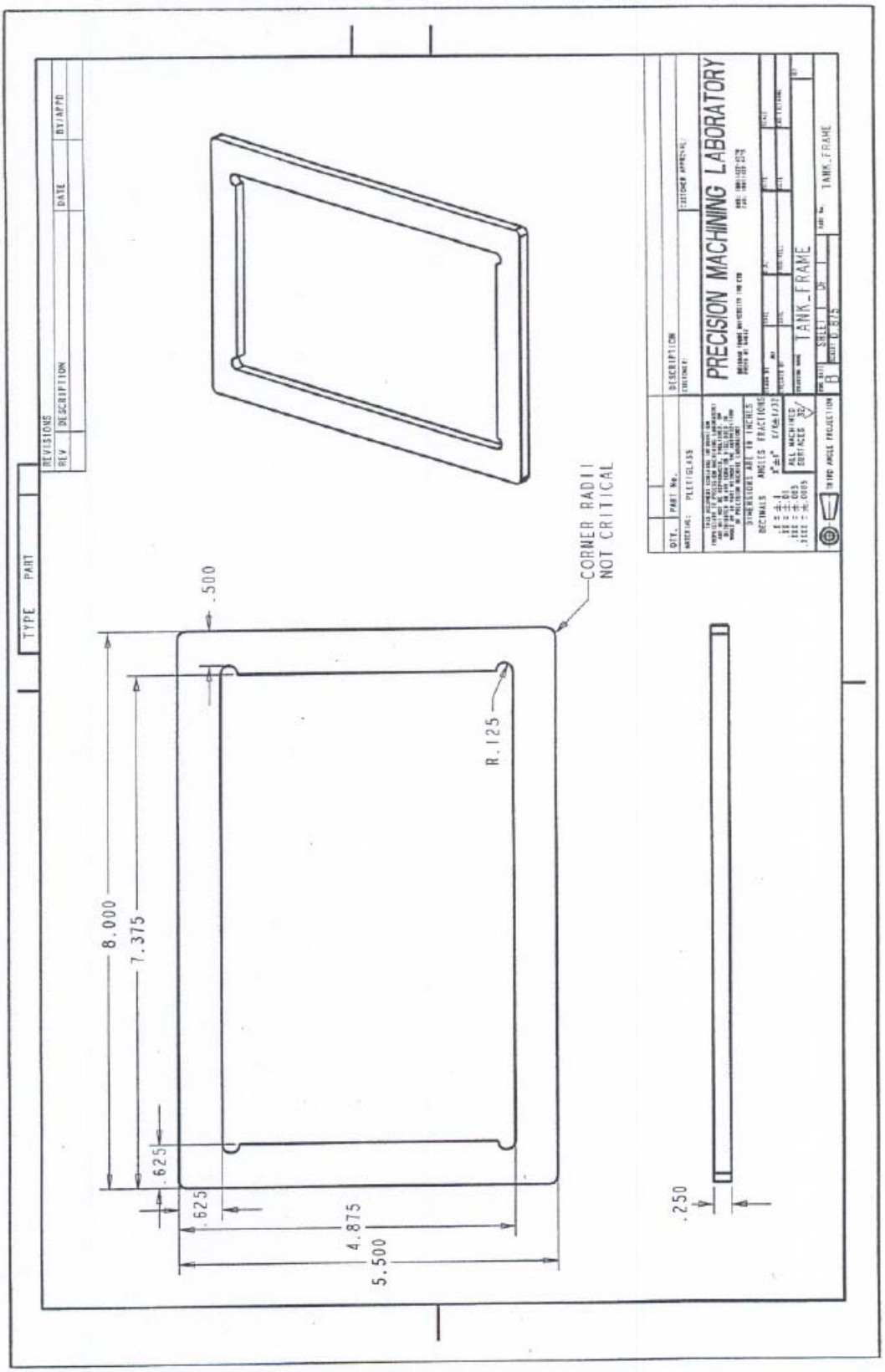

www.manaraa.com

www.manaraa.com

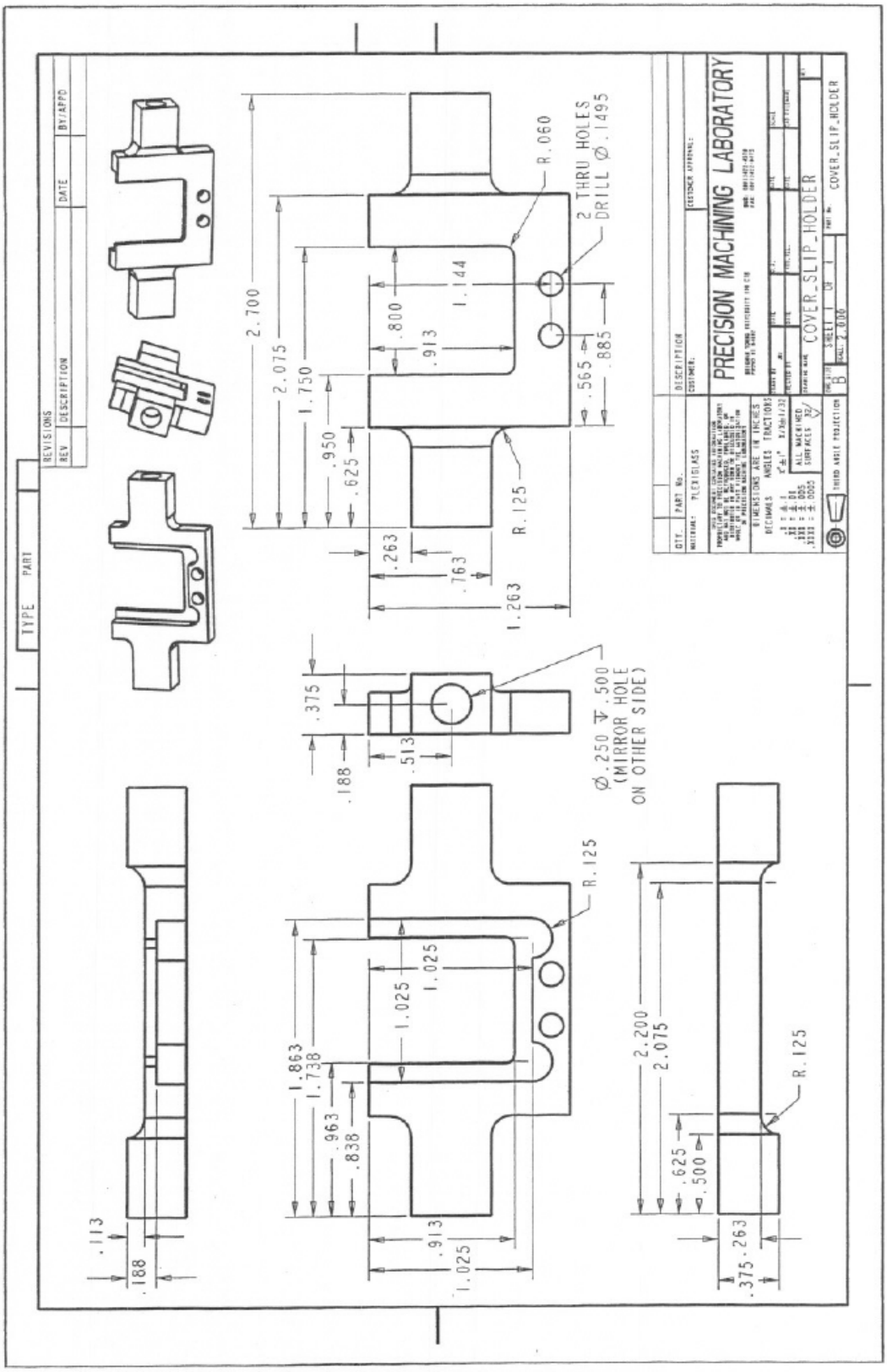

www.manaraa.com

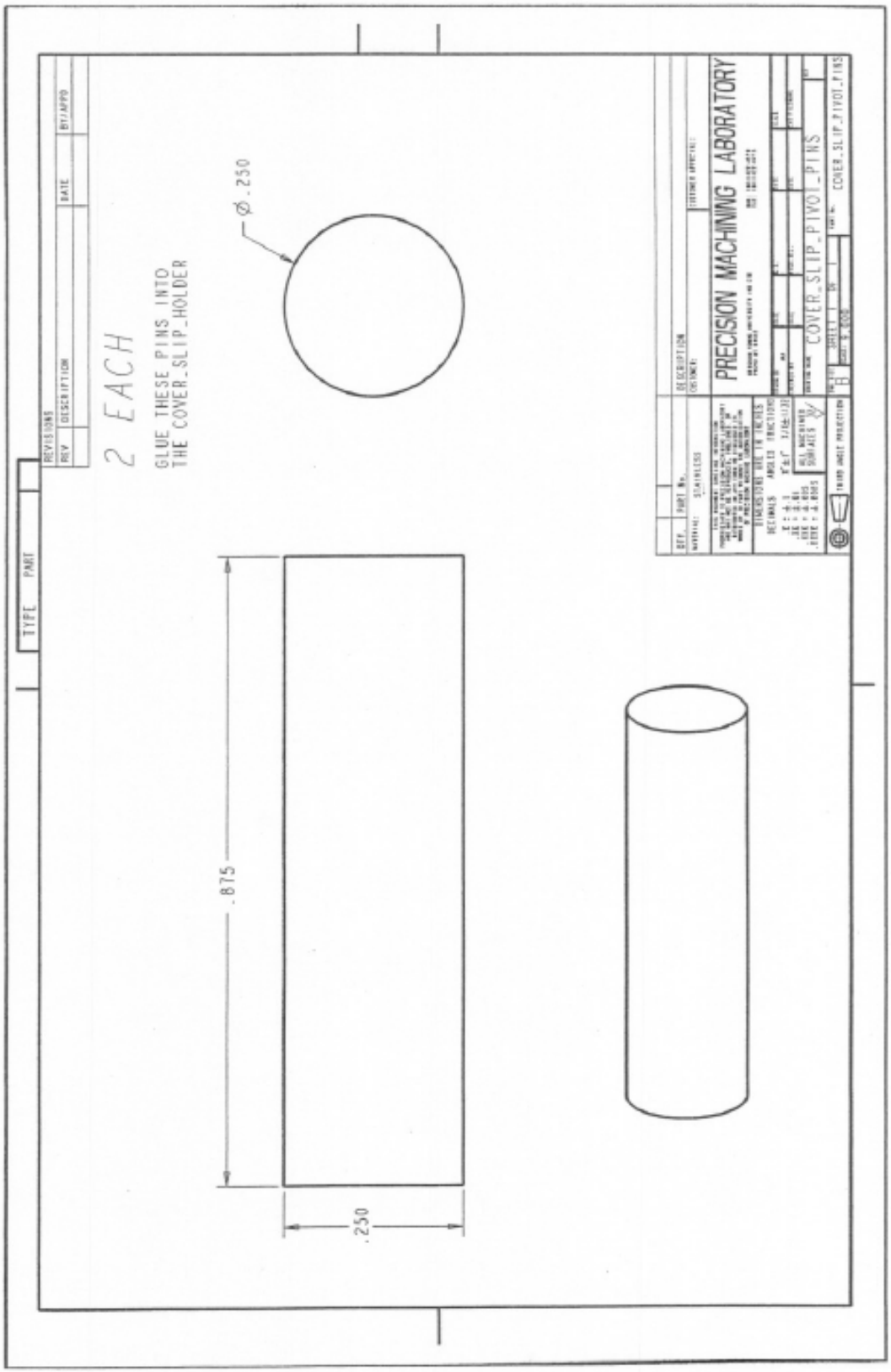

www.manaraa.com

www.manaraa.com

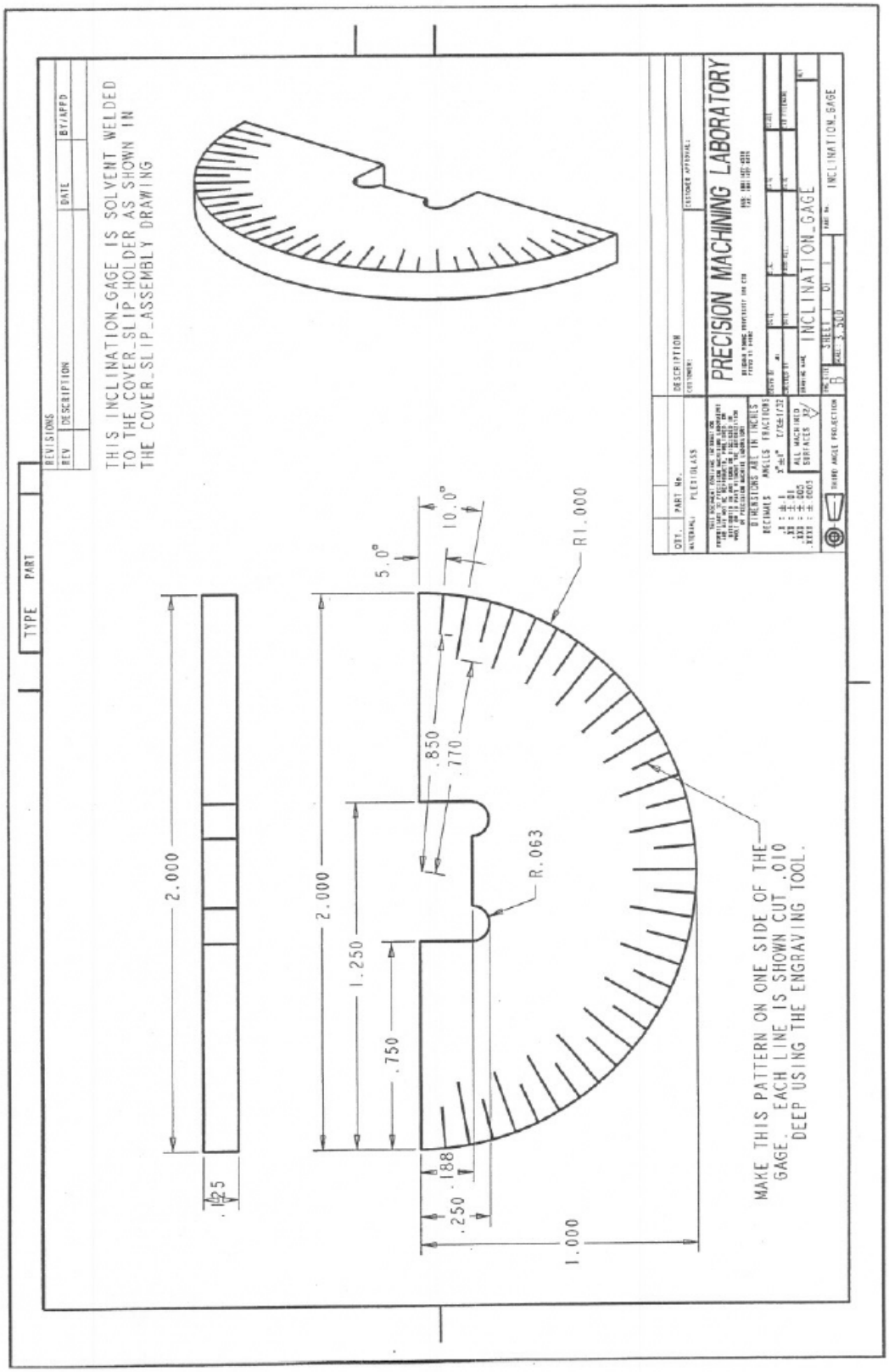

www.manaraa.com

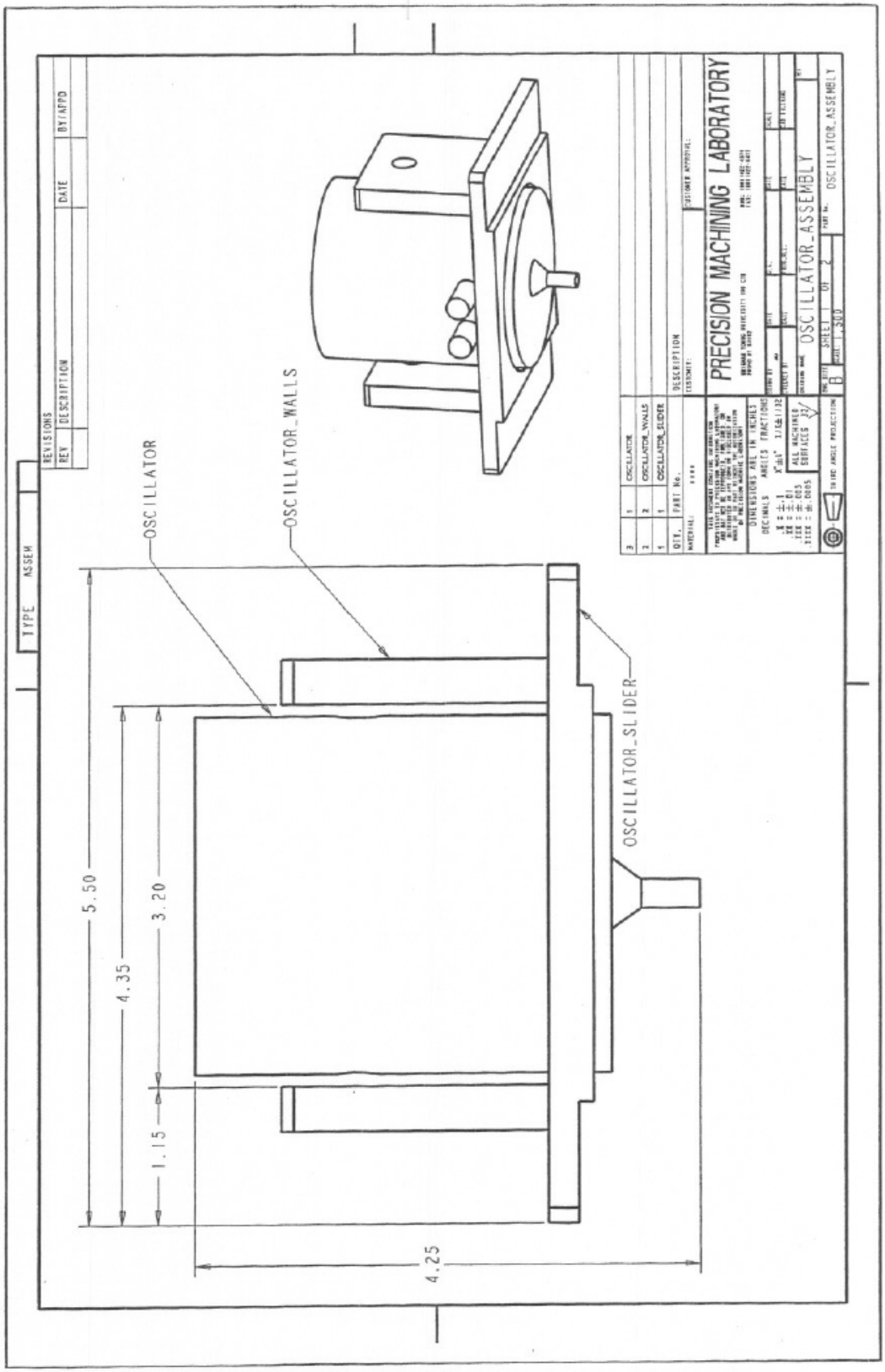

www.manaraa.com

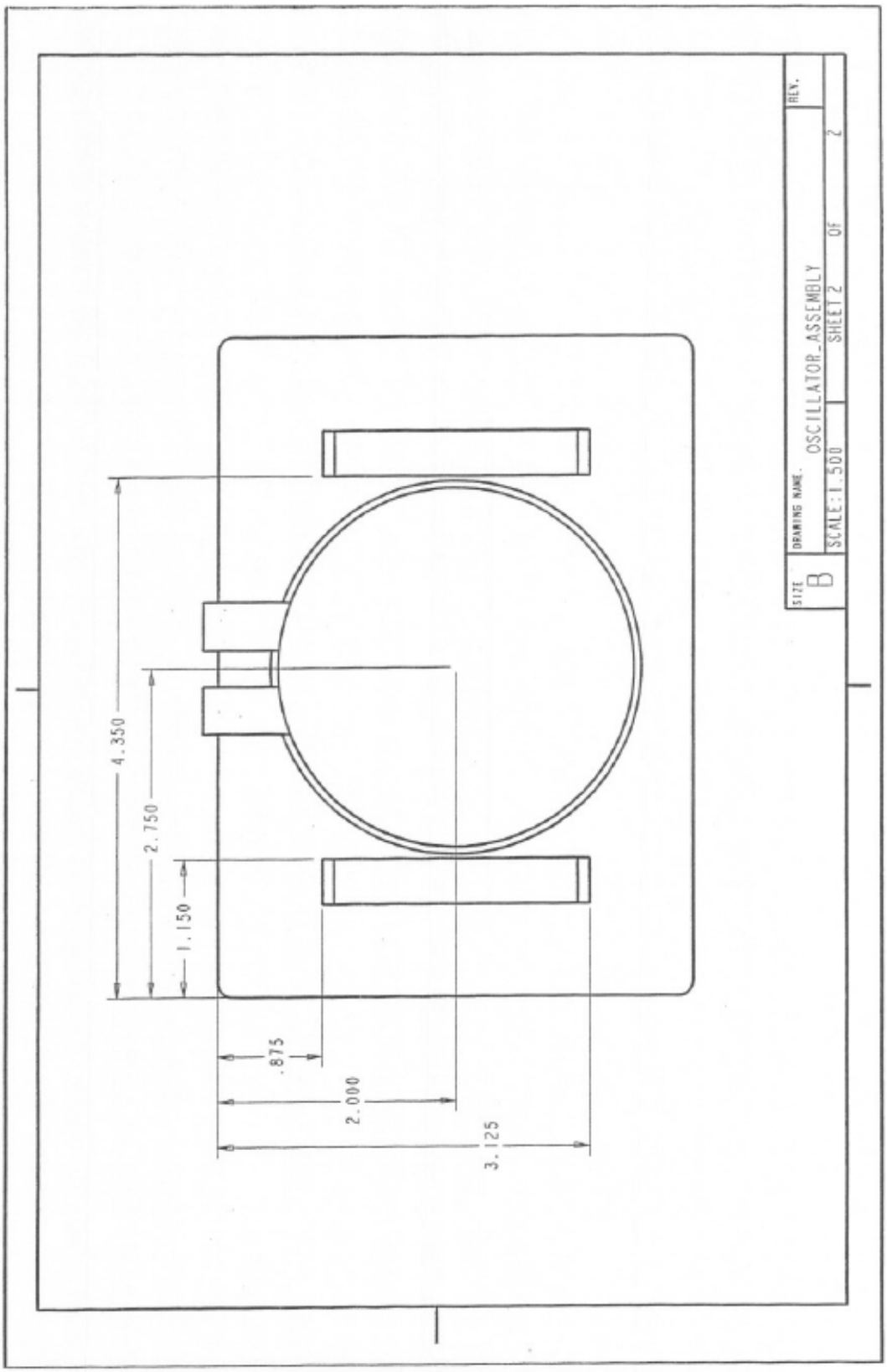

www.manaraa.com

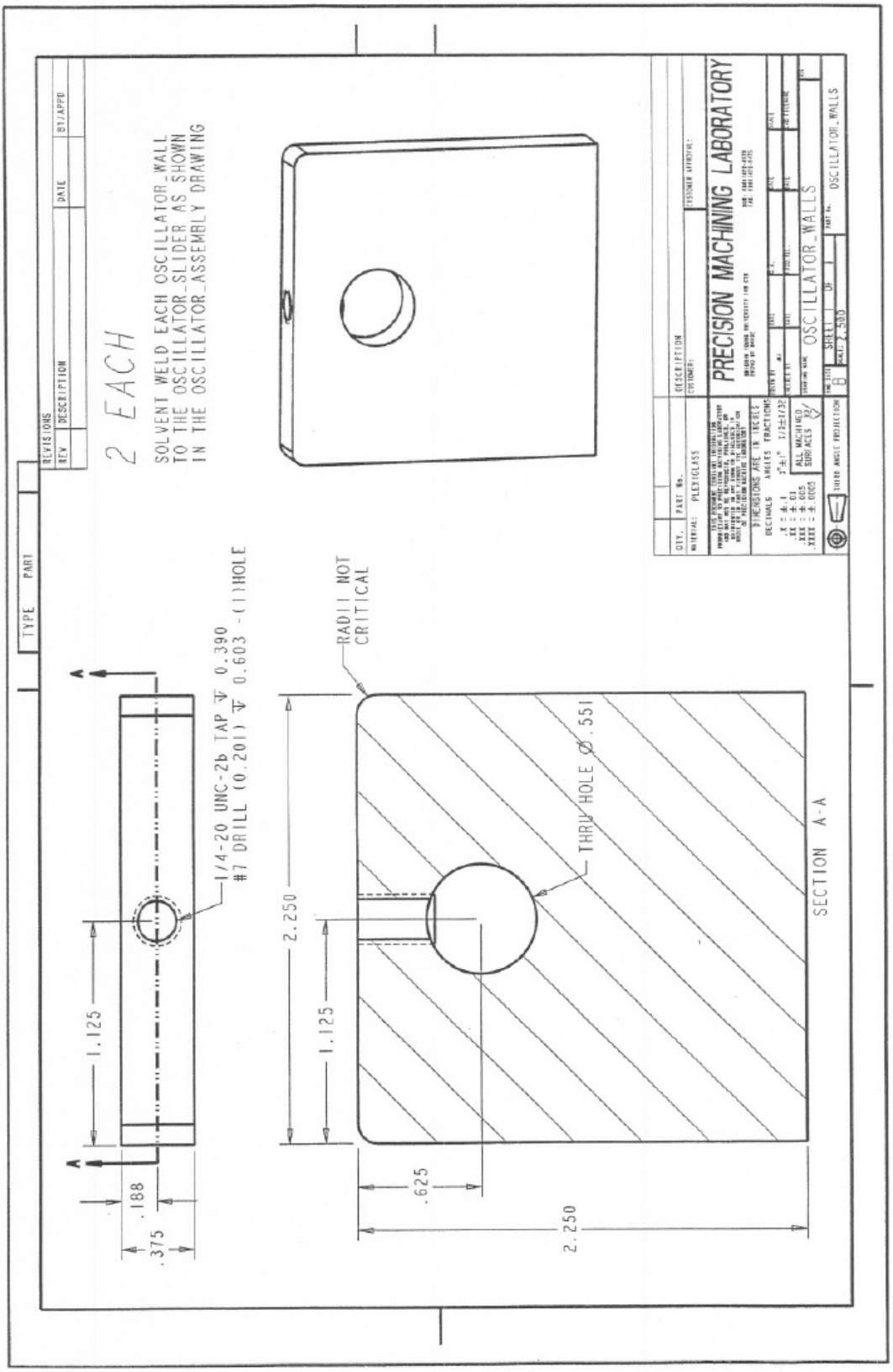

www.manaraa.com

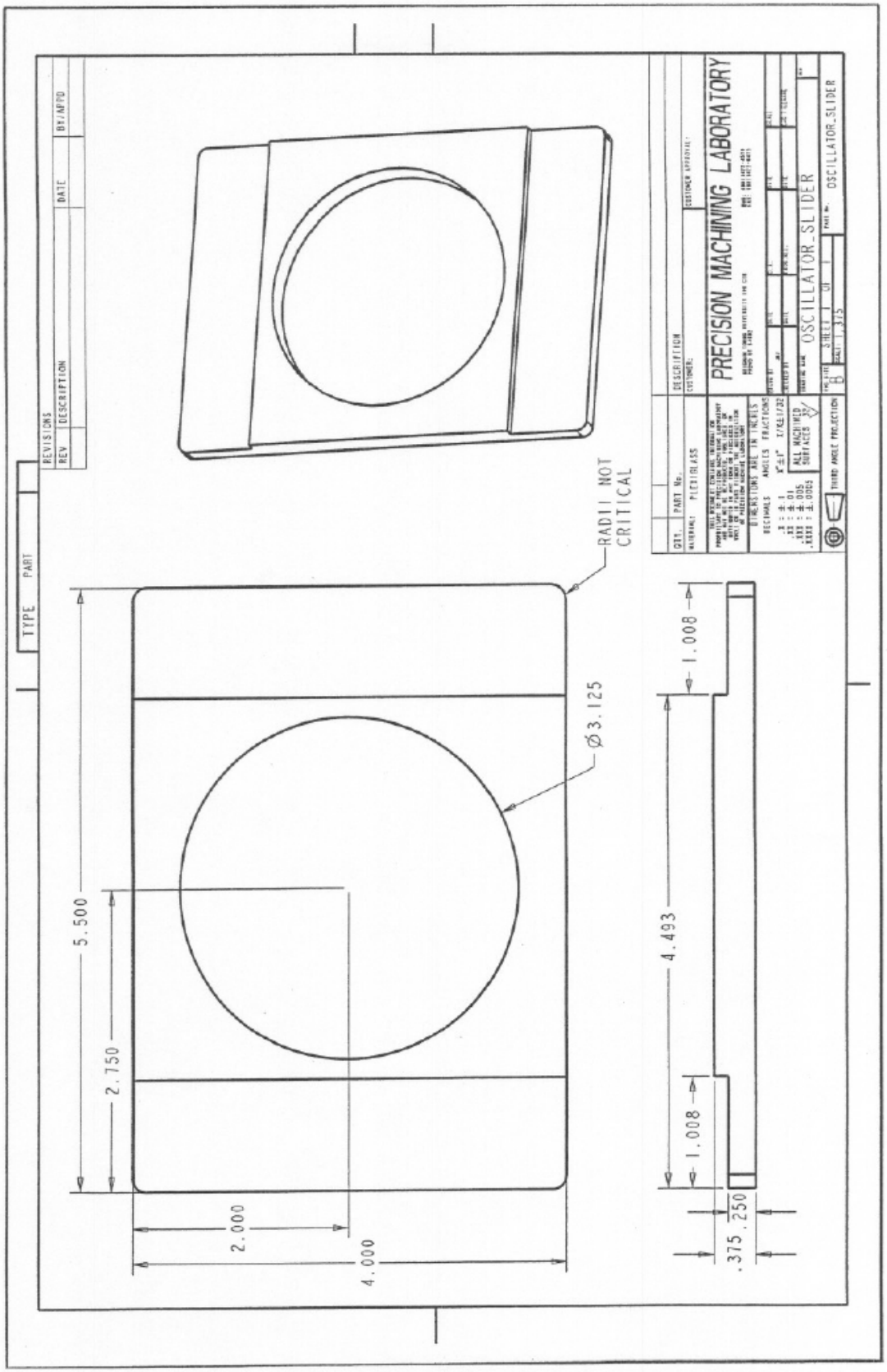

www.manaraa.com